Lecture #1 begins here

Introduction

What are Colloids?

The word "colloid" is not widely used in ordinary English, although you can find it listed in most dictionaries. This word was coined in the 1860's by Thomas Graham from the Greek word *kolla* meaning glue. Today the word is used in the technical literature to describe something related to glue but also quite different. For the purpose of this course, I will define colloid as follows:

> ***lyophobic*♣ *colloid*** – a state of mixtures of two immiscible components in which one component is finely divided as bubbles, drops or particles in a second (usually continuous) phase

By "finely divided" we mean that at least one dimension is in the range 10^{-9} m to 10^{-6} m. The size is perhaps the most important aspect of the definition – as we will see in a moment – because it is the size of the particles which distinuish this state of mixtures from others.

For comparison, let me give a similar definition for a more familiar state of mixtures:

> ***thermodynamic solution*** - a state of mixtures of two (miscible) components in which the molecules of one component (the solute) are each completely surrounded by molecules of the second component (the solvent).

The important difference is that in a solution the solute molecules are completely separated from each other, whereas in a colloid, clusters of molecules of one component are surrounded by a sea of the other component. The following figures shows three different states for mixtures of two components indicated by the black and white colors:

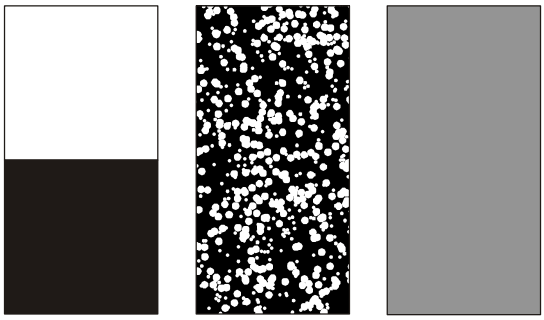

separated phases | colloid | thermodynamic solution

Consider two components like benzene and water. If we vigorous stir the mixture with a waring blender we can produce an emulsion of oil droplets in water. This is a simple and familiar example of a colloid.

> ***emulsion*** – droplets of one liquid finely divided in a second immiscible liquid (e.g. benzene in water)

The reason that these two components are immiscible in each other is that molecules of benzene would prefer to be in the vicinity of other benzene molecules rather than near molecules of water. While molecules in the interior of colloidal particles are "happy" because they are in contact with "friends," those on the surface of the particle (droplet) are "unhappy" because they can see "foes." The collective happiness of the entire group can be increased if all the oil droplets combine to form one large droplet. Then fewer molecules lie on the boundary between the two phases.

In this case, the colloidal state is not thermodynamically stable because it tends to revert to the original state of the mixture before mixing in which the oil and water for two separated layers of liquid. This represents the third state of mixtures of two components: ***totally separated phases***.

Other household examples of colloids include:

- salad dressing, mayonnaise (L/L)
- paint, ink, xerographic fluids (S/L)
- fog (L/G)
- smoke (S/G)
- magnetic recording tape (S/S)

Most of these familar household products are useful only if they maintain their colloidal state. For example, if the polymer particles in latex paint were to combine to form a continuous layer of polymer in the bottom of the can (with a layer of water on top), you would be unable to spread the polymer on the wall.

♣ lyophobic literally means solvent hating or solvent fearing. Wiktionary defines it as "having no affinity for the dispersion medium and thus easily precipitated."

So maintaining the colloidal state (which is often thermodynamically unstable) is an important problem in colloid science. Another important problem is the inverse of this problem: getting a colloidal dispersion to revert to separated phases. Once you spread the paint over the wall, you want the polymer particles to combine together to form a continuous film which will protect the substrate from the environment.

In this course, we will try to understand why colloids are generally unstable, how they can be partially stabilized, and once stabilized how they can be destabilized. We will also learn how to characterize colloids and we will learn about other kinds of behavior that they display.

Some Model Lyophobic Colloids

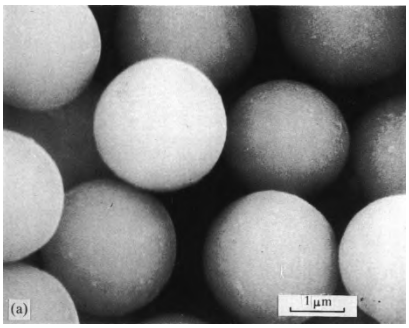

The above are 2 μm spheres of ZnS also known as sphalerite. These four micrographs were taken from Hunter Vol. 1, Fig. 1.5.2 and 3.

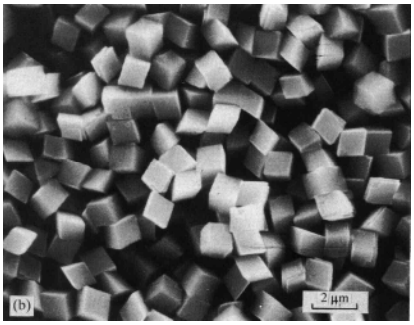

These are 1 μm cubes of $CdCO_3$.

Some Lyophilic Colloids

Besides mixtures of immiscible phases, there are also soluble macromolecules which have colloidal lengths or which self-assemble into structures having colloidal lengths. These are called

lyophilic*♦ *colloid – a thermodynamic solution of a macromolecule having colloidal dimensions or a small molecule which self-assembles to form structures having colloidal dimensions

Examples of macromolecules which are quite soluble in water are DNA, proteins, polysaccharides (starch) and poly(acrylic acid).

Small molecules which can self-assemble into colloidal structures are called

***surfactants*♥** – small molecules which display an affinity for the interfaces between two immiscible phases

By affinity, I mean tending to adsorb at these interfaces. A typical surfactant is sodium dodecylsulfate or SDS:

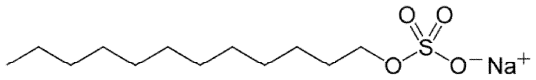

The zigzag portion of this molecule contains 12 methyl (CH_2) groups and is an alkane chain. If we eliminate the sulfate group, we have dodecane, which is an oil (immiscible in water but miscible in other oils). But owing to the polarity of the sulfate group (SO_4^-), SDS is quite soluble in water.

Not only do surfactants adsorb at interfaces, but they also tend to self-assemble to form larger structures in solution, as illustrated below

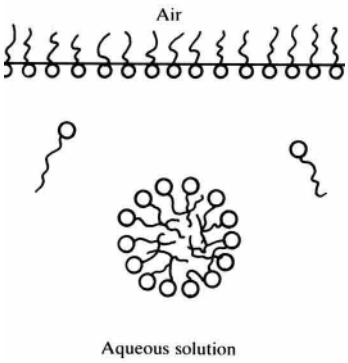

Adsorption of surfactants, tends to reduce the interfacial energy (surface tension) which can slow the rate of aggregation of thermodynamically

♦ lyophilic means solvent loving. Wiktionary defines it as "having an affinity for the dispersion medium and thus not easily precipitated."

♥ surfactant is a contraction of surface active agent

unstable lyophobic colloids. Later in the course, we will find that addition to surfactants to lyophobic colloids is essential to formulating many commerical products. The circular aggregate of SDS molecules is called a

micelle – an aggregate of surfactant molecules

While SDS tends to form spherical or cylindrical micelles (depending on conditions), other surfactants (e.g. phospholipids) form other shapes such as bilayers:

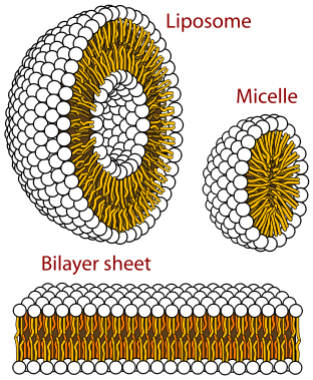

A spherical bilayer is called a ***vescicle***. When the structure is formed using phospholipids, it's called a ***liposome***. All cell membranes are bilayer sheets of phospholipids.

Importance of the Surface

The course title concerns "colloids" and "surfaces." The word "surface" means about the same in physical chemistry as it does in ordinary English:

surface (or ***interface***) – the boundary between any two immiscible phases

While we tend to think of surfaces or interfaces as being sharp, at the molecular level they are diffuse regions having a thickness on the order of 1 nm.

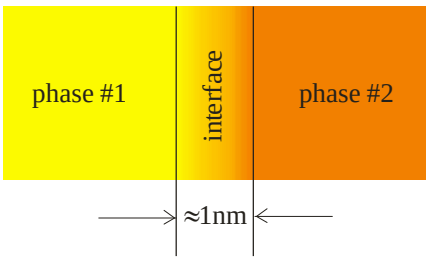

Regardless of whether we are talking about lyophilic or lyophobic colloids, the most important part of the definition is size of the structure: size matters alot. There are several reasons which will be revealed as the semester progresses. Let me give you one reason now.

As particle size decreases, the fraction of molecules of the particle which reside at the surface increases. To prove this, consider two concentric spheres whose radii differ by t = 1 nm, the "thickness" of the interface. Let's compare the volume of the interfacial shell

$$V_{\text{shell}} = \tfrac{4}{3}\pi(R+t)^3 - \tfrac{4}{3}\pi R^3$$

with the volume of the interior sphere

$$V_{\text{inner}} = \tfrac{4}{3}\pi R^3$$

Taking their ratio

$$\frac{V_{\text{shell}}}{V_{\text{inner}}} = \frac{\frac{4}{3}\pi(R+t)^3 - \frac{4}{3}\pi R^3}{\frac{4}{3}\pi R^3} = \left(1+\frac{t}{R}\right)^3 - 1$$

Taking t = 1 nm, we obtain the following values for this ratio:

R (m)	$\frac{V_{\text{shell}}}{V_{\text{inner}}}$
10^{-3} (1 mm)	3×10^{-6}
10^{-4}	3×10^{-5}
10^{-5}	3×10^{-4}
10^{-6} (1 μm)	0.003
10^{-7}	0.03
10^{-8}	0.33
10^{-9} (1 nm)	7

For particles of 1 mm (e.g. sand grains), the fraction of molecules in the interfacial region is negligible. For particles of 1 μm, the fraction is starting to become significant. For nanometer particles, there are actually more molecules in the interfacial region than in the interior.

Think of this interfacial region as a third phase whose thermodynamic properties lie somewhere between those of the interior phase and the exterior phase. As particle size decreases, the thermodynamic properties of the mixture changes, with the interfacial region playing an increasingly important role.

Surface Tension

The interface contributes to the Gibbs free energy of a mixture. That contribution is proportional to the interfacial area; the proportionality constant is called the

interfacial tension – Gibbs free energy per unit area of interface between *any* two immiscible phases

surface tension – Gibbs free energy per unit area of surface between a liquid and its vapor (or air)

In equation form, these definitions correspond to

$$\gamma = \left(\frac{\partial G_{mix}}{\partial A} \right)_{T,P,N_j}$$

where γ is surface or interfacial tension, G_{mix} is the Gibbs free energy of the mixture, A is interfacial area, T is temperature, P is pressure and N_j is the number of moles of each component j.

Surface tension as a force

Recall from thermodynamics that systems tend to spontaneous transform thermselves into that state having the minimum energy. The simplest experiment which demonstrate the existence of surface tension is the following.♠ Consider a soap film supported by a rectangular wire frame in which one edge of the frame is moveable:

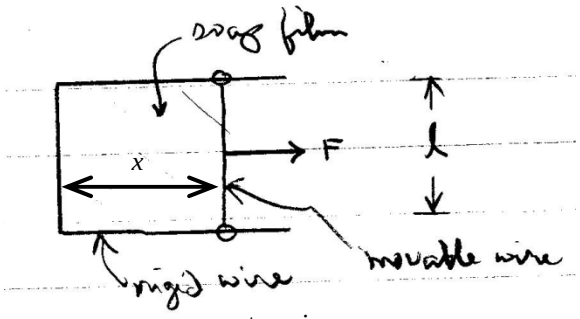

top view

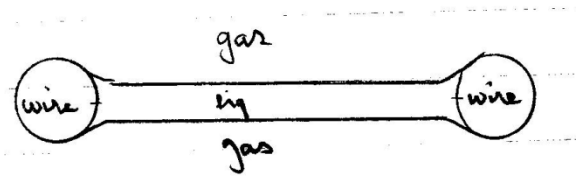

side view
(vertical scale of film exaggerated)

The soap film satisfies the definition of a colloid because at least one dimension (the thickness) is in the range of 1 nm to 1 micron.

♠ This also demonstrates the importance of surfaces to colloids.

The soap film has two faces, so the total interfacial area is

$$A = 2xl$$

The tendency to minimize the area gives rise to a measurable force exerted on the moveable wire:

$$F = 2\gamma l$$

This force actually has to be continuously applied to the moveable wire to keep it stationary. Rearranging

$$\gamma = \frac{F}{2l} = 72.7 \text{ mN/m for water at } 20^{\circ}\text{C}$$

Recall that the "2" in this equation arises between for a soap film, there are *two* air-water interfaces which contribute to the force, each of length l. Notice also that the length l is measured along a direction which is perpendicular to the direction of the force.

Surface tension as an energy

Now consider an experiment in which we stretch the soap film by pulling on the moveable wire with a force F causes the wire to move a distance dx:

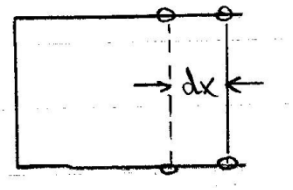

This has increased the area of air-water interface by

$$dA = 2l\,dx$$

We did work to create this new interface

$$dW = F\,dx = 2\gamma l\,dx$$

Dividing these two equations:

$$\frac{dW}{dA} = \frac{2\gamma l\,dx}{2l\,dx} = \gamma = 72.7 \text{ mJ/m}^2 \text{ for water at } 20^{\circ}\text{C}$$

Thus you can see that γ can be considered to be the energy per unit area of the new surface created by moving the wire to expand the film.

Surface tension causes a number of facinating phenomena, which are demonstrated in the film by Lloyd Trefethen (MechE Dept, Tufts U, 1963) shown in class.

Particle Characterization

Shape

The performance of a colloid as a product is often determined by physical properties -- size, shape, density -- as well as chemical composition.

One example is the iron oxide particles commonly found in audio and video recording tape as well as floppy disks, hard disks etc. These particles are composed of γ-Fe_2O_3 (maghemite), which is a particular phase (denoted by the γ) of this ferric oxide which has good magnetic properties.

Size and shape is also important. The best recording properties are obtained using needle-shaped (acicular) particles typically 20×120 nm in size.

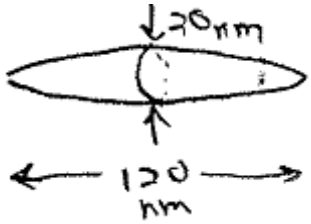

Generally, small particles are preferred since, ideally, each particle could store a single bit of information. Then the smaller the particle, the higher the density of information storage:

large size $\rightarrow$ low info density

But there is a limit to how small the particles can be. For small particles, the magnetic dipole undergoes significant thermal fluctuations, which means that any stored information would be lost:

small size $\rightarrow$ (super)paramagnetic

Thus there is an optimum size.

Another example of a colloidal product is latex paint which consists of 200 nm spheres typically of some acrylic polymer. Here the shape isn't so important. The emulsion polymerization process happens to produce spheres. Thin films of these polymers would tend to be clear. TiO_2 particles are sometimes added as a pigment to produce an opaque white film.

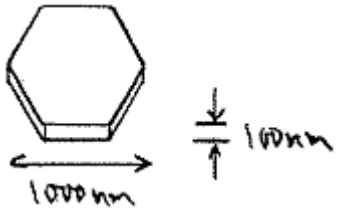

Another common shape is the platelet. Many clays used for ceramicsnaturally occur as hexagonal plates typically on the order of 100x1000 nm in size.

Barium ferrite is a magnetic material which also exists as hexagonal platelets, but much smaller in size. This material maintains its ferromagnetic properties at much smaller size and so it is of considerable interest for magnetic recording. One difficulty is getting it dispersed.

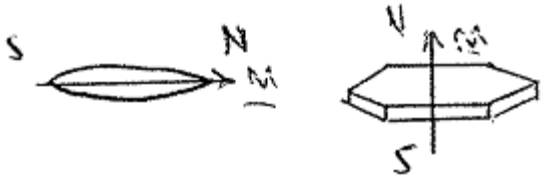

The magnetic dipole is usually aligned with the shorter geometric axis with the ferrites whereas the dipole is aligned with the long axis in ferric oxides.

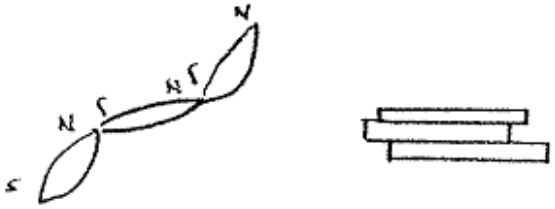

Strong magnetic attractions cause these particles to aggregate with the dipoles aligned north-to-south. This produces long necklace-like structures with the ferric oxides and poker-chip stacks with the ferrites. The stack of poker chips is much harder to disperse.

Ellipsoids or Spheroids

A (triaxial) ***ellipsoid*** is a generalized version of a sphere. The mathematical equation of a ***sphere*** in rectangular coordinates (x,y,z) is

$$x^2 + y^2 + z^2 = R^2$$

where R is the radius of the sphere. The equation of an ellipsoid is

$$\left(\frac{x}{R_x}\right)^2 + \left(\frac{y}{R_y}\right)^2 + \left(\frac{z}{R_z}\right)^2 = 1$$

which has three different radii. The volume of a ellipsoid is given by

$$V = \frac{4}{3}\pi R_x R_y R_z$$

A formula also exists for the surface area but it involves special functions (**http://mathworld.wolfram.com/Ellipsoid.html**).

A sphere has all three radii equal. If only two of the three radii are equal, the object is called an ***spheroid***. There are two different types of spheroids: prolate and oblate. Both are obtained by rotating an ellipse around one of the principal axes.

The equation of an ellipse is the 2-D analog of that for an ellipsoid:

$$\left(\frac{x}{R_x}\right)^2 + \left(\frac{y}{R_y}\right)^2 = 1$$

An ellsipse having $R_x > R_y$ is shown below:

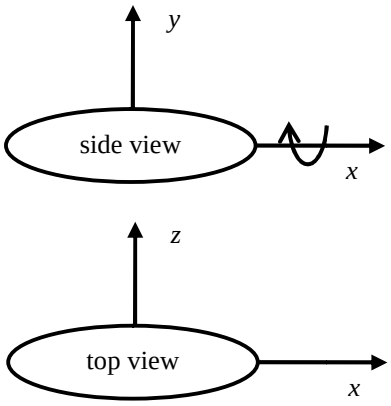

Rotating this same ellipse around the x-axis results in a cigar-shaped object called a ***prolate ellipsoid***.

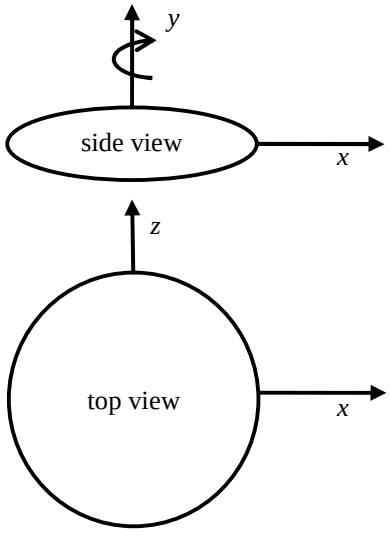

If instead, we rotate around the y-axis we obtain a pill-shaped objected called an ***oblate ellipsoid***.

Particle Size Distribution

Most sols are not composed of identical particles. Nearly always there will be a range of particle size. To describe the distribution of particle sizes, we might subdivide the total range of sizes into a number of intervals and then count the number of particles in each interval.

This process is called classification of the particles: we are assigning each particle to a class and then counting the members of each class. Here are the data from Table 1.5 on p32 of Hiemenz:

Class boundaries $<d<$ (μm)	Class mark d_i (μm)	Number of particles n_i
0–0.1	0.05	7
0.1–0.2	0.15	15
0.2–0.3	0.25	18
0.3–0.4	0.35	28
0.4–0.5	0.45	32
0.5–0.6	0.55	70
0.6–0.7	0.65	65
0.7–0.8	0.75	59
0.8–0.9	0.85	45
0.9–1.0	0.95	38
1.0–1.1	1.05	19
1.1–1.2	1.15	4

A plot of the count n_i of each class i versus the size d_i of that class is called a histogram. The following plot is the data tabulated above and is Fig. 1.18a:

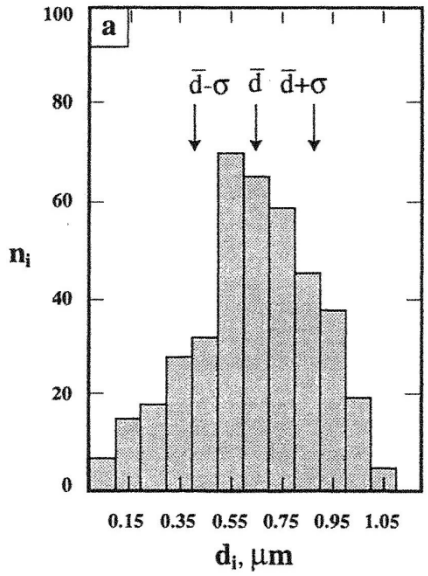

Such a distribution can be characterized by its mean $\bar{d}$ and its standard deviation σ, which are calculated as:

$$\bar{d} = \bar{d}_n \equiv \frac{\sum_i n_i d_i}{\sum_i n_i} = \sum_i \underbrace{\frac{n_i}{\sum_i n_i}}_{f_i} d_i = \sum_i f_i d_i$$

and

$$\sigma = \sqrt{\sum_i f_i \left(d_i - \bar{d}\right)^2}$$

where

$$f_i \equiv \frac{n_i}{\sum_j n_j}$$

is the fraction of particles which are in class *i*. The above mean is called the ***number average*** diameter. There are other reasonable mean values which are also defined:

$$\bar{d}_s \equiv \left(\overline{d^2}\right)^{1/2} \quad \text{where} \quad \overline{d^n} \equiv \sum_i f_i \, d_i^n$$

is called the ***surface average*** diameter, and

$$\bar{d}_v \equiv \left(\overline{d^3}\right)^{1/3}$$

is called the ***volume average*** diameter. Finally,

$$\bar{d}_z \equiv \left(\overline{d^6}\right)^{1/6}$$

is call the ***Z-average***. These four measures of the average diameter are not equal. Generally the larger the exponent on *d*, the more heavily larger diameters are weighted in the average; thus

$$d_n < d_s < d_v < d_z$$

The reason for so many definitions of average is that different experiments for measuring the average diameter weigh the various classes differently. For example, light scattering yields the Z-average (also called the ***intensity average***) whereas centrifugation rate yields the surface average but centrifugation equilibrium yields the volume average.

Most histograms of particle sizes are fit reasonably well by a ***Gaussian*** shape:

$$f(x) = \frac{1}{\sqrt{2\pi\sigma^2}} \exp\left[-\frac{\left(x-\bar{x}\right)^2}{2\sigma^2}\right] \qquad (1)$$

which is called a ***normal distribution***. When the particle size distribution is quite broad, sometimes yields better fit is obtained using a ***log-normal distribution***:

$$f(x) = \frac{1}{\sqrt{2\pi\sigma^2}} \exp\left[-\frac{\left(\ln x - \ln \bar{x}_g\right)^2}{2\left(\ln \sigma_g\right)^2}\right] \qquad (2)$$

Eq. (1) yields the familiar bell shape of a Guassian when you plot f vs x on linear coordinates whereas (2) gives the bell shape of a Gaussian when you plot f vs x on semi-log coordinates, with the x-axis being the logarithmic one.

Sometimes it's more convenient or more accurate to plot the ***cumulative distribution***; in other words, the fraction of particles having a size smaller than *x*:

$$F(x) = \int_{-\infty}^{x} f(x')\,dx'$$

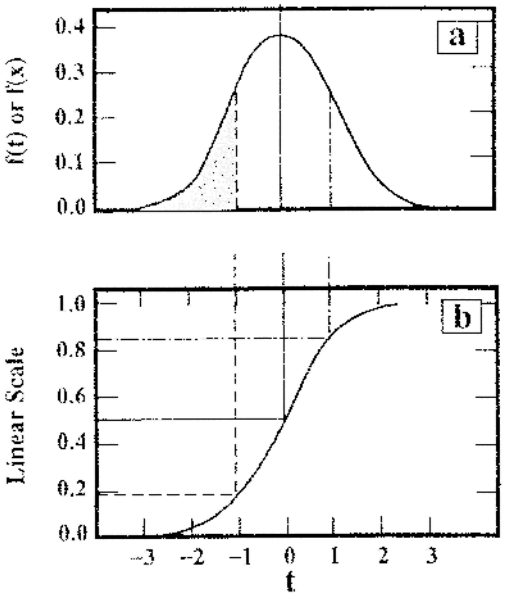

Lecture #2 begins here

Trefethen's film.

Brownian Motion

Reading: Hiemenz Sect. 2.6

One of the ways colloidal dispersions differ from other mixtures is that the particles exhibit Brownian motion.

Brownian motion - random movement of a particle as a consequence of thermal agitation

Suppose we were able to track, for example, a single gas molecule as it undergoes collisions with other gas molecules. The trajectory might look something like that shown below (except in 3-D). The trajectory of a Brownian particle in a liquid would look similarly random except that the mean-free path (length of straight paths between collisions) is much shorter.

1-D Random Walk

To simplify the mathematics, let's confine our attention to 1-D motion -- for example, motion along a capillary tube.

Assumptions:

- particle can only move left or right in steps of equal length
- left or right steps are equally probable, but particle cannot remain at its present location (every t seconds, it must move left or right)

Let $P(m,N)$ denote the probability that a particle is located at position m (an integer) after taking N steps (also an integer). Starting at 0, after N steps, the particle must be located at some point between $-N$ and $+N$:

$$-N \le m \le +N$$

Also the sum of the probabilities must always equal unity (i.e. the particle must exist somewhere):

$$\sum_{m=-\infty}^{\infty} P(m,N) = 1$$

Now let's try to determine $P(m,N)$ subject to the assumptions stated above.

N = 0: this is just the initial condition. We will start the particle at the origin, so:

$$P(m,0) = \begin{cases} 1 & \text{if } m = 0 \\ 0 & \text{if } m \neq 0 \end{cases}$$

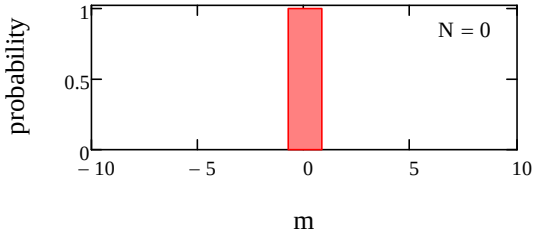

N = 1: possible locations are m=+1 or -1, which are equally probable, so:

$$P(m,1) = \begin{cases} \frac{1}{2} & \text{if } |m| = 1 \\ 0 & \text{if } |m| \neq 1 \text{ (including 0)} \end{cases}$$

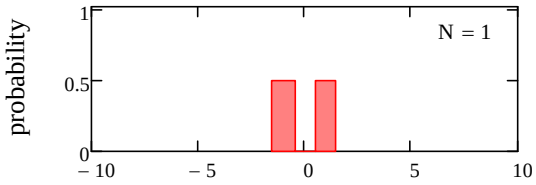

N = 2: there are four possible sequences for these 2 events

1st step	2nd step	m	$P(m,2)$
L	L	-2	1/4
L	R	0	1/4
R	L	0	1/4
R	R	+2	1/4

Each of these outcomes has equal probability, leaving

$$P(m,2) = \begin{cases} \frac{1}{2} & \text{if } m = 0 \\ \frac{1}{4} & \text{if } |m| = 2 \\ 0 & \text{otherwise} \end{cases}$$

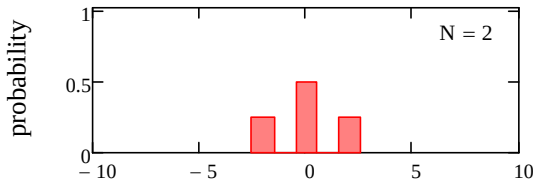

Arbitrary *N*: suppose I toss a coin N times. The probability of a H heads and T tails can be determined from elementary statistics as:

$$\left\{\begin{array}{c}\text{probability of}\\ H \text{ heads, } T \text{ tails}\\ \text{in any order}\end{array}\right\} = \frac{N!\left(\frac{1}{2}\right)^N}{H!T!} \quad \text{with } N = H+T \qquad (3)$$

Suppose I move one step to the right if the coin toss yields a head and one step to the left if the toss yields a tail. To get m>0 we clearly need to take more heads than tails. Indeed, the final position depends only on the number of heads relative to the number of tails:

$$m = H - T$$

but $$N = H + T$$

Solving simultaneously for H and T:

$$\left.\begin{aligned} H &= \frac{N+m}{2} \\ T &= \frac{N-m}{2} \end{aligned}\right\} \qquad (4)$$

Substituting (4) into (3):

$$P(m,N) = \begin{cases} \dfrac{N!\left(\frac{1}{2}\right)^N}{\left(\frac{N+m}{2}\right)!\left(\frac{N-m}{2}\right)!} & \text{if } N+m = \text{even} \\ 0 & \text{if } N+m = \text{odd} \end{cases}$$

The zero result for $N+m$ = odd can be inferred from (4). Since the number of heads H and the number of tails T are integers, then (4) implies that $2H = N+m$ and $2T = N–m$ must both be even numbers. In particular $N+m$ cannot be an odd integer, so we assign zero probability to this outcome.

Lecture #3 begins here

N*→∞**: When N becomes very large we can use ***Sterling's approximation:

$$\ln(n!) = \left(n+\tfrac{1}{2}\right)\ln(n) - n + \tfrac{1}{2}\ln(2\pi) + O\left(n^{-1}\right)$$

and a second approximation (valid when $|m| \ll N$), which is a Taylor series expansion of the logarithm function around unit value for its argument:

$$\ln\left(1 \pm \frac{m}{N}\right) = \pm\frac{m}{N} - \frac{1}{2}\left(\frac{m}{N}\right)^2 + O\left[\left(\frac{m}{N}\right)^3\right]$$

With these two approximations, our expression for probability becomes a little easier to calculate:

$$P(m,N) \approx \begin{cases} \left(\dfrac{2}{\pi N}\right)^{1/2} \exp\left(-\dfrac{m^2}{2N}\right) & \text{if } N+m = \text{even} \\ 0 & \text{if } N+m = \text{odd} \end{cases} \qquad (5)$$

Probability Density

Our goal is to derive Einstein's famous equation: in random walk the mean-square displacement grows in direct proportion to the time of the walk:

$$\left\langle x^2 \right\rangle = 2Dt \qquad (6)$$

Now let's try to relate (5) to Brownian motion in gases and liquids. What is the length of a step? How big is N?

To answer these questions, it is convenient to keep in mind the kinetic theory of gases. The distance a gas molecule travels between collisions is the ***mean free path***:

$$\text{mean-free path} = \begin{cases} 10^{-7}\,\text{m} & \text{for gases near STP} \\ 10^{-10}\,\text{m} & \text{for liquids} \end{cases}$$

Thus the step sizes can be of atomic dimensions, which would be virtually impossible to follow. The rate of stepping can be equated with the collision frequency:

$$\text{collision freq} \approx \begin{cases} 10^{10}\,\text{sec}^{-1} & \text{for gases near STP} \\ 10^{13}\,\text{sec}^{-1} & \text{for liquids} \end{cases}$$

In the experiments I have in mind, we would be tracking a single colloidal particle through a light microscope using video microscopy, which might be capable of 30 frames/sec. Thus there is no hope of seeing individual steps; we can only sample at intervals of many steps.

Then the discontinuity between odd and even values of $N+m$ will never be resolved. So let's smooth out (5) by replacing it with

$$P(m,N) \approx \frac{1}{2}\left(\frac{2}{\pi N}\right)^{1/2} \exp\left(-\frac{m^2}{2N}\right) \qquad (7)$$

where the factor of ½ in front arises from averaging odd and even values. Let l denote width of elementary step; then

$$x = ml \qquad (8)$$

is the final position of the particle after N steps. Also let τ denote the time interval for elementary steps; then

$$t = N\tau \qquad (9)$$

is the time required for N steps. Finally let Δx denote the spatial resolution of position measurements. Based on the arguments above, we expect $\Delta x \gg l$. The probability of finding the particle between x and $x+\Delta x$ is the sum of

$$\left\{\begin{matrix}\text{probability of finding it}\\ \text{between } x \text{ and } x+\Delta x\end{matrix}\right\} = \sum_{m=\frac{x}{l}}^{m=\frac{x+\Delta x}{l}} P(m,N)$$

$$\approx \frac{\Delta x}{l}\frac{1}{2}\left(\frac{2}{\pi N}\right)^{1/2} \exp\left(-\frac{m^2}{2N}\right) \qquad (10)$$

where the second equation substitutes (7) is approximate because it treats the exponential as a constant over this narrow (differential) interval of m. Dividing this sum of probabilities by the spatial interval Δx yields the probability density $p(x,t)$. After substituting (8) and (9), we have

$$p(x,t) \equiv \frac{\sum P}{\Delta x} \approx \left(\frac{\tau}{2\pi l^2 t}\right)^{1/2} \exp\left(-\frac{\tau x^2}{2l^2 t}\right) \qquad (11)$$

The net effect of the approximations is to take us from a discrete description of the random walk process to a continuous description (i.e. m was constrained to take on integer values whereas x is not integer). Unlike $P(m,N)$ (which is discontinuous), $p(x,t)$ is a smooth continuous function. In effect, we have averaged out the singularities in P by accepting a coarser description of the random walk process.♣

Some properties of $p(x,t)$: it has units of m^{-1}, it has Gaussian shape (see below) and

$$\int_{-\infty}^{\infty} p\,dx = 1$$

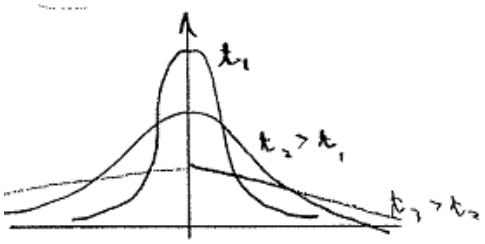

We can use (11) to re-write (10):

$$\left\{\begin{matrix}\text{probability of finding it}\\ \text{between } x \text{ and } x+\Delta x\end{matrix}\right\} = p(x,t)\,dx$$

In effect, we have replaced Δx by a differential quantity dx, which just acknowledges that Δx is sufficiently small that the exponential function of x is essentially constant over the interval between x and $x+dx$.

To calculate the average value of $x(t)$ for a large number of random walks, we take the probability of finding a particular x, multiply by x, and add up the result for each x:

$$\langle x \rangle = \int_{-\infty}^{\infty} x\,p(x,t)\,dx = 0$$

Substituting $p(x,t)$ from (11) and integrating, the result is zero mean x, independent of time t. This integral must vanish because $p(x,t)$ is an even function while xp is odd:

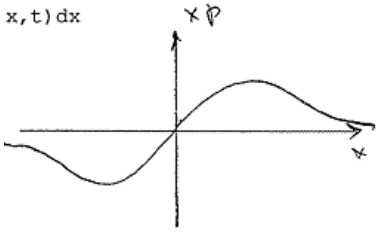

Similarly we can calculate the mean square displacement which does not vanish:

$$\langle x^2 \rangle = \int_{-\infty}^{\infty} x^2\,p(x,t)\,dx = \frac{l^2}{\tau}t \qquad (12)$$

Notice that the the mean-square displacement is proportional to t and the portionality coefficient has units of $m^2\ sec^{-1}$ – just as in (6).

1-D Diffusion from a Point Source

Reading: Hiemenz Sect. 2.5

♣ Actually the singularities in (5) are an artifact of assuming uniform step size. In reality, each elementary step has a different length; then these discontinuities disappear.

Now we will try to show that the coefficient of t in the above expression is just the usual diffusion coefficient (times two). First let me carefully define what I mean by diffusion coefficient (D). According to ***Fick's 1st law of diffusion***:

$$N_x(x,t) = -D\frac{\partial C(x,t)}{\partial x} \qquad (13)$$

where N_x is the flux (rate of transport per unit area) of particles in the x-direction. What is the difference between Brownian motion and diffusion?

Brownian motion - random walk of a single particle

diffusion - net flux of an ensemble of particles (particle transport rate/area)

The "ensemble" is a set of particles (or small molecules) which is statistically large enough so that the average behavior is reproduced if the diffusion experiment is repeated.

Conservation of particles (a mass balance) for diffusion in the x-direction only requires

$$\frac{\partial C}{\partial t} + \frac{\partial N_x}{\partial x} = 0$$

Substituting (13) into the above equation yields ***Fick's 2nd law of diffusion***:

$$\frac{\partial C}{\partial t} = D\frac{\partial^2 C}{\partial x^2}$$

We are going to look at the particular solution of this equation which satisfies the following initial condition♦

$t = 0$: $\qquad C(x,0) = \frac{n}{A}\delta(x)$

and boundary conditions:

$x \to \pm\infty$: $\qquad C(\pm\infty, t) \to 0$

This mathematical problem describes the following experiment. n particles (the ensemble) are initially distributed uniformly over the x=0 plane inside a tube of cross sectional area A. At time zero they are released and diffuse away in the +x and –x directions.

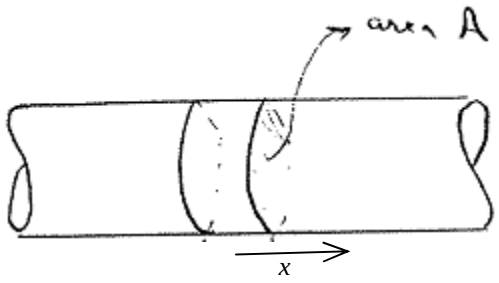

The particular solution to this mathematical problem is

$$C(x,t) = \frac{n/A}{\sqrt{4\pi Dt}}\exp\left(-\frac{x^2}{4Dt}\right)$$

Comparing this result to (11), we see that the two results have the same dependence on x and t. Indeed the two equations are identical if we make the following substitutions:

$$D = \frac{l^2}{2\tau} \qquad (14)$$

and $\qquad p(x,t) = \frac{C(x,t)}{n/A}$

Moreover, substituting (14) into (12) yields (6):

$$\langle x^2 \rangle = 2Dt \qquad (6)$$

for Brownian motion in 1-D. The same result applies to the other two dimensions:

$$\langle x^2 \rangle = \langle y^2 \rangle = \langle z^2 \rangle = 2Dt$$

The corollaries for 2-D and 3-D are

$$\langle r^2 \rangle = \langle x^2 + y^2 \rangle = 4Dt$$

$$\langle r^2 \rangle = \langle x^2 + y^2 + z^2 \rangle = 6Dt$$

whose proof will be left for a homework.

♦ $\delta(x)$ is called the "delta function" and it's defined such that for any continuous function $F(x)$, the following relationship holds:

$$\int_{-\infty}^{+\infty} F(x)\delta(x - x_0)\,dx \equiv F(x_0)$$

Lecture #4 begins here

Sedimentation

Reading: Hiemenz §§2.2-2.3

We have just seen how tracking the Brownian motion of single colloidal particles with the aid of a microscope can allow us to measure the diffusion coefficient *D*. Einstein went on to use *D* to calculate Avogadro's number N_A from

$$N_A = \frac{R_{gas}T}{Df} \tag{15}$$

where R_{gas} = 8.31 J mol^{-1} ^{o}K^{-1} is the universal gas constant, T is absolute temperature and f is the friction coefficient of the same particle having diffusion coefficient D. So what's this friction coefficient? and what's the basis for the equation above? Why does the gas constant appear when we are not dealing with a gas?

The Friction Coefficient

Suppose we apply a force $\mathbf{F}_{\text{app}}$ to a colloidal particle initially at rest. The force causes the particle to accelerate in the direction of the applied force. Once it begins to move through the fluid, the particle also experiences a drag force, which can be predicted from Stokes formula:

$$\mathbf{F}_{drag} = -\underbrace{6\pi\eta R}_{f}\mathbf{v} \tag{16}$$

for spheres of radius R in a fluid having viscosity η. Notice that this force acts in the direction opposing the velocity **v**. A similar relationship applies for nonspherical particles, where the proportionality constant multiplying –**v** is call the ***friction coefficient*** *f*. The drag force offsets some of the applied force so that the sphere then accelerates more slowly until it reaches its final or terminal velocity $\mathbf{v}_\infty$ at which the drag force is equal to the applied force but acts in the opposite direction:

$$-\mathbf{F}_{drag} = \underbrace{6\pi\eta R}_{f}\mathbf{v}_\infty = \mathbf{F}_{app}$$

Solving for the terminal velocity:

$$\mathbf{v}_\infty = \frac{1}{f}\mathbf{F}_{app} \tag{17}$$

where the new proportionality constant $(1/f)$ is called the ***hydrodynamic mobility***.

While the nature (gravity, electrical etc.) of $\mathbf{F}_{\text{app}}$ is not important, the most common force is gravity. For a sphere of density ρ_s immersed in a fluid of density ρ_f, the gravitation force acting on the sphere is the difference between its weight and the weight of the fluid displaced by it (Archimedes law):

$$\mathbf{F}_{app} = \mathbf{F}_{grav} = \tfrac{4}{3}\pi R^3\left(\rho_s - \rho_f\right)\mathbf{g} \tag{18}$$

where **g** is the acceleration of gravity, a vector pointing to the center of the earth and having magnitude of 9.81 m/sec^2.

Sedimentation Equilibrium: Analysis #1

Reading: Hiemenz §2.8

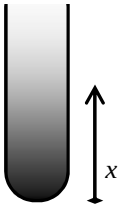

Eq. (15) results from comparing two independent approaches to describing sedimentation equilibrium. The first approach is via mass transfer. Suppose we disperse N identical colloidal particles in a test tube of cross-sectional area A and allow them to sediment for a long time. As soon as their concentration begins to build up near the bottom of the test tube, diffusion will occur which opposes further sedimentation. Eventually an equilibrium concentration profile is establishes such that the downward sedimentation rate is exactly balanced by upward diffusion at every point in the test tube:

$$\underbrace{\underbrace{-\frac{F_{grav}}{f}}_{v_x}C}_{\text{sedimentation}} \underbrace{-D\frac{dC}{dx}}_{\text{diffusion}} = 0 \tag{19}$$

The shape of concentration profile can be obtained by integrating this equation

$$C(x) = A\exp\left(-\frac{F_{grav}}{Df}x\right) \tag{20}$$

where A is some integration constant chosen so that the total number of particles equals what was added initially

$$\int_{x_{bot}}^{x_{top}} C(x)\,dx = \frac{N}{A}$$

Although easily calculated, the exact value of A is not important to the current problem.

Lecture #5 begins here

Sedimentation Equilibrium: Analysis #2

The second approach to predicting sedimentation equilibrium is via thermodynamics. Recall that a given chemical component *i* of a mixture distributes itself between phases such that at equilibrium:

$$\mu_i \text{ in phase \#1} = \mu_i \text{ in phase \#2}$$

where μ_i is called the ***chemical potential*** of component *i*. Within a given phase, each component will distribute itself such that its chemical potential is the same at each point, or

$$\nabla \mu_i = \mathbf{0} \quad \text{or} \quad \mu_i = \text{const}$$

For an ***ideal solution***, the chemical potential is calculated using

$$\left(d\mu_i\right)_{T,P} = R_{gas}T \; d\ln C_i \tag{21}$$

For components which experience an interaction force from a source outside the system, we need to modify the criteria for phase equilibrium:

$$\mu_i + \Phi_i \text{ in phase \#1} = \mu_i + \Phi_i \text{ in phase \#2}$$

where Φ_i is the potential energy of component *i* arising from that force. Within a given phase, each component will now distribute itself such that the sum of its chemical potential and the potential energy is the same at each point, or

$$\nabla\left(\mu_i + \Phi_i\right) = \mathbf{0} \quad \text{or} \quad \mu_i + \Phi_i = \text{const}$$

For colloidal particles in our test tube, which experience a gravitational force given by (18), their potential energy can be calculated from

$$\Phi_i(x) = N_A F_{grav} x$$

where we have multiplied by Avogadro's number to get the same units of energy per mole of particles as in (21). At equilibrium, thermodynamics requires

$$\frac{d\mu_i}{dx} + \frac{d\Phi_i}{dx} = R_{gas}T\frac{d\ln C}{dx} + N_A F_{grav} = 0$$

Integrating:

$$C(x) = A\exp\left(-\frac{N_A F_{grav}}{R_{gas}T}x\right) \tag{22}$$

Now the exponents in (20) and (22) must be the same, so:

$$\frac{\cancel{F_{grav}}}{Df} = \frac{N_A \cancel{F_{grav}}}{R_{gas}T}$$

Solving this for N_A yields (15):

$$N_A = \frac{R_{gas}T}{Df} \tag{15}$$

Sedimentation Length

Dividing Avogadro's number into the gas constant yields

$$k = \frac{R_{gas}}{N_A} = 1.3805\times10^{-23}\ \frac{\text{J}}{^\circ\text{K}} \tag{23}$$

which is called ***Boltzmann's constant***. kT = 4.11×10^{-21} J (at 25ºC) is the characteristic thermal energy of single molecules or single colloidal particles. (22) can then be re-written as

$$C(x) = A\exp\left(-\frac{F_{grav}x}{kT}\right)$$

Let's define the sedimentation length *l* such that

$$F_{grav}\,l \equiv kT$$

Thus *l* represents the vertical distance over which the particle concentration changes by a factor of $e = 2.71$. It also gives an idea of how thick the sediment layer becomes if the particle concentration remains dilute: say $N/A \to 0$. Because the weight of a particle scales with the cube of its radius, this sedimentation length is quite sensitive to particle size. Consider particles of a hypothetical material having a specific gravity of 2. The sedimentation length for particles of different size are shown in the following table.

$2R$	l
1 mm (sand)	10^{-6} nm (sub-atomic)
0.1 μm (colloid)	1 mm
1 nm (molecule)	1 km

The calculated lengths *l* vary from sub-atomic to a kilometer.

Determining Particle Size from Sedimentation Equilibrium

For some colloidal particles, it is possible to establish sedimentation equilibrium with a dilute

solution and then to measure the concentration profile $C(x)$. Plotting the concentration on semi-log coordinates should yield a straight line:

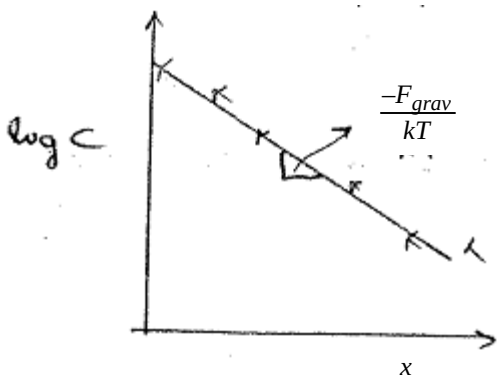

The slope of this line should be negative and its magnitude equals the ratio of the gravitational force to kT:

$$\text{slope} = -\frac{F_{grav}}{kT} = -\frac{1}{l}$$

Since kT is known, F_{grav} can be determined which can then be converted into a particle size R using (18)

$$F_{grav} = \tfrac{4}{3}\pi R^3 \left(\rho_s - \rho_f\right) g \qquad (18)$$

Extension to Nonspherical Particles

For nonspherical particles, the formulas for volume and friction coefficient used above are not valid. Instead, we can write (18) as

$$F_{grav} = V\left(\rho_s - \rho_f\right) g = \underbrace{V\rho_s}_{m}\left(1 - \frac{\rho_f}{\rho_s}\right) g \qquad (24)$$

where m is the mass of one particle. Stokes law can be written as (17):

$$v_\infty = \frac{1}{f} F_{grav} \qquad (17)$$

Combining these two equations yields

$$v_\infty = \frac{m}{f}\left(1 - \frac{\rho_f}{\rho_s}\right) g \qquad (25)$$

Thus by measuring the terminal sedimentation velocity, we can infer the ratio m/f.

Centrifugal Sedimentation

Reading: Hiemenz §2.4.

For small particles, the gravitational sedimentation length might be too large to be measured. In this case, we might measure the concentration profile caused by centrifugal forces rather than gravity.

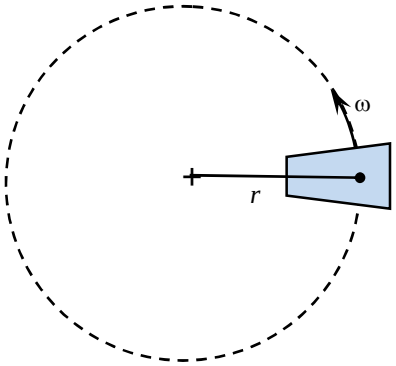

A centrifuge is a device in which a sample is rotated in a plane around some axis. If the distance of the sample from the axis of rotation is r and the rotation rate is ω (radians per time), then the centrifugal acceleration is

$$g_{centrifuge} = r\omega^2$$

Subsituting this quantity for g in (18) yields the centrifugal force on particles:

$$F_{centrifugal} = \tfrac{4}{3}\pi R^3 \left(\rho_s - \rho_f\right) r\omega^2 \qquad (26)$$

Today's ultracentrifuges (the size of a washing machine) are capable of accelerations up to 10^6 g which greatly extends downward the range of particle sizes which can be measured.

Experiments either measure $C(r)$ for sedimentation equilibrium or the terminal velocity generated by the centrifugal force. Case 1) If the sample size Δr is very small compared to r, centrifugal sedimentation equilibrium is analyzed by plotting $C(r)$ on semi-log coordinates and the slope of the straight line is converted to size using the analog of (18) or (24) with the g replaced by $r\omega^2$.

Case 2) If the sample size Δr is not negligibly small compared to r, then a plot of ln $C(r)$ vs r will be curved downward. The analysis leading to the mass of the particles will now be more complicated and is left for a homework assignment.

Sedimentation rate of small molecules in an ultracentrifuge is often analyzed by imaging the concentration profile though a ***Schlieren lens***, which reveals gradients in the refractive index of the solution. When the concentration of solute varies with position, so does the index of refraction, thus creating a gradient in refractive index.

In fig. (a) below, we see the evolution of the concentration profile with time (the four curves). As sedimentation occurs far from equilibrium, the solution at the top of the sample (small *r*) becomes free of solute; the abrupt increase in concentration marks a "front" between a solute-free solution and the solution bearing solute moves downward (toward larger *r*) at the rate of sedimentation of the molecules.

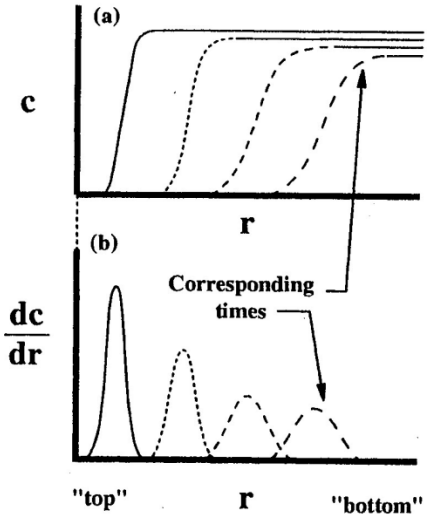

The Schlieren lens images the concentration gradient *dc*/*dr* sketched in (b). An actual Schlieren image from an ultracentrifuge is shown below [taken from Faucher & Koleske, *Science* **147**, 1152 (1965)].

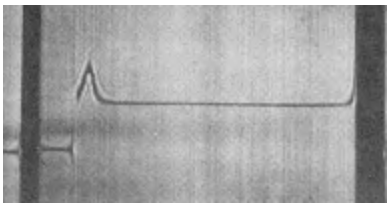

By tracking the speed of the peak, we can infer the sedimentation velocity *dr*/*dt*. The resulting speed is usually reported as the sedimentational coefficient defined by

$$s \equiv \frac{dr/dt}{\omega^2 r} = \frac{1}{\omega^2}\frac{d\ln r}{dt} = \frac{1}{\omega^2}\frac{\ln(r_2/r_1)}{t_2 - t_1} \qquad (27)$$

The units of *s* are sec. In particular

$$10^{-13}\ \text{sec} = 1\ \text{svedberg} = 1\ \text{S}$$

which is named after T. Svedberg who won the Nobel in chemistry the same year as Perrin won the physics prize (1926). Replacing v_∞ in (25) by *dr*/*dt* and *g* by $r\omega^2$, we obtain

$$\frac{dr}{dt} = \frac{m}{f}\left(1 - \frac{\rho_f}{\rho_s}\right) r\omega^2 \qquad (28)$$

or

$$s = \frac{dr/dt}{r\omega^2} = \frac{m}{f}\left(1 - \frac{\rho_f}{\rho_s}\right) \qquad (29)$$

Notice that, even if *r* varies significantly across the cell, the value of *s* should be independent of *r* and can be calculated from the displacement of the Schieren peaks using (27) and translated into *m*/*f* using the equation above.

Example: Prob. 2 from Hiemenz, Chapt. 2

Solution: The problem statement provides *C* vs *r* for sedimentation equilibrium at 25ºC in a centrifuge rotating at 12,590 rpm. Centrifugal sedimentation differs from gravitation sedimentation in that the force depends on position.

Replacing $v_x = F_{grav}/f$ in (19) by *dr*/*dt* in (28) and *dC*/*dx* by *dC*/*dr*:

$$\frac{m}{f}\left(1 - \frac{\rho_f}{\rho_s}\right) r\omega^2 C - D\frac{dC}{dr} = 0$$

which is a first-order separable ODE. Separating yields

$$\frac{dC}{C} = \frac{m}{Df}\left(1 - \frac{\rho_f}{\rho_s}\right)\omega^2 r\, dr$$

Integration yields

$$\ln C(r) = \tfrac{1}{2}\frac{m}{Df}\left(1 - \frac{\rho_f}{\rho_s}\right)\omega^2 r^2 + \text{const}$$

Using (15) and (23):

$$Df = kT$$

and the concentration profile becomes

$$\ln C(r) = \underbrace{\frac{m\omega^2}{2kT}\left(1 - \frac{\rho_f}{\rho_s}\right)}_{\text{slope}} r^2 + \text{const}$$

So a plot of ln*C* vs r^2 should be linear. The data given yields

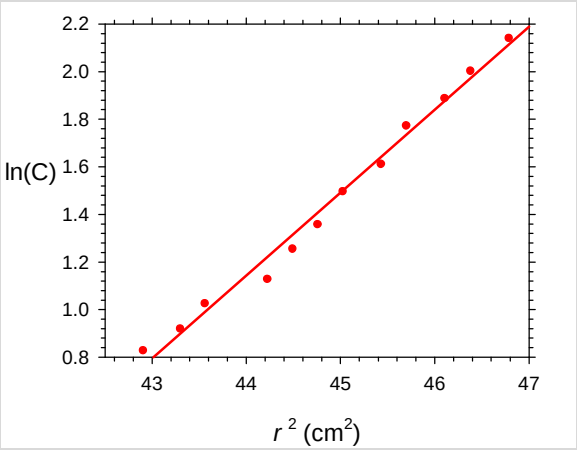

The line is a best-fit linear regression having the following slope:

$$\text{slope} = \frac{m\omega^2}{2kT}\left(1-\frac{\rho_f}{\rho_s}\right) = 0.349 \text{ cm}^{-2} \qquad (30)$$

Some of these quantities can be calculated from the info given in the problem statement:

$$\omega = \frac{12,590 \text{ rev}}{\text{min}} 2\pi \frac{\text{radians}}{\text{rev}} = 1.318\times10^3 \text{ sec}^{-1}$$

$$kT = \left(1.3807\times10^{-23}\frac{\text{J}}{^\circ K}\right)(298^\circ K) = 4.11\times10^{-21} \text{ J}$$

We are told the protein has a density of 1.370 gm/cm^3. So

$$1-\frac{\rho_f}{\rho_s} = 1-\frac{1}{1.370} = 0.270$$

Solving (30) for the apparent mass m of one molecule:

$$m = 6.11\times10^{-20} \text{gm}$$

Avogadro's number of these molecules equals the apparent molecular weight of the protein:

$$M = 6.02\times10^{23} m = 3.68\times10^4 \frac{\text{gm}}{\text{mol}}$$

Knowing the mass and density of one sphere allows us to calculate its apparent radius:

$$R_0 = \left(\frac{3m}{4\pi\rho_s}\right)^{1/3} = 2.20 \text{ nm}$$

and apparent friction coefficient:

$$f_0 = 6\pi\eta R_0 = 3.69\times10^{-8}\frac{\text{gm}}{\text{sec}}$$

where we have substituted a viscosity of $\eta = 8.9\times10^{-4}$ Pa-sec (0.89 cp) at 25ºC.

Question 2a) asks whether the sample appears to be monodisperse (i.e. one size). The first three points of the graph above appear to have a different slope from the remaining points and in Hiemenz's solution he expects you to follow up on this. Below are shown separate regressions for the two sets of points:

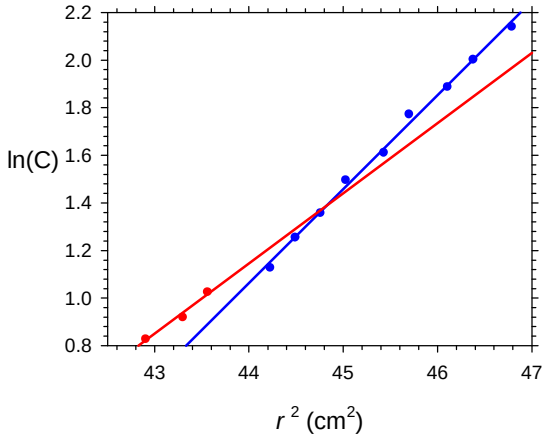

While you might be able to make a case for two sizes, that case is not compelling. The fact that the first "blue" point lies below the red line detracts significantly from the case. If the sample were polydisperse, you would expect the slope to increase monotonically with r. Instead, the slope (of a line drawn) between the 3rd and 4th point actually decreases. Moreover the single regression on the earlier graph is a reasonable fit even for the first three points. Thus I think Hiemenz is trying to read more into this data than can be justified. My experience suggests that a simpler interpretation (i.e. one size) is often more reliable and defensible than the more complex interpretation (i.e. two sizes).

Lecture #6 begins here

Question 2b) states that the sedimentation coefficient s of this sample is known to be 2.7 S and asks for the (true) value of the friction coefficient f. Once the mass m is known from sedimentation equilibrium, the friction coefficient can be deduced by measuring the sedimentation speed. s is defined by (29); solving for f and substituting s = 2.7 S = 2.7×10^{-13} sec:

$$f = \frac{m}{s}\left(1-\frac{\rho_f}{\rho_s}\right) = 6.12\times10^{-8}\frac{\text{gm}}{\text{sec}}$$

and $$\frac{f}{f_0} = 1.66$$

So why is f not equal to f_0? There are two common reasons.

Nonspherical Shape

One reason for the difference is that f_0 was calculated from the mass assuming the particle is a sphere. No such assumption was made in calculating f from the sedimentation coefficient. Nonspherical shape usually increases the friction coefficient for the same volume (or mass) of particle.

Solvation

A second reason is that water molecules can attach themselves to particles or large molecules. This is called hydration (in the case of water) or solvation (in the more general case).

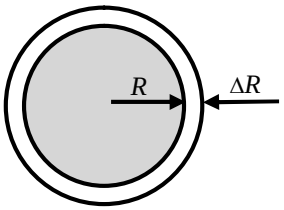

Adding a rigid layer of water on the outside of the sphere would also increase the friction coefficient (by increasing the hydrodynamic radius of the sphere) without changing the net weight of the sphere:

$$F_{grav} = \underbrace{\tfrac{4}{3}\pi R^3 \rho_s}_{\text{solid}} + \underbrace{\tfrac{4}{3}\pi\left[\cancel{\left(R+\Delta R\right)^3} - R^3\right]\rho_f}_{\text{fluid layer}}$$

$$\underbrace{-\tfrac{4}{3}\pi\cancel{\left(R+\Delta R\right)^3}\rho_f}_{\text{displaced fluid}}$$

$$= \tfrac{4}{3}\pi R^3\left(\rho_s - \rho_f\right)$$

net weight is the true weight less weight of displaced water. Attaching a layer of water increases both the true weight and the weight of the displaced water by the same amount, leading to no change in the net weight.

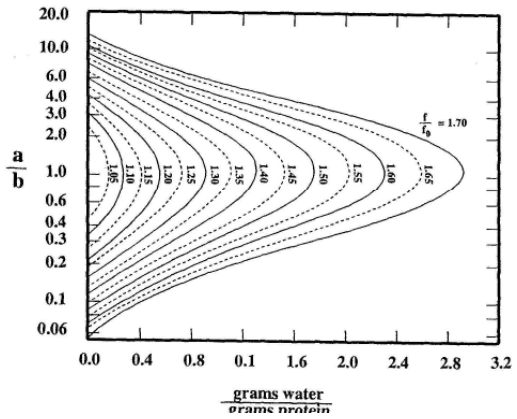

Fig. 2.9 in Hiemenz (above) shows different combinations of these two explanations which can yield a given value for f/f_0. For example, our ratio of 1.66 can be obtained if the particles are ellipsoids having an axis ratio of 12:1 (prolate) or 0.07:1 (oblate); or spheres could yield this f/f_0 if 2.7 grams of water is bound to every gram of anhydrous solid.

Light Scattering

Now we are going to examine the scattering of light by small particles. Static light scattering is widely used to size colloidal particles. Dynamic light scattering is used both for size determination and charge determination.

Nature of Light

Light consists of electric and magnetic fields which oscillate with time at a frequency on the order of 10^{15} sec^{-1}; these fields also oscillate with position. Visible light has a period in the oscillation with position on the order of 0.5 μm which is in the middle of the colloidal size range. These electric and magnetic fields are governed by Maxwell's equations:

Coulomb's law: $\nabla\cdot\mathbf{D} = \rho_e$

Ampere's law: $\nabla\times\mathbf{H} = \boxed{\frac{\partial\mathbf{D}}{\partial t}} + \mathbf{j}$

Faraday's law: $\nabla\times\mathbf{E} = -\frac{\partial\mathbf{B}}{\partial t}$

$$\nabla\cdot\mathbf{B} = 0$$

Maxwell's equations are for light what conservation of momentum, energy and mass are for transport phenomena: they govern all behavior of these quantities. The symbols appearing in these equations have the following names and units:

Symbol	Name	Units
ρ_e	space charge density	coul m^{-3}
j	electric current density	coul s^{-1} m^{-2}
E	electric field intensity	volt m^{-1}
H	magnetic field intensity	amp turn m^{-1}
D	electric displacement	coul m^{-2}
B	magnetic induction	weber m^{-2} = volt s m^{-2}

Regarding the propagation of light in vacuum, air or other simple dielectrics, we can take the charge ρ_e and current **j** to be zero. We need to supplement Maxwell's equations with constitutive equations: a statement of how matter responds to oscillating electric and magnetic fields.

Some examples of constitutive equations in mechanics include Hooke's law (for how an elastic solid responds to stress) or Newton's law of viscosity (for how a viscous fluid responds to stress). The electromagnetic constitutive equations for an isotropic material are:

$\mathbf{D} = \varepsilon\mathbf{E}$, $\varepsilon(\omega)$ = electric permittivity
$\mathbf{B} = \mu\mathbf{H}$, $\mu(\omega)$ = magnetic permeability

Just as Newton's law of viscosity is a linear relation between stress and rate of deformation, these constitutive relations also describe a linear response. ε and μ represent physical properties of the material, which happen to depend on the frequency of the oscillations.

For propagation of light through a dielectric, Maxwell's equation can be combined to obtain

$$\nabla^2\mathbf{E} = \underbrace{\mu\varepsilon}_{1/c^2}\frac{\partial^2\mathbf{E}}{\partial^2 t} \qquad (31)$$

which is the familiar ***wave equation***. From our previous experience with wave equations, we know that the coefficient με is related to the speed of propagation; in particular, the coefficient of the time-derivative is $1/c^2$, so

$$c = \frac{1}{\sqrt{\mu\varepsilon}} = \text{speed of wave propagation} \qquad (32)$$

One particular solution of the wave equation is a ***linearly polarized plane wave***

$$\mathbf{E}(\mathbf{r},t) = \mathbf{E}_0\exp\left[i\left(\omega t - \mathbf{k}\cdot\mathbf{r}\right)\right] \qquad (33)$$

where $i = \sqrt{-1}$ and **k** is a vector pointing in the direction of propagation of the wave with magnitude

$$k = \frac{\omega}{c} = \frac{2\pi}{\lambda}$$

where λ is the wavelength. It is customary to use the complex exponential to describe the oscillating time and position dependence rather than sines and cosines because differentiating with respect to time or position is easier. For example, taking the curl of (33) we get

$$\nabla\times\mathbf{E} = -i\mathbf{k}\times\mathbf{E}$$

and taking the partial time derivative, we get

$$\frac{\partial\mathbf{E}}{\partial t} = i\omega\mathbf{E}$$

Thus both differentiation opererations a replaced by a simpler multiplication. The appearance of *i* in expression (33) makes it mathematically complex. To convert between the complex exponential and

sines and cosines, recall Euler's formula for complex numbers

$$e^{iz} = \cos z + i \sin z$$

Introduction of physically extraneous imaginary values is a mathematical convenience. The general idea is to replace cosz by e^{iz} (which introduces an extraneous *i*sinz), then perform operations like differentiation and drop the extraneous imaginary part in the final answer.

A linearly polarized plane wave is the kind of light produced by a simple HeNe laser such as a laser pointer. If desired, we could also calculate the magnetic field **H** for a linearly polarized plane wave, which is given by

$$\mathbf{H}(\mathbf{r},t) = \frac{\mathbf{k}\times\mathbf{E}(\mathbf{r},t)}{\omega\mu} = \frac{1}{\mu\omega}\mathbf{k}\times\mathbf{E}_0 \exp\left[i\left(\omega t - \mathbf{k}\cdot\mathbf{r}\right)\right]$$

It turns out that **E**, **H** and **k** are mutually orthogonal vectors.

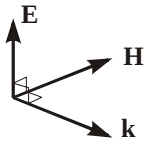

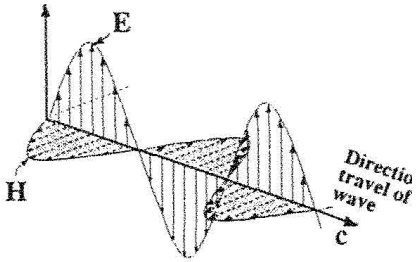

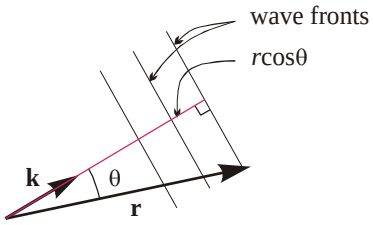

(33) is called a ***plane wave*** because, at a particular *t*, the surfaces of constant **E** are planes; in particular, surfaces having **E** = $\mathbf{E}_0$ are ***wave fronts***. For plane waves, these fronts are planar and the planes are orthogonal to the ***wave vector*** **k** and are spaced a wavelength apart. To see this, note that

$$\mathbf{k}\cdot\mathbf{r} = kr\cos\theta$$

Consider a plane which is orthogonal to **k**. All points **r** on this plane have the same value for *r*cosθ (and that value is the length of the red line in the figure above): as θ increases, *r* increases but cosθ decreases in such a way that their product remains constant. Since **k**·**r** = const on this plane, so is **E**.

The intensity of light is also the flux of energy carried by the wave:

$$\Pi(\mathbf{r},t) \equiv \mathbf{E}\times\mathbf{H} = \frac{1}{\mu\omega}E_0^2\mathbf{k}\cos^2\left(\omega t - \mathbf{k}\cdot\mathbf{r}\right)$$

Averaging over either one cycle of time or over one wavelength yields

$$\langle\Pi\rangle = \frac{1}{2\pi/\omega}\int_0^{2\pi/\omega}\Pi(t)\,dt = \frac{1}{2\mu\omega}E_0^2\mathbf{k} \;[=]\frac{\text{J}}{\text{m}^2-\text{sec}} \quad (34)$$

Atomic Polarization

Reading: Hiemenz §5.2

Perhaps the simplest problem to consider is the scattering by a single hydrogen atom in a vacuum.

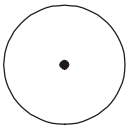

no applied electric field

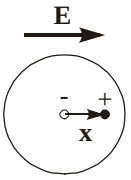

We can think of a hydrogen atom as a proton surrounded by a spherical cloud of negative charge of equal magnitude. In the absence of any applied electric field, the center of negative charge coincides with the center of positive charge.

When a static electric field is applied, the positive nucleus is pulled in direction of the electric field, while the oppositely charged cloud is pulled in the opposite direction. A displacement between the centers of positive and negative charge occurs. The result is that a ***dipole moment*** has been induced in the atom. If **x** is the vectorial displacement between the centers of positive and negative charge, and *e* is the quantity of charge (in this case, its the elemental charge on one proton), then the induced dipole is

$$\mathbf{p} \equiv e\mathbf{x}$$

Lecture #7 begins here

The magnitude of this dipole is zero when *E* is zero and increases linearly as *E* increases. The direction of **p** is parallel to the direction of **E**:

$$\mathbf{p} = \alpha\mathbf{E} \quad (35)$$

where α is a material property called the ***molecular polarizability***. Thus, even molecules which do not possess a permanent dipole moment acquire a dipole moment throught the shift in their electron cloud by the applied electric field. The oscillation of this dipole with time (since **E** oscillates with time) is what leads to "scattering" much like the signal from a radio transmitter which uses a dipole antenna.

In the case of a single spherical electron cloud, the polarizability is given by

$$\alpha = 4\pi\varepsilon_0 R^3 \tag{36}$$

where R is the radius of the cloud and

$$\varepsilon_0 = 8.854\times10^{-12}\ \frac{\text{Coul}^2}{\text{N-m}^2}$$

is the permittivity of vacuum, which is the proportionality constant in ***Coulomb's law***:

$$F = \frac{1}{4\pi\varepsilon_0}\frac{q_1 q_2}{R^2}$$

For charges in media other than vacuum, ε_0 in Coulimb's law is replaced by the permittivity for that media ε. ε is also related to the speed of light: see (32). The ratio of the speed of light in vacuum c_0 to the speed of light in some other medium c is defined as the refractive index of the material

$$n \equiv \frac{c_0}{c} = \frac{\sqrt{\mu\varepsilon}}{\sqrt{\mu_0\varepsilon_0}} = \sqrt{\frac{\varepsilon}{\varepsilon_0}} \tag{37}$$

Most transparent media have the same value of magnetic permeability μ so this property cancels out.

Now ε is a property of a continuum whereas α in (36) is a property of single molecules or atoms. The two properties are related by the ***Clausius-Mosotti equation*** (also called the Lorentz-Lorenz formula):

$$\alpha = \frac{3\varepsilon_0}{N}\frac{\varepsilon-\varepsilon_0}{\varepsilon+2\varepsilon_0} = \frac{3\varepsilon_0}{N}\frac{n^2-1}{n^2+2} \tag{38}$$

where N is the number of molecules per unit volume; the second relation results from substitutuing (37). For dilute gases, n is only slightly larger than unity (e.g. air at STP has n = 1.0003). Then we can approximate

gases: $$\alpha = \frac{3\varepsilon_0}{N}\frac{n^2-1}{n^2+2} \approx \frac{2\varepsilon_0}{N}(n-1) \tag{39}$$

Radiation from an Oscillating Point Dipole

Reference: Lipson & Lipson, p80-85, 313-317

Reading: Hiemenz §5.3

We have just seen that electric fields can induce a dipole moment in all material — even if the atoms or molecules do not possess a permanent dipole of their own. Next, we will see that oscillation in this dipole generates electromagnetic radiation in all directions from this oscilling dipole.

Let the induced point dipole oscillate with a frequency ω at the origin of spherical coordinates

at **r** = **0**: $$\mathbf{p} = \mathbf{p}_0\, e^{i\omega t}$$

The particular solution to the wave equation (31) which describes the far-field ($kr \gg 1$) solution to the radiation from the oscillating dipole is

$$\mathbf{E}^{\text{rad}}(\mathbf{r},t) = \frac{k^2}{4\pi\varepsilon_0}\underbrace{(\mathbf{n}\times\mathbf{p}_0)}_{\mathbf{e}_\phi}\times\mathbf{n}\frac{e^{i(\omega t+kr)}}{r} \propto \mathbf{e}_\theta \tag{40}$$

where r is the magnitude of the position vector **r** and **n** is a unit vector in the direction of **r**

$$\mathbf{n} \equiv \frac{\mathbf{r}}{r}$$

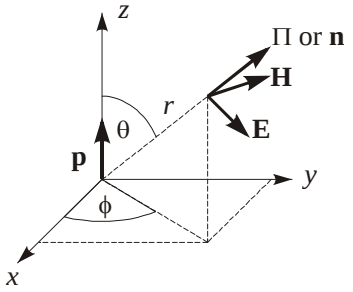

(40) is called a ***spherical wave***. The local energy flux associated with this spherical wave is given by

$$\Pi = \text{Re}\{\mathbf{E}\}\times\text{Re}\{\mathbf{H}\} = \frac{k^4 p_0^2 c\sin^2\theta}{16\pi^2\varepsilon_0}\frac{\sin^2(\omega t-kr)}{r^2}\mathbf{n} \tag{41}$$

The total power emanating from this point can be calculated by integrating the flux over any closed surface containing the oscillating dipole, and then averaging the result over one period of the oscillations:

$$\langle P\rangle = \frac{k^4 p_0^2 c}{12\pi\varepsilon_0} \underset{k=2\pi/\lambda}{=} \frac{4\pi^3 p_0^2 c}{3\varepsilon_0\lambda^4} \propto \lambda^{-4} \tag{42}$$

Note the sensitivity to the wavelength of the incident light, whose frequency and speed of propagation are the same as the scattered light. Visible light varies in wavelength from about

violet or blue: $\lambda = 400$ nm

red: $\lambda = 700$ nm

$$\frac{\langle P\rangle_{red}}{\langle P\rangle_{blue}} = \left(\frac{700}{400}\right)^{-4} = 0.11$$

Clearly red light has a longer wavelength and scatters much less light then does blue:

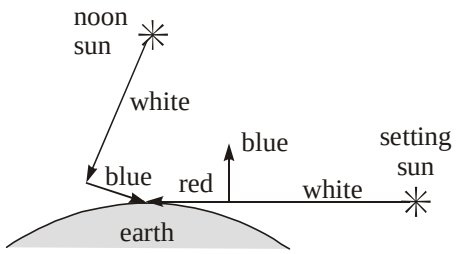

This is why the daytime sky appears blue and sunsets (and sunrises) appear red. During daytime, we don't look directly at the sun, but at white light which is scattered off of molecules of air and water in the atmosphere. Since the blue portion of the spectrum is scattered more intensely, the sky appears blue. On the other hand, at sunset we are looking almost directly at the sun. So we see the light which has not been scattered away. Thus the setting sun appears red.

The amplitude of the oscillating dipole is proportional to the strength of the electric field of the incident light according to (35) and the proportionality constant is given by (36). This links the scattered intensity given by (41) (averaged over one cycle) to the incident intensity given by (34). Their ratio is dimensionless

$$\frac{i}{I_0} \equiv \frac{\left\langle \Pi_r^{sca} \right\rangle}{\left\langle \Pi_x^{inc} \right\rangle} = \frac{\pi^2 \alpha^2}{2\varepsilon_0^2 \lambda^4 r^2} \sin^2\theta \qquad (43)$$

Scattering from Small Particles: Rayleigh Scattering

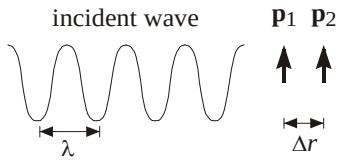

(41) represents the energy flux radiating from a single H atom or other fluctuating dipole. Suppose instead of one, we have two H atoms close enough together that they see the same incident electic field so that the two induced dipole oscillate in unison. Generally, this requires that the distance separating them is very small compared to the wavelength of the incident light.

$$\Delta r << \lambda \qquad (44)$$

Then the net dipole induced is just twice what it would have been if only one H atom had been present. Similarly, if you had a cluster of *m* atoms very close together, they would generate a dipole moment *m* times as large as one.

Suppose we have particles of one phase dispersed in a second phase. The analog of (36) can be deduced by calculating the apparent dipole moment induced in a spherical particle of radius *R* and permittivity ε_s by a uniform electric field externally applied in the surrounding phase (e.g. water) having permittivity ε_f. Assuming both phases are dielectrics the result turns out to be

$$\alpha_{particle} = \underbrace{4\pi\varepsilon_f R^3}_{3V\varepsilon_f} \frac{\varepsilon_s - \varepsilon_f}{\varepsilon_s + 2\varepsilon_f} \qquad (45)$$

The important result is that the polarizability of small particles is proportional to their volume. While this was also true of (36), the proportionality constant is different. This difference arises because the electron cloud of an H atom was treated as a good conductor whereas the particles (and the surrounding fluid) are treated as insulators. In particular, different electrical properties show up in the derivations (left for a Hwk problem). Finally the analog of requirement (44) is

$$R << \lambda$$

Scattering from Dilute Gases

Now (43) gives the scattering from a single atom or molecule. For a dilute gas, the gas molecules will be far enough apart to be considered as independent scatterers; then the scattering from a sample volume is obtained from (43) by multiplying by the number of scatterers inside the sample volume. Multiplying (43) by *N* molecules per unit volume and substituting α from (39) we obtain

gases: $$\frac{i_s}{I_0} = \frac{i}{I_0} N = \frac{2\pi^2 (n-1)^2}{\lambda^4 r^2 N} \sin^2\theta$$

gives the dimensionless scattering intensity per unit sample volume.

Scattering from Liquid Solutions

For condensed phases like liquids, the molecules are too close together to behave like independent

scatters. Instead, for every molecule whose dipole oscillates with a particular phase there is another molecule which oscillates 180º out of phase causing destructive interference in the total scattering. A perfectly uniform pure liquid then scatters no light. Nonetheless experiments do reveal some scattering from pure liquids. Scattering is caused by inhomogeneities in the local density of the liquid caused by thermal agitation.

Solutions having a solute dissolved in the liquid also scatter some light. Some of this scattering comes from density fluctuations in the pure liquid and some comes from fluctuations in the concentration of solute. The theory is quite involved and goes beyond the scope of this course. We will just give the final result:

$$\frac{i_s}{I_0} = \frac{2\pi^2 \left[n\left(dn/dC\right)\right]^2 kTC}{\lambda^4 r^2 \left(\partial \pi_{osm}/\partial C\right)} \sin^2 \theta$$

where π_{osm} and n is the osmotic pressure and refractive index of the solution having mass concentration C of solute. At infinite dilution, all solutions behave ideally and the osmotic pressure is given by van't Hoff's law (see Hiemenz §3.2):

$$\pi_{osm} = \frac{RT}{M} C$$

where M is the molecular weight of the solute. At higher concentrations, the osmotic pressure becomes a Taylor series expansion in the concentration, which is called a virial expansion. At low concentrations, we can truncate after the second term, leaving

$$\pi_{osm} = RT\left(\frac{C}{M} + BC^2\right)$$

where B is called the 2nd virial coefficient which contains information of the intermolecular interaction between solute molecues. Using this second expression for the osmotic pressure, the scattering becomes

$$\frac{i_s}{I_0} = \frac{KC}{1/M + 2BC} \frac{\sin^2 \theta}{r^2} \qquad (46)$$

where $$K \equiv \frac{2\pi^2 \left[n\left(dn/dC\right)\right]^2}{N_A \lambda^4}$$

In the limit of zero concentration of solute C, the scattering goes to zero as expected.

Lecture #8 begins here

Static Light Scattering Experiments: Turbidity

One type of experiment is to measure the intensity of light transmitted through the sample I_t relative to the intensity of incident light I_0.

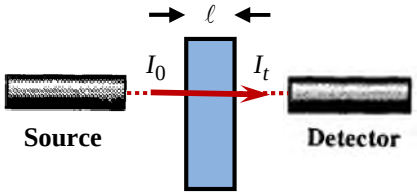

Sample

Generally, the amount of light transmitted will be less than that incident for two reasons: 1) some of the light might be absorbed by molecules in the sample or 2) light might be scattered by the sample. We will assume that no light is absorbed. Then

$$I_t = I_0 - I_s$$

where I_s is the amount scattered. Owing to scattering the intensity of light monotonically decays with distance x travelled through the sample. Consider the change in intensity across a slice of sample dx which is thin enough so that the intensity changes by a negligibly small amount

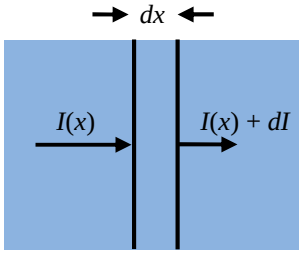

The change in intensity dI is expected to be negative and amount of the decrease is expected to be proportional to the intensity $I(x)$ itself and to the number of scatterers in the slice; the latter is expected to proportional to the volume or thickness of the slice:

$$dI = -\tau\, I(x)\, dx$$

where the proportionality constant is called the ***turbidity***. Integrating across the full pathlength of the sample:

$$I\left(x\right) = I_0 e^{-\tau x}$$

In particular $I_t \equiv I(\ell) = I_0 e^{-\tau\ell}$

Solving for τ:

$$\tau = \frac{1}{\ell}\ln\frac{I_0}{I_t} = \frac{1}{\ell}\ln\frac{I_0}{I_0 - I_s}$$

which is the analog of ***Beer's law*** for the specific absorption coefficient (except that the decrease in intensity here is due to turbidity – not absorption). In most scattering experiments, the fraction change in intensity is very small, then the logarithm function can be replaced by a one-term Taylor series approximation:

$$\tau \approx \frac{I_s}{\ell I_0} \quad \text{for} \quad \frac{I_s}{I_0} \ll 1$$

Next we calculate I_s from a surface integral of i_s over a sphere of radius r :

$$\tau \approx \frac{I_s}{\ell I_0} = \int_0^{2\pi} d\phi \int_0^{\pi} \frac{i_s}{I_0} r^2 \sin\theta \, d\theta$$

where θ and φ are the two angles in spherical coordinates. The ratio of intensities calculated above is called the ***turbidity***. When the scattering is given by (46), the turbidity becomes

$$\tau = \frac{16\pi KC}{3\left(1/M + 2BC\right)} \tag{47}$$

Two types of experiments can be performed.

Expt. #1) Measure τ vs. λ. If a spectrophotometer is used, we can vary the wavelength of the incident light. Our theory is based on turbidity being caused by scattering. Then

$$\tau \propto \lambda^{-4}$$

Then a plot of log τ versus log λ should be linear with a slope of –4. Obtaining this result is strong confirmation that turbidity is due to scattering. The other major source of turbidity is absorbance of light by the sample. But absorbance typically displays non-monotonic behavior with wavelength: peaks of turbidity occur at specific wavelengths at which absorbance takes place.

Expt. #2) Measure τ vs. *C*. If our solute is a polymer of unknown molecule weight *M*, this data will allow us to determine *M*. The equations above express concentration *C* in mass per volume, which can be determined without knowing the molecular weight. (47) can be rearranged to yield a straight line in its dependence on *C*:

$$\frac{HC}{\tau} = \frac{1}{M} + 2BC \tag{48}$$

where $H \equiv \frac{16\pi K}{3} = \frac{32\pi^3\left[n\left(dn/dC\right)\right]^2}{3N_A\lambda^4}$

Below is plotted turbidity data for polystyrene solutions in methylethyl ketone obtained at 25ºC using light having λ = 436 nm. Results for three different fractions (having different molecular weights) are shown:

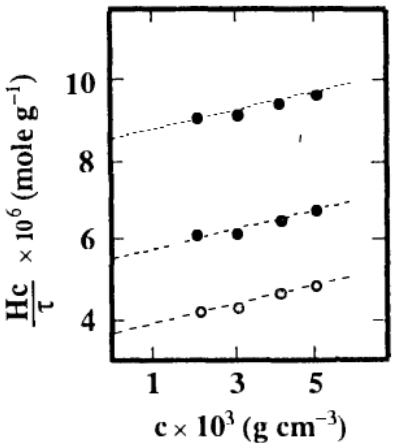

The linearity of the points is consistent with expectations based on (48). This equation suggests that the intercept of the straight lines is the molecular weight of each fraction (116, 180 and 270 kDa) and the slope could also be used to infer *B*.

Polydisperse Samples

Suppose that each fraction is polydisperse. In other words, suppose that in volume *V*, we have n_i moles of polystyrene having molecular weight M_i. What type of average molecular weight is obtained with this turbidity experiment? To answer this question, we assume that each fraction contributes independently of other fractions to the total turbidity and total concentration measured:

$$C_{tot} = \sum_i C_i = \sum_i \frac{n_i M_i}{V} \tag{49}$$

$$\tau_{tot} = \sum_i \tau_i \tag{50}$$

The average molecular weight is defined by the intercept of (48):

$$\frac{HC_{tot}}{\tau_{tot}} = \frac{1}{\overline{M}} \quad \text{and} \quad \overline{M} = \frac{\tau_{tot}}{HC_{tot}} \tag{51}$$

The contribution to turbidity of each fraction can also be calculated from (48):

$$\frac{HC_i}{\tau_i} = \frac{1}{M_i} \quad \text{or} \quad \tau_i = HC_i M_i \qquad (52)$$

Substituting (49), (50) and (52) into (51):

$$\overline{M} = \frac{\tau_{tot}}{HC_{tot}} = \frac{\sum_i \tau_i}{H\sum_i C_i} = \frac{\sum_i HC_i M_i}{H\sum_i \frac{n_i M_i}{V}}$$

$$= \frac{\sum_i \frac{n_i M_i}{V} M_i}{\sum_i \frac{n_i M_i}{V}} = \frac{\sum_i n_i M_i^2}{\sum_i n_i M_i} \equiv M_w$$

Thus the appropriate average is the ***weight-average*** molecular weight of the mixture (since the contribution of each term to the average is weighted by the molecular weight).

Static Light Scattering Experiments: Angle Dependence

Light scattering experiments today typically use a laser as a light source. The sample is held in a 1 cm diameter glass cylinder a few cm long (the small black square in the schematic below). The detector is usually a photomultiplier tube (PMT) which is held by a goniometer, a device which allows the detector to be rotated around a vertical axis through the center of the sample to detect light scattered in various angles relative to the direction of the incident light.

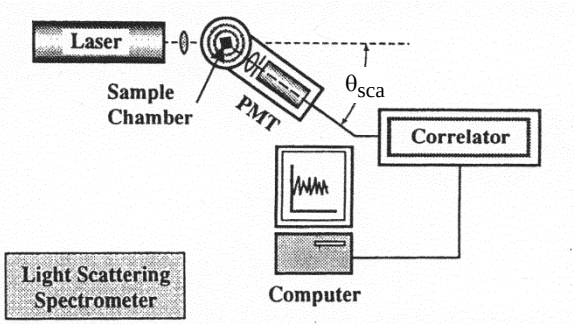

Usually the goniometer rotates in a horizontal plane. This plane contains both the wave vector $\mathbf{k}_{inc}$ for the incident beam as well as the wave vector $\mathbf{k}_{sca}$ for the scattered rays. The plane containing both of these wave vectors is called the ***scattering plane***. The angle between these two vectors is the scattering angle θ_{sca}:

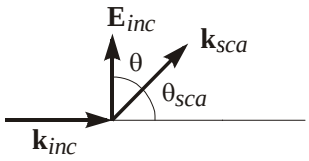

The scattering angle θ_{sca} is not the same as the polar angle in spherical coordinates θ which is the angle measured from the axis aligned with the electric field for the incident light (see sketch on page 20).

The angular dependence of scattering depends on the polarization of the incident light. **Case 1)** If the incident beam is a LPPW with the electric field oriented horizontally (in the scattering plane), then

$$\theta_{sca} = \pi/2 - \theta$$

and (43) predicts that the scattering intensity behaves like

$$\langle \Pi_r \rangle \propto \sin^2\theta = \sin^2\left(\frac{\pi}{2} - \theta_{sca}\right) = \cos^2\theta_{sca} \qquad (53)$$

which is plotted as the red curve in the polar plot below (a figure eight on its side).

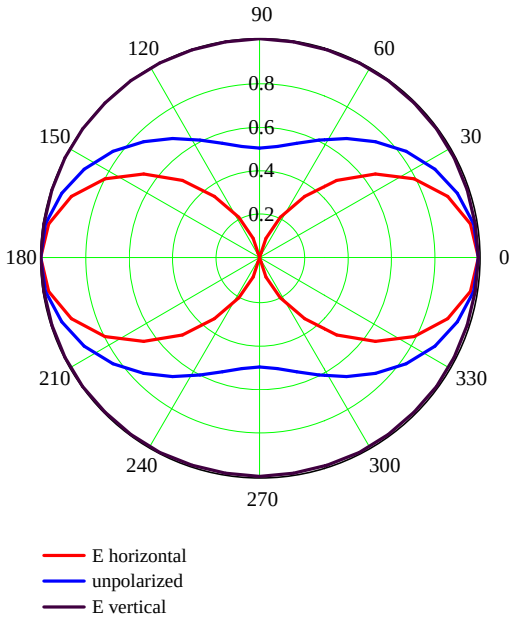

Case 2) On the other hand, if the incident light is polarized such that $\mathbf{E}_{inc}$ is vertical, then the scattering plane coincides with the equatorial plane of the sphere which has $\theta = \pi/2$ for all points. Varying the scattering angle varies the second angle of spherical coordinates (i.e. the azimuthal angle ϕ). If $\theta = \pi/2$ for all scattering angles, then (43) predicts that the scattering intensity behaves like a constant:

$$\langle \Pi_r \rangle \propto \sin^2\theta = \sin^2\left(\frac{\pi}{2}\right) = 1 \qquad (54)$$

which is a constant for different scattering angles (shown as the black circle in the polar plot above).

Case 3) Light from the sun (and most light sources other than lasers) is ***unpolarized***, which means that the electric field of the light is not oriented in a particular direction (except that **E** is always perpendicular to **k** but this still leaves a degree of freedom). Then the angular dependence of scattering turns out to be the arithmetic average of horizontal and vertical polarization [i.e. (53) and (54)]:

$$\langle \Pi_r \rangle \propto \frac{1+\cos^2\theta_{sca}}{2}$$

which is plotted as the blue curve in the figure above.

Scattering from Larger Particles: Rayleigh-Debye Scattering

Reference: van de Hulst, p85f and Kerker, p414.

Reading: Hiemenz §§5.5, 5.6

Rayleigh scattering requires that all the dipoles of each particle must be oscillating in unison. This will be true only if each atom in the particle sees the same electric field. Generally, this requires that the largest dimension of a particle must be very small compared to the wavelength of the incident light:

$$2R < \lambda/20 \qquad (55)$$

Atoms in larger particles are not oscillating in unison. As a result, their scattering intensity does not add linearly as Rayleigh scattering theory assumes.

Rayleigh recognized these effects and took them into account in a series of papers published in 1910, 1914 and 1918. Further contributions were made by Debye in 1915. The basic problem is to compute the total phase difference between radiated light reaching the detector from an arbitrary pair of atoms in the particle. This total phase difference will determine if interference is constructive (as assumed in Rayleigh scattering theory) or destructive, or somewhere in between.

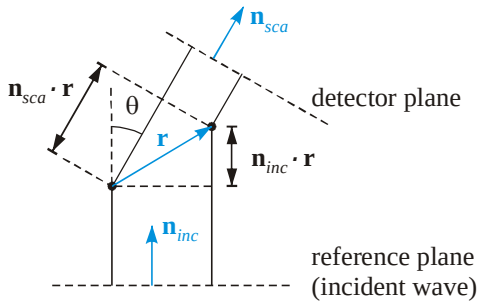

The sketch above shows two arbitrary atoms (the two dots) separated by a vectorial displacement **r**. Also shown are two unit vectors: $\mathbf{n}_{inc}$ denotes the direction of incident LPPW and $\mathbf{n}_{sca}$ denotes the scattering direction. These two vectors also define the plane of scattering.

The dot at the right is further from the incident light source (the reference plane for incident wave) than the dot at the left by a distance $\mathbf{n}_{inc}\cdot\mathbf{r}$. This causes a phase lag (in radians) of

$$\delta_1 = k\mathbf{n}_{inc}\cdot\mathbf{r}$$

where $k = 2\pi/\lambda$ for the incident light. But the same dot is actually closer to the detector plane by a distance $\mathbf{n}_{sca}\cdot\mathbf{r}$. This causes a negative phase lag of

$$\delta_2 = -k\mathbf{n}_{sca}\cdot\mathbf{r}$$

The total phase difference is obtained by adding

$$\delta(\mathbf{r}) \equiv \delta_1 + \delta_2 = k(\mathbf{n}_{inc}-\mathbf{n}_{sca})\cdot\mathbf{r} \qquad (56)$$

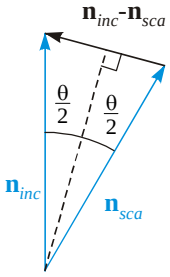

The figure above shows the vector addition (subtraction). From the geometry of the right triangle formed by bisecting the isosceles triangle, we can deduce that the length of the difference vector is

$$\left|\mathbf{n}_{inc}-\mathbf{n}_{sca}\right| = 2\sin\frac{\theta}{2}$$

and so on. Once we have δ, the phase factor is calculated as $e^{i\delta}$. This is then summed over all pairs of atoms in the two bodies:

$$\int_{\mathbf{r}_1} dV \int_{\mathbf{r}_2} dV \left\{ e^{i\delta(\mathbf{r}_1-\mathbf{r}_2)} \right\} = \left| \int e^{i\delta} dV \right|^2$$

To make it dimensionless, we divide by volume squared:

$$P(\theta) = \frac{\left| \int e^{i\delta} dV \right|^2}{V^2} \qquad (57)$$

The result depends on the scattering angle for a particular shape and size of particle representing the region V. This is called the ***form factor***.

Form Factor for Spheres

Rayleigh (1914) worked out the result for a sphere of radius a:

sphere $$P(\theta) = \left[\frac{3}{u^3} (\sin u - u \cos u) \right]^2 \qquad (58)$$

where $$u \equiv 2ka \sin\frac{\theta_{sca}}{2} = \frac{4\pi a}{\lambda} \sin\frac{\theta_{sca}}{2} \qquad (59)$$

Here P is a dimensionless correction factor – not the total power radiating from the scatterer.

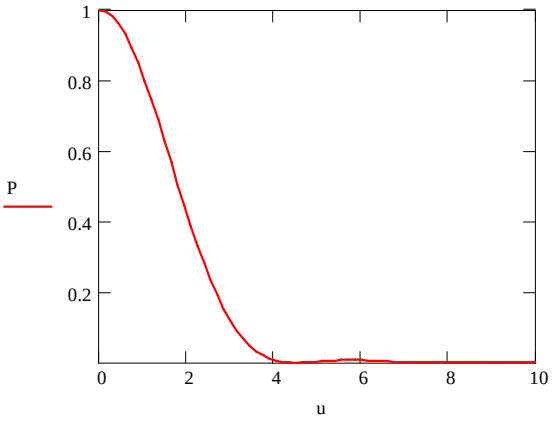

The function $P(u)$ is plotted above. It seems to decay almost monotonically to zero.

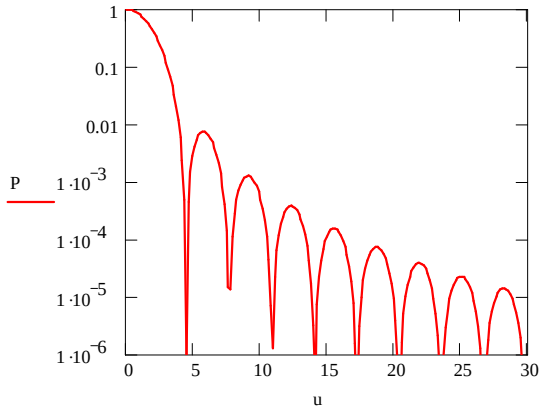

But if we plot the same data on semi-log coordinates (above), we see quite different behavior. Note the appearance of many maxima separated by deep cusps (values of u at which P vanishes). This leads to some complicated scattering patterns when the particle size exceeds a certain value.

Form Factor for Random Coils, Rods, Disks

The form factor for other shapes has also been worked out and the results are shown in the figure below (p433 of Berg):

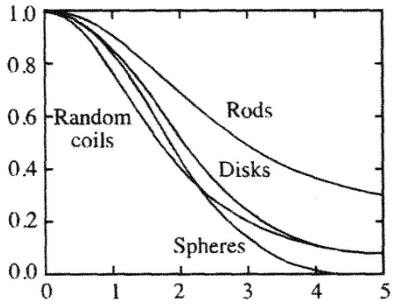

where the x-axis is u defined by (59) except that the sphere radius a is replaced by the disk radius, half the rod length or the radius of gyration of random coils. Note that the functional form of $P(u)$ differs for different shapes.

This form factor is used to correct the angular dependence of simple Rayleigh theory for the effect of interference arising because not all the atoms in a particle are oscillating in unison. For example, scattering from solutions is described by (46) in terms of i_s/I_0.

$$\underbrace{\frac{i_c(\theta_{sca})}{I_0}}_{\text{corrected}} = \underbrace{\frac{i_s(\theta_{sca})}{I_0}}_{\substack{\text{uncorrected} \\ \text{Rayleigh}}} P(\theta_{sca}) \qquad (60)$$

If we are only interested in the scattering relative to that scattered forward in the direction of the incident

light, we could substitute $i_s/I_0 = \cos^2(\theta_{sca})$, which was used for the plots below.

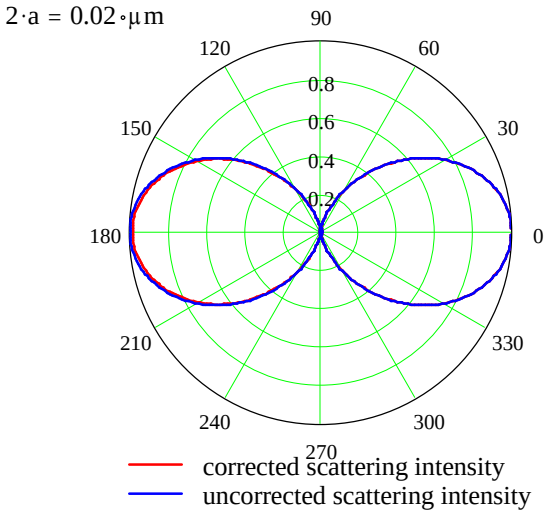

The above polar plot shows the scattering pattern for 20 nm polystyrene (PS) latex spheres (n = 1.67) in water (n = 1.33) when illuminated by a HeNe laser (λ_0 = 623.8 nm in vacuum or $\lambda_1 = \lambda_0/n_1$ = 469 nm in water). These particles are very small compared to the wavelength: 20nm/λ_1 = 0.043. The pattern in red is virtually indistinguishable from $\cos^2(\theta_{sca})$ (given in blue), i.e. the simple Rayleigh theory. Recall from (55) that the simpler Rayleigh theory was valid for particles whose diameter was less than 1/20 = 0.05 of the wavelength.

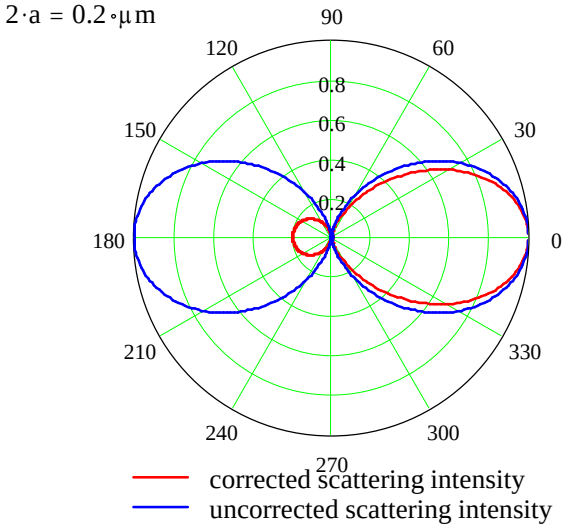

Raising the particle size an order of magnitude to 200 nm (above) causes the backscattering to become significantly weaker than the forward scattering, but even forward scattering is beginning to show some deviation from $\cos^2(\theta_{sca})$.

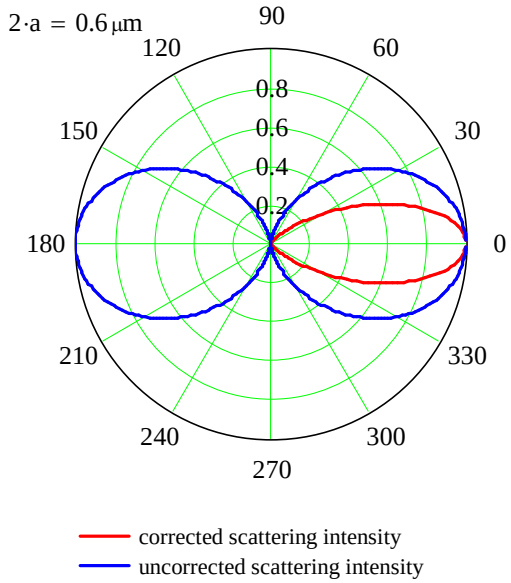

Increasing the particle radius a bit more to 0.6 μm (above), which is just a little larger than the wavelength in water (0.6 μm/λ_1 = 1.3), causes the backscattering pattern to disappear from the figure above left while the forward scattering pattern has become significantly distorted: with scattering falling off more sharply with angle than Rayleigh's simple theory predicts.

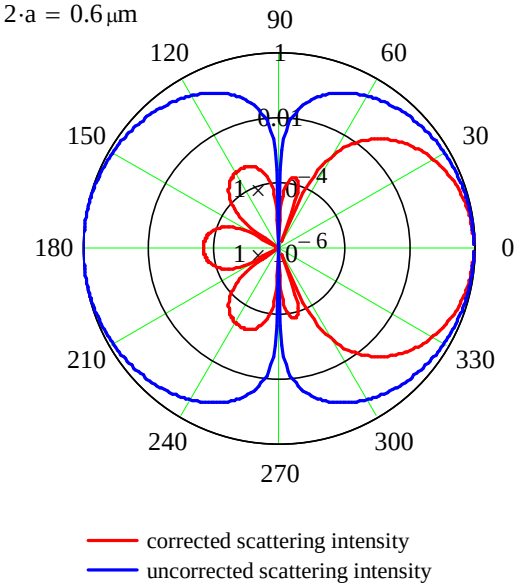

Actually, backscattering has not completely vanished as can be seen in the figure above right in which the radial axis has been made logarithmic.

Lecture #9 begins here

Inferring Size from Angle Dependence

For Rayleigh scatterers, the angular dependence of scattering contains no information on the size of the scatterer. But for particles which are large enough to have a form-factor different from unity, the angular dependence contains information about the size.

For example, the plot below shows the angular dependence of scattering intensity calculated for polystyrene (PS) latex spheres of different size ($2a$ = 0, 0.2, 0.4, 0.6, 0.8 and 1.0 μm) in water. The incident light from a HeNe laser has λ_0 = 515.5 nm in vacuum (or λ = 387.6 nm in water) and is horizontally polarized. Then the uncorrected angular dependence from Rayleigh scattering is $\cos^2(\theta_{sca})$

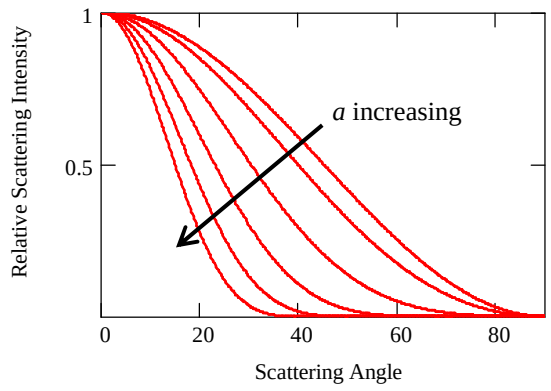

The strong intensity dependence on size has been removed by normalizing the scattering results by the scattering at zero degrees. Nonetheless, you can clearly see that size affects the rate of decay with scattering angle at small angles.

In the limit of small scattering angles, we can approximate the form factor (58) using a Taylor series

$$P(u) = 1 - \tfrac{1}{5}u^2 + O(u^4)$$

Truncating after the u^2 term and substituting u from (59)

$$P \approx 1 - \frac{16\pi^2 a^2}{5\lambda^2}\sin^2\left(\frac{\theta_{sca}}{2}\right) \qquad (61)$$

and taking the *ln* of both sides:

$$\ln P(\theta) \approx -\frac{16\pi^2 a^2}{5\lambda^2}\sin^2\left(\frac{\theta}{2}\right)$$

Then a plot of ln$P$ vs $\sin^2(\theta/2)$ should be linear and its slope would permit evaluation of the particle size.

Scattering from Solutions: Zimm Plots

To obtain the size M of an unknown polymer solute, we can vary either the scattering angle θ_{sca} or the mass concentration C of the polymer.

The Rayleigh scattering result is given by (46); multiplying by the appropriate form factor for a random coil polymer:

$$\frac{i_c}{I_0} = \frac{i_s}{I_0}P(\theta_{sca}) = \frac{KC}{1/M + 2BC}\frac{\sin^2\theta}{r^2}P(\theta_{sca}) \qquad (46)$$

Recall that $\sin^2\theta = \cos^2\theta_{sca}$ for horizontal polarization of the incident light, $\sin^2\theta = 1$ for vertical polarization, and $\sin^2\theta = (1+\cos^2\theta_{sca})/2$ for unpolarized light.

Experimental data is usually plotted in terms of the ***Rayleigh ratio*** which is defined as

$$R_\theta \equiv \frac{r^2}{\sin^2\theta}\frac{i_c}{I_0} = \frac{KC}{1/M + 2BC}P(\theta_{sca})$$

In the same way that turbidity was transformed to create a quantity that was linear in C [see (48)], we can also transform the Rayleigh ratio

$$\frac{KC}{R_\theta} = \left(\frac{1}{M} + 2BC\right)\frac{1}{P(\theta_{sca})}$$

Substituting the counterpart to (61) which is appropriate for random coils:

$$\frac{KC}{R_\theta} = \left(\frac{1}{M} + 2BC\right)\left[1 + \frac{16\pi^2\overline{R_g^2}}{3\lambda^2}\sin^2\left(\frac{\theta_{sca}}{2}\right)\right] \qquad (62)$$

where $\overline{R_g^2}$ is the mean-square radius of gyration of a random polymer coil (another measure of its size).♠ The minus sign in (61) becomes a plus sign because the term in square brackets represents the inverse.

♠ The shape of a "random coil polymer" resembles a Brownian random walk in 3-D. Just like the mean-square displacement is proportional to time, the mean-square radius of gyration is proportional to the number of monomer segments (like the number of steps). See §2.7 in Hiemenz for more information.

Below is a graph of scattering data (black points) in which both scattering angle and polymer concentration are varied. The data is for cellulose nitrate dissolved in acetone.

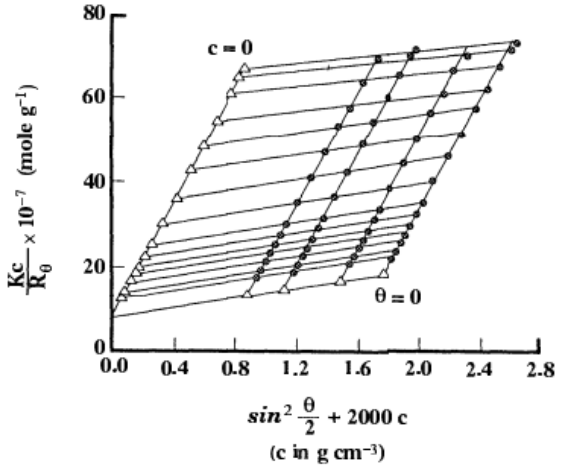

The nearly vertical lines through the black points represent regressions of data for the same concentration but different scattering angles. The triangles at the bottom of these lines represent the extrapolation to zero scattering angle. The nearly horizontal lines represent regressions of data for the same scattering angle but different concentrations. The triangles at the left end of each of these lines represents the extrapolation to zero concentration.

The regression of either set of triangles should yield the same y-intercept. The value of this intercept is the limit of (62) for both $C \to 0$ and $\theta_{sca} \to 0$:

$$\lim_{\substack{C\to 0 \\ \theta_{sca}\to 0}} \frac{KC}{R_\theta} = \frac{1}{M}$$

The slopes of the two lines through the two sets of triangles also have meaning which can be inferred from (62):

$$\frac{dy(\theta, C=0)}{d\sin^2\frac{\theta}{2}} = \frac{16\pi^2\overline{R_g^2}}{3\lambda^2 M}$$

$$\frac{dy(\theta=0, C)}{dC} = 2B$$

Application to Flocculation Studies

Later in this course, we will discuss aggregation (or flocculation) of colloidal dispersion. Light scattering can also be used to study the rate of this process. If I use (45) instead of (36) in (35) and (43), then multiply by the number of particles per unit volume *N*, the Rayleight ratio behaves like

$$R_\theta \propto NV^2 \qquad (63)$$

where *V* is the volume of one scatterer. During flocculation two independent scatterers combine to form a single scatterer having twice the volume

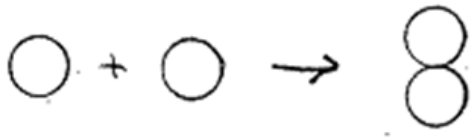

If all singlets combined in this way we would be obtain half as many particles with each one having twice the volume. But according to (63), this would change the scattering by a factor of $(1/2)2^2 = 2$. As aggregation proceeds, the scattering increases at a rate that related to the rate of aggregation.

Dynamic Light Scattering Experiments

Reading: Hiemenz §5.8

The scattering signal from small sample volumes tends to be noisy. But this "noise" actually contains information regarding the size of the scatterers. For example, the figure below (taken from Berg, p439) shows the raw scattering signal for three different sizes of polystyrene latex particles: 0.085 μm (a), 0.220 μm (b) and 1.011 μm (c):

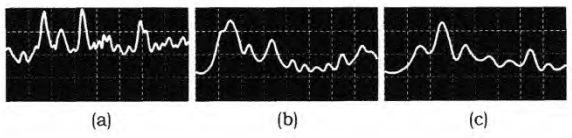

While each signal is some random fluctuation around a mean value, larger particles clearly have slower fluctuations than smaller particles. These fluctuations arise because the PS particles undergo Brownian motion so the relative distance between any two particles in the sample volume changes with time. This changes the nature of the interference in light scattered from any two particles from complete constructive interference to complete destructive interference. The rate of change is related to the diffusion coefficient of the Brownian particles.

The extraction of the diffusion coefficient from such noisy data involves computing the autocorrelation of the scattering intensity

$$C(t_d) \equiv \lim_{T\to\infty}\left\{\frac{1}{T}\int_{t_0}^{t_0+T} i(t)\,i(t+t_d)\,dt\right\} \qquad (64)$$

This function describes how strongly the intensity measured at some later time $t+t_d$ is correlated with the intensity at current time t. For example, if $i(t+t_d)$ is strongly correlated to $i(t)$ (for example if $t_d=0$), then their product will be $i^2(t)$ and we obtain

$$C(0) = \langle i^2 \rangle$$

On the other hand, at very large delay times, we expect that $i(t+t_d)$ will be completely uncorrelated to $i(t)$. For half of the t's in the integral, $i(t+\tau)$ will be greater than the mean $\langle i \rangle$ and for the other half $i(t+t_d)$ will be smaller than the mean. If there is no correlation, we just replace $i(t+t_d)$ by $\langle i \rangle$. Then (64) yields

$$C(\infty) = \langle i \rangle^2 \qquad (65)$$

For virtually all functions $i(t)$, $\langle i^2 \rangle > \langle i \rangle^2$ and $C(t_d)$ decays monotonically from one limit to the other as the delay time t_d increases.

For monodisperse particles (all have same size), the normalized autocorrelation function decays exponentially with the delay time t_d:

$$\underbrace{\frac{C(s,t_d)}{\langle i \rangle^2}}_{g_2(s,t_d)} = 1 + \underbrace{\frac{\langle i^2 \rangle - \langle i \rangle^2}{\langle i \rangle^2}}_{\xi} \exp\left(-2s^2 D t_d\right) \qquad (66)$$

where ξ is an instrument constant and

$$s = \frac{4\pi}{\lambda}\sin\frac{\theta_{sca}}{2}$$

Example 5.5: Experimental results for the enzyme phosphofructokinase in water at 20ºC is given by the graph below. If the density of the enzyme (protein) is 1.35 g/cm^3, find the apparent molecular weight.

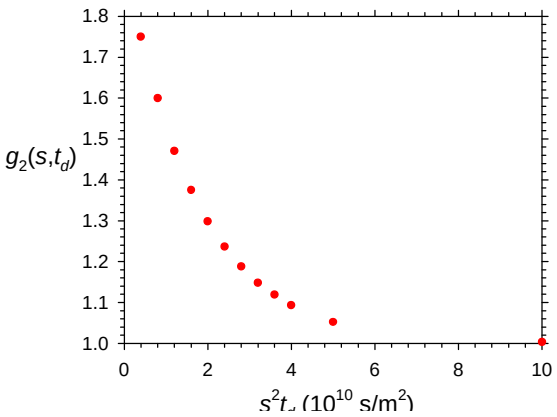

Solution: Replotting the data so as to get a straight line:

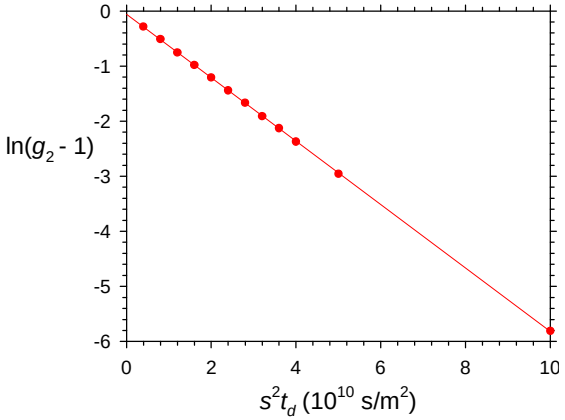

According to (66), the slope of this line is:

$$\text{slope} = -2D = -5.78\times10^{-11}\,\frac{\text{m}^2}{\text{s}}$$

or

$$D = 2.88\times10^{-11}\,\frac{\text{m}^2}{\text{s}}$$

Treating the enzyme as a sphere, we can infer its hydrodynamic radius by substituting Stokes law (16) into Einstein's equation (15). The result is called the ***Stokes-Einstein equation*** for the diffusion coefficient:

$$D \overset{\text{Einstein}}{=} \frac{kT}{f} \overset{\text{Stokes}}{=} \frac{kT}{6\pi\eta a_H}$$

Solving for the ***hydrodynamic radius*** a_H; then substituting k = 1.381×10^{-23} J/ºK, T = 293ºK, η = 0.001 Pa-sec and D = 2.88×10^{-11} m^2/sec:

$$a_H = \frac{kT}{6\pi\eta D} = 7.4 \text{ nm}$$

The molecular weight of this enzyme is 478 kg/mol and the density is 1.35 gm/cm^3. These values can be used to estimate the mass and volume of one molecule:

$$m = \frac{478\ \text{kg}}{6.02\times10^{23}} = 7.94\times10^{-22}\ \text{kg}$$

$$v = \frac{7.94\times10^{-22}\ \text{kg}}{1.35\frac{g}{cm^3}} = 5.87\times10^{-25}\ \text{m}^3$$

Treating this volume as a sphere, we can calculate an apparent radius:

$$a = \left(\frac{3v}{4\pi}\right)^{1/3} = 5.2\ \text{nm}$$

As with sedimentation equilibrium and sedimentation rate, these two ways of estimating the size of the enzyme yield different values

$$\frac{a_H}{a} = 1.43$$

The volume v represents the "dry" volume. Any bound water would add to this volume and the apparent radius, although the required increase in radius (7.4 – 5.2 = 2.2 nm) is much larger than a single water molecule. A more likely explanation is that the enzyme is not spherical in shape. An ellipsoid having the same volume v would have a larger friction coefficient f than a sphere, which would correspond to a smaller D and a larger apparent hydrodynamic radius a_H.

Lecture #10 begins here

Surface Tension

The video *Surface Tension in Fluid Mechanics* **530.427 S961** (which we viewed) contained many demonstrations of bubble, drop and particle motion caused by surface tension. In this chapter, we will analyze several of the phenomena demonstrated by this video.

Molecular Origin of Surface Tension

In thermodynamics, the Gibbs free energy is an extensive property of material whose value is proportional to the mass or volume of material. When the system consists of a mixture of two or more phases, the free energy also contains a contribution which is proportional to the surface area between the phases. This contribution is called ***surface tension*** (units are energy per unit area or force per unit length).

Such a contribution arises from intermolecular forces. All molecules experience van der Waals attraction for one another. Consider a single water molecule buried deep in a pool of water. Such a molecule is represented by the blue dot in the lower right of the figure below. This interior water molecule is surrounded on all sides by other water molecules and is pulled equally in all directions (indicated by the four arrows). As a result it feels no net force.

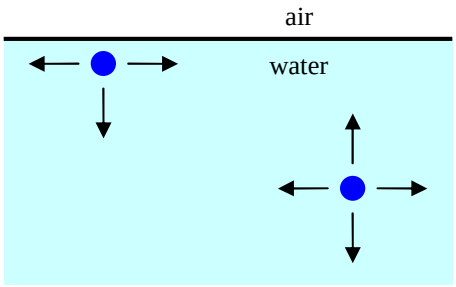

Next, consider a second water molecule located next to the air/water interface. Such a molecule is represented by the blue dot in the upper left of the figure above. Owing to the very low density of air compared to water, there are virtually no molecules located above our interfacial water molecule. Consequently, the intermolecular forces acting on it are no longer balanced: it feels a net force pulling it normal to the interface into the pool.

All liquid molecules near the interface experience a net force normal to the interface pulling them back into the liquid. Each interfacial molecule then moves away from the interface, but conservation of mass causes another molecule to take its place. In the absence of other forces, the molecules of the liquid phase will rearrange themselves to minimize the interfacial area. Thus small droplets tend to be spherical because that geometry has the smallest area for a given volume.

Expanding Area of Soap Films

From a continuum point of view, the tendency to minimize interfacial area is achieved by assigning a contribution to the free energy of the air-water mixture which is proportional to the interfacial area. That contribution is called ***surface tension*** which we will denote by γ.

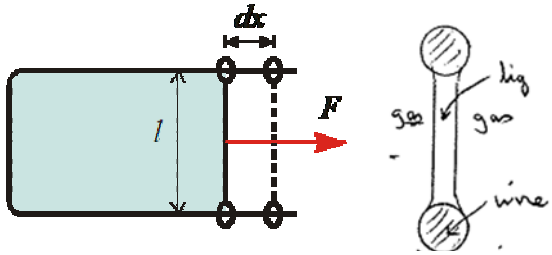

top view end view

To understand the consequences of surface tension, consider a soap film (colored area in sketch above) supported by a rectangular wire frame, in which the right side of the wire frame is a slide wire which can be moved either right or left. Suppose we apply a force F and drag the slide wire to the right a distance dx. The amount of work done is $F\,dx$. This work goes into increasing the surface area of the soap film by $2l\,dx$ which increases the free energy by $2\,\gamma\,l\,dx$.♣ The factor of two arises because the soap film has two air-water interfaces: one each on the top and bottom. Assuming there are no irreversible losses of energy:

$$dW = F\,dx = 2\gamma\,l\,dx$$

where γ is the surface tension. Dividing out the dx we have

$$F = 2\gamma\,l \qquad (67)$$

This force must be continuously applied to overcome the thermodynamic tendency to reduce the interfacial area and keep the film from shinking in area.

Values of the surface tension for various liquids are shown at several temperatures in Table 1. Strictly speaking, the term "surface tension" refers to the interfacial free energy between a liquid and its vapor.

♣ The volume of liquid held in the film is a constant, so the film also thins a little as the area is increased.

Table 1
Surface Tension for Common Liquids*

Mol. formula	Name	γ in mN/m 10°C	25°C	50°C	75°C	100°C
Br_2	Bromine	43.68	40.95	36.40		
Cl_2O_2S	Sulfuryl chloride		28.78			
Cl_3OP	Phosphoryl chloride		32.03	28.85	25.66	
Cl_3P	Phosphorus trichloride		27.98	24.81		
Cl_4Si	Silicon tetrachloride	19.78	18.29	15.80		
H_2O	Water	74.23	71.99	67.94	63.57	58.91
H_4N_2	Hydrazine		66.39			
Hg	Mercury	488.55	485.48	480.36	475.23	470.11
CCl_4	Tetrachloromethane		26.43	23.37	20.31	17.25
CS_2	Carbon disulfide	33.81	31.58	27.87		
$CHBr_3$	Tribromomethane		44.87	41.60	38.33	
$CHCl_3$	Trichloromethane		26.67	23.44	20.20	
CH_2Br_2	Dibromomethane		39.05	35.33	31.61	
CH_2Cl_2	Dichloromethane		27.20			
CH_2O_2	Formic acid		37.13	34.38	31.64	
CH_2I	Iodomethane	32.19	30.34			
CH_3NO	Formamide		57.03	54.92	52.82	50.71
CH_3NO_2	Nitromethane	39.04	36.53	32.33		
CH_4O	Methanol	23.23	22.07	20.14		

*Taken from *CRC Handbook of Chemistry & Physics*, 87th edition, 2006-7.

Table 2
Surface vs Interfacial Tensions*

Surface and interfacial tensions of some liquids (in mN m^{-1}) at 293 K (from Aveyard and Haydon 1973, p. 70, with permission)

	Liquid–vapour	Water–liquid	$-d\gamma/dT$ (liquid–vapour) (mN m^{-1} K^{-1})
Water	72.75	—	0.16
Octane	21.69	51.68	0.095
Dodecane	25.44	52.90	0.088
Hexadecane	27.46	53.77	0.085
Benzene	28.88	35.00	0.13
Carbon tetrachloride	26.77	45.0	—
Mercury	476	375	—

$d\gamma/dT$ for the hydrocarbon–water interface is 0.09 mN m^{-1} K^{-1}.

*taken from Hunter, Vol. 1, page 233.

However, when the density of the gas phase is much less than the liquid, replacing the vapor by a mixture of vapor and air usually doesn't change the value of the interfacial free energy.

Replacing the gas phase by second immiscible liquid does however change the interfacial free energy. The term ***interfacial tension*** is the generic term used for the interfacial free energy per unit area between two arbitrary (immiscible) phases. Table 2 shows the effect of replacing the gas phase in contact with various organic liquids by liquid water. At least in these examples, the resulting interfacial tension between liquids lies between the surface tensions for the two liquids.

Laplace Pressure

One manifestation of surface tension is that it induces a hydrostatic pressure difference across a curved interface: the concave side of the interface has higher pressure. Recall the demonstration in Trefethen's video in which he blows a soap bubble at the end of a pipe, then holds his finger over the end of the tube. When he removed his finger and unblocks the tube, the soap bubble shinks forcing air out through the tube. This demonstates that at equilibrium, the pressure inside the bubble is greater than outside.

Consider a spherical soap bubble of radius R composed of a liquid having surface tension γ. Consider a force balance about the upper hemisphere:

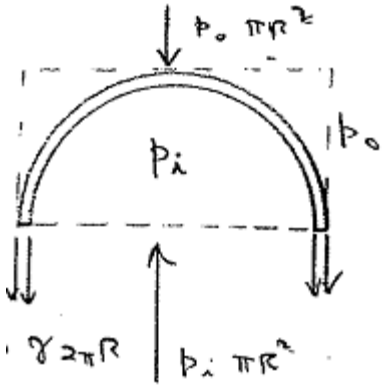

Surface tension pulls downward with a force equal to the product of surface tension γ and the perimeter of the soap film $2\pi R$ [see (67)]. But we need to double this because the soap film has both an inner and out surface and both pull downward. Also acting downward is the hydrostatic pressure outside the bubble p_o. This exerts a downward force equal to the product of the pressure and the projected area of the sphere πR^2. The total of the downward forces is

downward: $2\times 2\pi R\gamma + \pi R^2 p_o$

This is balanced by the upward force of hydrostatic pressure p_i inside the bubble:

upward: $\pi R^2 p_i$

Equating these two forces and solving for the pressure difference:

soap bubble: $$p_i - p_o = \frac{4\gamma}{R}$$

If instead of a soap bubble, we had a liquid drop in air (or an air bubble immersed in liquid), we would not need to double the perimeter. Then the pressure difference turns out to be:

liquid drop: $$p_i - p_o = \frac{2\gamma}{R} \qquad (68)$$

Notice that it doesn't matter when the condensed phase is inside or outside, the pressure is always higher on the concave side of the interface (i.e. inside the sphere).

Example: Calculate Δp for a 1 mm air bubble submerged in water at 20°C; at this temperature, the surface tension of water is 73 mN/m (see Table 2).

Solution: Using (68):

$$p_i - p_o = \frac{2\gamma}{R} = \frac{2\left(73\frac{\text{mN}}{\text{m}}\right)}{0.0005\text{ m}} = 292\text{ Pa} = 0.003\text{ atm}$$

which is surely measureable but not large. To get a pressure difference of 1 atm, we need a diameter of $2R = 2.88\ \mu$m.

A sphere is a particular shape of interface. More generally, two radii of curvature are needed to characterize a curved surface and the pressure difference is given by the Young-Laplace equation.

This derivation of the Young-Laplace equation is adapted from Hunter, Vol 1.

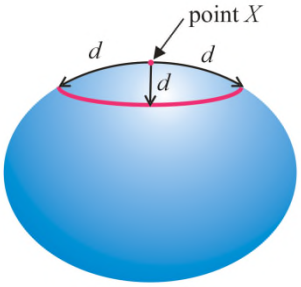

Consider a drop of liquid (see figure above) having surface tension γ in air. A spheroidal cap is bounded by a contour (the thick pink line) which is everywhere the same distance d from some arbitrary point X on the surface. The three distances denoted d might not look equal in the diagram owing to perspective.

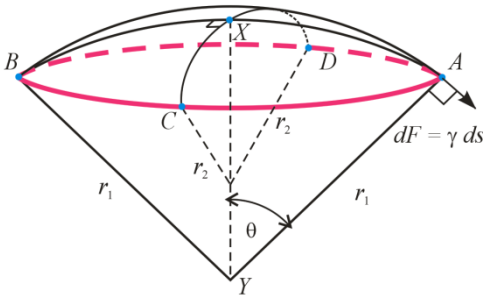

In the sketch above, the edge of the spheroidal cap has been re-drawn and re-scaled as the pink line labelled *ACBDA*. Contours *AB* and *CD* (which lie completely on the surface of the drop) both contain the point *X* and form a right angle at point *X*. In the limit that $d\to 0$, both *AB* and *CD* become circular arcs of radius r_1 and r_2, respectively. From the differential geometry of surfaces (Weatherburn, 1930), the directions of *AB* and *CD* (which are perpendicular) can be chosen such that r_1 is a maximum (R_1) and r_2 is a minimum (R_2). Furthermore the sum of the reciprocals is

independent of the orientation of the two perpendicular axes *AB* and *CD*:

$$\frac{1}{r_1}+\frac{1}{r_2}=\frac{1}{R_1}+\frac{1}{R_2}=H$$

This sum of the reciprocals of the radii is called the ***mean curvature*** of the surface at point *X*, r_1 and r_2 are called the ***radii of curvature*** and R_1 and R_2 are called the ***principal radii of curvature***.

In the same way that a force *F* was needed to overcome the thermodynamic tendency of the soap film to shink in (67), the remainder of the surface must exert a force to keep the area of the spherical cap from shinking. This force is exerted tangent to the surface as shown in the figure and its magnitude for a differential arc length *ds* (the analog of *l*) is

$$dF=\gamma\, ds$$

The component of this force normal to the surface (i.e. in the direction of the line *XY*) is

$$dF_{\text{vertical}}=\gamma\, ds\sin\theta$$

but when $d\to 0$, this angle is that subtended by an arc of length *d* and radius r_1:

$$\lim_{d\to 0}\theta=\frac{d}{r_1}$$

and

$$\lim_{d\to 0}\sin\theta=\theta=\frac{d}{r_1}$$

Thus

$$\frac{dF_{\text{vertical}}}{ds}=\gamma\frac{d}{r_1}$$

This is the contribution to the vertical component of the force from point *A*. Averaging similar contributions from points B, C and D yields

$$\frac{dF_{\text{vertical}}}{ds}=\frac{\gamma d}{2}\left(\frac{1}{r_1}+\frac{1}{r_2}\right)=\frac{\gamma d}{2}\left(\frac{1}{R_1}+\frac{1}{R_2}\right)$$

Since the sum of the reciprocals of the radii is independent of orientation, we can integrate over the entire edge of the spherical cap. In the limit $d\to 0$, the edge is just a circle of radius *d*.

$$F_{\text{vertical}}=\frac{\gamma d}{2}\left(\frac{1}{R_1}+\frac{1}{R_2}\right)\underbrace{\int_{\substack{\text{edge}\\ \text{of cap}}} ds}_{2\pi d}$$

or

$$F_{\text{vertical}}=\gamma\pi d^2\left(\frac{1}{R_1}+\frac{1}{R_2}\right)$$

This vertical component of force on the cap is acting downward. But the drop is not is motion; so another force of equal magnitude but opposite direction must be acting on the cap.

This force is hydrostatic pressure: the pressure inside the drop is higher than the pressure outside by Δp. The upward force due to this higher pressure is Δp multiplied by the area of the disk (πd^2):

$$\Delta p\,\pi d^2=\gamma\pi d^2\left(\frac{1}{R_1}+\frac{1}{R_2}\right)$$

or

$$\Delta p=\gamma\left(\frac{1}{R_1}+\frac{1}{R_2}\right)$$

which is called the ***Young-Laplace equation***. The sum of the two radii reciprocals is called the ***curvature*** *J* of the surface:

$$J=\frac{1}{R_1}+\frac{1}{R_2}$$

Note that a flat surface has both radii infinite: $R_1 = R_2 = \infty$ and $J = 0$. In other words, a flat surface has zero curvature.

Implication for Phase Equilibrium

Curvature can have a profound effect on phase equilibria. For example, small water drops have a higher vapor pressure than bulk liquid at the same temperature. The reason is that the pressure inside the drop is higher, which increases its Gibbs free energy.

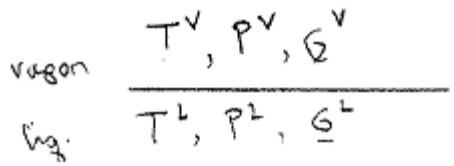

First consider the usual problem of phase equilibrium of a one-component system (say pure water) between a liquid and its vapor at a flat interface. Thermal, mechanical and chemical equilibrium require:

$$T^V = T^L = T$$

$$P^V = P^L = P_0(T)$$

$$\underline{G}^V = \underline{G}^L = \underline{G}_0$$

where $P_0(T)$ is the vapor pressure and $\underline{G}$ is the molar free energy of either phase. There is only one pressure at which the two phases coexist for a given temperature and that is the vapor pressure.

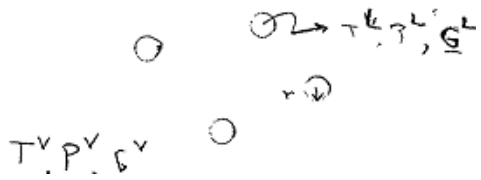

Now consider a second system at the same temperature composed of uniform liquid drops in equilibrium with their vapor. Because of the curved interface, the mechanical equilibrium requirement is different, making the pressure inside the liquid higher than that of the vapor:

$$T^V = T^L = T$$

$$P^L - P^V = \frac{2\gamma}{r} \tag{69}$$

$$\underline{G}^V = \underline{G}^L \tag{70}$$

The pressure of both phases might be different from that with a flat interface. The effect of pressure on the Gibbs free energy can be calculated from:

$$\left(\frac{\partial \underline{G}}{\partial P}\right)_T = \underline{V}$$

where $\underline{V}$ is the molar volume. Changing the pressure of the vapor from the vapor pressure $P_0(T)$ to whatever P^V is causes the following change in the free energy of the vapor:

$$\int_{\underline{G}_0}^{\underline{G}^V} d\underline{G} = \int_{P_0}^{P^V} \underline{V}^V dP \overset{\text{ideal gas law}}{=} \int_{P_0}^{P^V} \frac{RT}{P} dP$$

where the second equation substitutes the ideal-gas law for the molar volume of the vapor. Integrating

$$\underline{G}^V - \underline{G}_0 = RT \ln \frac{P^V}{P_0(T)}$$

A similar integration can be performed for the liquid. One difference is that the molar volume of the liquid is practically independent of pressure:

$$\underline{G}^L - \underline{G}_0 = \underline{V}^L \left(P^L - P_0(T)\right)$$

According to (70), the left-hand sides of the above two equations are the same, so the right-hand sides must also be equal:

$$RT \ln \frac{P^V}{P_0(T)} = \underline{V}^L \left(P^L - P_0(T)\right)$$

Finally, we substitute P^L from (69):

$$RT \ln \frac{P^V}{P_0(T)} = \underline{V}^L \left(P^V + \frac{2\gamma}{r} - P_0(T)\right)$$

$$= \underbrace{\underline{V}^L \left(P^V - P_0(T)\right)}_{\text{neglible}} + \frac{2\gamma \underline{V}^L}{r} \approx \frac{2\gamma \underline{V}^L}{r}$$

Assuming the increase in vapor pressure $P^V - P_0$ is small compared to the Laplace pressure $2\gamma/r$, we can neglect the first term. Solving for the new vapor pressure P^V:

for drops: $$P^V = P_0(T) \exp\left(\frac{2\gamma \underline{V}^L}{rRT}\right)$$

which is called ***Kelvin's equation***. Note that as $r \to \infty$, it correctly predicts no change in vapor pressure. But as r becomes smaller, the vapor pressure increases. One effect of this is that small drops evaporate much more quickly than you would otherwise expect.

If we repeat this analysis for bubbles of water vapor in a liquid, the vapor pressure is reduced rather than increased:

for bubbles: $$P^V = P_0(T) \exp\left(-\frac{2\gamma \underline{V}^L}{rRT}\right)$$

Example #1: Evaluate the vapor pressure of water in droplets at 20°C as function of drop size.

Solution: γ = 72.8 mN/m and P_0 = 17.535 mmHg. The molar volume of liquid water can be calculated from its density ρ and molecular weight M:

$$\underline{V}^L = \frac{M}{\rho} = 18.0 \text{ cc/gmol}$$

Then Kelvin's equation becomes

$$P^V = P_0 \exp\left(\frac{1.08 \text{ nm}}{r}\right)$$

Substituting in various values of r:

r	P^V/P_0	$\frac{2\gamma}{r}/P_0$	P^L/P_0
10^{-1} m	1.000	0.001	1.001
10^{-3} m = 1 mm	1.000	0.063	1.063
10^{-6} m = 1 μm	1.001	62.9	63.9
10^{-7} m	1.01	629	630
10^{-8} m	1.11	6,293	6,295
10^{-9} m = 1 nm	2.93	62,934	62,937

Thus the effect is not significant except for nanoparticles. Notice that the pressure in both phases increases as the droplets get smaller.

Subcooled Vapor. The main importance of Kelvin's equation is that it allows vapors to become supersaturated. In order for a vapor to condense into a liquid, small nuclei must first be formed. Since the vapor pressure of such small droplets can be many times larger than the usual vapor pressure, homogeneous nucleation is usually prevented by Kelvin's equation. Instead nucleation may take place on a wall, or on a piece of dust or other nucleation site.

Example #2: Let's repeat this example for small bubbles of water vapor in liquid, but let's increase the temperature to 100ºC where the vapor pressure of water is P_0 = 760 mmHg or 1 atm:

Solution: Then Kelvin's equation becomes

$$P^V = P_0 \exp\left(-\frac{1.08\text{ nm}}{r}\right)$$

Substituting in various values of r:

r	P^V/P_0	$\frac{2\gamma}{r}/P_0$	P^L/P_0
1 m	1	1.437e-6	1
0.1	1	1.437e-5	1
0.01	1	0	1
1e-3 m = 1 mm	1	0.001	0.999
1e-4	1	0.014	0.986
1e-5	1	0.144	0.856
1e-6 m = 1 μm	0.999	1.437	-0.438
1e-7	0.989	14.37	-13.38
1e-8	0.898	143.696	-142.798
1e-9 m = 1 nm	0.341	1436.96	-1436.619

Notice that some of the (absolute) pressures (indicated in red) are negative. This of course is physically unrealistic and suggests that two phases cannot co-exist for bubbles this small.

Superheated Liquid. Consider a dispersion of small gas bubbles in a liquid. Now the liquid is on the convex rather than the concave side of the interface. So the pressure in the liquid phase will be lowered rather than raised. For this reason it is difficult to get homogeneous nucleation of gas bubbles when you raise the temperature of a liquid or lower its temperature.

When you heat water on a stove, you will see bubbles first form on the wall, not in the interior, Of course, there is a slightly higher temperature at the wall. If I tried to boil water at room temperature by lowering the pressure, bubbles would again form only at the wall.

Unless we are extremely careful, there will be pockets of air on the rough wall which has been incompletely wet by the liquid. Even if these pockets are only 10^{-7} cm in size, it will be much easier for water vapor to expand these pockets than to nucleate new bubbles in the bulk.

Lecture #11 begins here

Capillary Rise

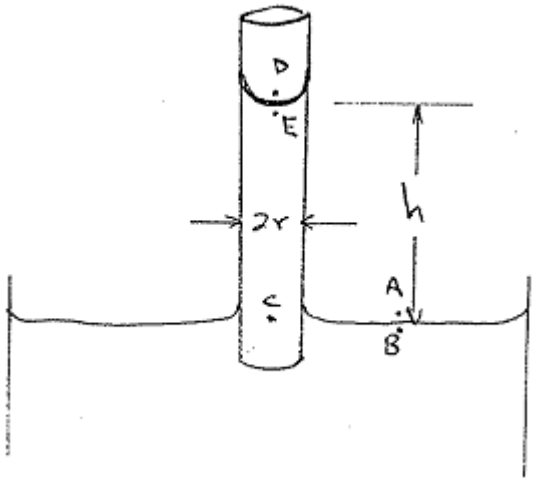

When one end of an open capillary tube♣ is dipped into a pool of liquid, the liquid will be drawn into the tube to a level above the horizontal surface of liquid in the pool. In the figure above, this rise is the distance h. This phenomenon is called ***capillary rise***.

For a circular capillary tube composed of a material which is fully wetted by the liquid (i.e. zero contact angle: see next section), the shape of the meniscus (the air-water interface inside the capillary) is a hemisphere having the same radius r as the capillary tube. Application of (68) reveals that the liquid has a lower pressure than the air on the concave side of the interface:

♣ A capillary is a long tube having a small bore (from Latin *capillus* meaning hair).

$$p_D - p_E = \frac{2\gamma}{r} \tag{71}$$

Owing to its very low density, the hydrostatic pressure in the air is everywhere 1 atm. The pressure is also 1 atm in the liquid at the same elevation at the horizontal interface (its curvature is zero so no Laplace pressure difference) of the pool in the large beaker:

$$p_A = p_B = p_C = p_D = \text{latm} \tag{72}$$

The weight of the fluid in the capillary tube causes $p_C > p_E$:

$$p_C - p_E = \rho g h \tag{73}$$

Since $p_C = p_D$ according to (72), the left sides of (71) and (73) are equal, so the right-hand sides must also be equal:

$$\rho g h = \frac{2\gamma}{r}$$

Solving for the capillary rise height h:

$$h = \frac{2\gamma}{\rho g r}$$

The derivation above assumes a hemispherical shape for the meniscus. More generally, the shape depends on the contact angle θ which will be discussed in an upcoming section:

$$h = \frac{2\gamma}{\rho g r}\cos\theta \tag{74}$$

Now $\cos\theta$ is positive for fluids which wet the capillary (water will wet clean glass) and negative for nonwetting fluids (e.g. mercury on glass). So the meniscus inside the capillary can be either higher or lower than the bulk liquid outside:

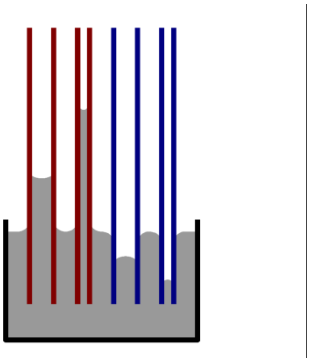

Note that the product rh is a property only of the fluid. The square root of this product is a number which has units of length and is called the ***capillary constant***:

$$a \equiv \sqrt{rh} = \sqrt{\frac{2\gamma}{\rho g}} \tag{75}$$

The expression (74) for capillary rise can be re-written in terms of the capillary constant:

$$h = \frac{a^2}{r}\cos\theta$$

Example: Compute the capillary rise of benzene in a clean glass capillary with 1 mm diameter. Assume $\cos\theta = 1$.

Solution: γ = 29 mN/m at 20°C and ρ = 0.879 g/cm^3. Eq. (74) gives h = 1.35cm using r = 0.05cm. Eq. (75) gives a = 0.259 cm.

Contact Angle

Surface tension arises because molecules residing near the surface of a liquid possess a higher energy than molecules in the bulk of the liquid. This difference in energy results from the greater number of neighbors which bulk molecules have compared to surface molecules.

These same differences between surface molecules and bulk molecules applies to solids as well as liquids. Thus we might anticipate that solids have a kind of surface tension associated with them.

One important difference is that solids cannot deform to minimize their surface energy. So the manifestation of surface energy of solids is a little more subtle. An important illustration of surface energy in solids is the contact angle.

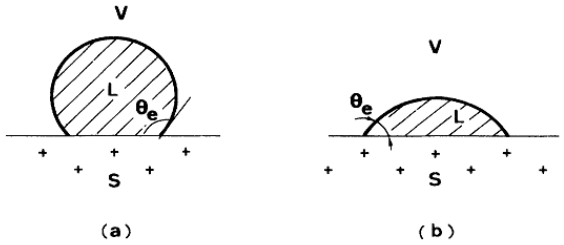

When a drop of fluid is placed on a solid, the drop may assume a variety of shapes, depending not only on the volume of the drop and its surface tension, but also on the solid. The figure above shows the same drop applied to two different solids.

At equilibrium, the drop will form some angle with the solid. This is called the contact angle. This angle is independent of the size of the drop, but it does depend on the particular solid and liquid used. Thus, the contact angle represents an equilibrium property of the solid/liquid interface.

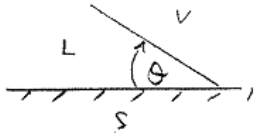

By convention, contact angles are always measured through the liquid and $0<\theta<180°$:

contact angle -- measured through the liquid from the L/S interface to the tangent to L/V interface at the 3-phase contact line

- $\theta < 90°$ -- Liquid is said to wet solid
- $\theta > 90°$ -- Liquid does not wet solid
- $\theta = 0°$ -- Liquid is said to spread on solid

Some typical values:

water on clean glass at 25°C: $\theta = 0$
mercury on clean glass at 25°C: $\theta = 140°$

As it turns out, the contact angle can be greatly altered by contamination, especially of the solid surface. The reason for this becomes obvious as soon as we draw a connection between contact angle and surface tension. Then any surface contamination might be explained through a change in the surface energy.

Derivation of Young's Equation

The fundamental equation governing contact angles is

$$\gamma_{LV}\cos\theta = \gamma_{SV} - \gamma_{SL} \tag{76}$$

which is called ***Young's equation*** (a.k.a. Young-Dupré equation) after Thomas Young who proposed this equation in 1805.

γ_{LV} is the surface tension associated with the liquid-vapor interface. Recall that surface tension can be thought of as a contribution to free energy which is proportional to the surface area. Solid surfaces also have energy and γ_{SV} and γ_{SL} are the analogous energies for the solid-vapor and solid-liquid surfaces. However γ_{SV} and γ_{SL} are called ***interfacial tension***s instead of surface tension (which is reserved for liquid-vapor surfaces).

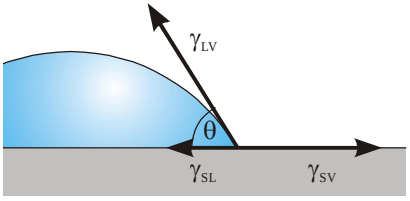

There are at least two different methods of deriving this equation.

Partial Proof #1: The first is to consider the interfacial tensions as forces exerted on the three-phase contact line. A balance of the horizontal components of the forces yields

$$\underbrace{\gamma_{LV}\cos\theta + \gamma_{SL}}_{\text{left forces}} = \underbrace{\gamma_{SV}}_{\text{right force}}$$

One problem with this derivation is that the vertical forces are not balanced. Supporters argue that the contact line cannot move vertically so this balance is not relevant.

Partial proof #2: A second approach is to say that the drop assumes that shape for a given volume V which minimizes the total interfacial energy.

$$G = \gamma_{LV} A_{LV} + \gamma_{SL} A_{SL} + \gamma_{SV} A_{SV} \qquad (77)$$

If V is sufficiently small so that gravity does not contribute significantly to the energy of the drop, then we can assume that the LV interface is spherical (because that shape generally minimizes the LV surface area for a given volume).

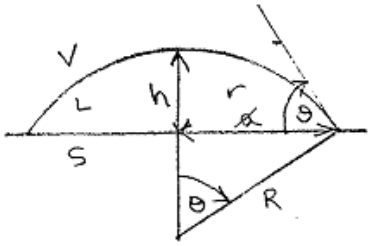

Then the liquid must be a segment of a sphere of radius R (also known as a spherical cap of height h). A spherical cap has the following area and volume:

$$A_{LV} = \pi\left(h^2 + r^2\right) \qquad (78)$$

$$V = \frac{\pi h}{6}\left(h^2 + 3r^2\right) \qquad (79)$$

The base of the "cap" is a disk of radius r whose area is

$$A_{SL} = \pi r^2 \qquad (80)$$

Finally the solid-vapor area is the remainder of the total area of the plane not wet by liquid:

$$A_{SV} = A_{plane} - A_{SL} \qquad (81)$$

Our task is to find the shape which minimizes the free energy of the system, given by (77). The figure above contains four variables: r, h, R and θ. The geometry of a right triangle provides two constraints among them: see (86) and (87) below. Specifying the volume of the spherical cap, (79) provides a third constraint: 4 unknowns less 3 constraints leaves only one degree of freedom for minimizing G. So let's consider that the total interfacial energy can be written as a function of r alone:

$$G = G(r)$$

at the min: $dG/dr = 0$

Assume some change dr: what is the corresponding dG? Note that dr will cause compensating changes in both the solid-liquid and solid-vapor areas dA_{SL} and dA_{SV}: According to (80) and (81)

$$dA_{SL} = -dA_{SV} = d\left(\pi r^2\right) = 2\pi r\, dr \qquad (82)$$

(77) requires:

$$\begin{aligned} dG &= \gamma_{LV} dA_{LV} + \gamma_{SL} dA_{SL} + \gamma_{SV} dA_{SV} \\ 0 &= \gamma_{LV} dA_{LV} + \left(\gamma_{SL} - \gamma_{SV}\right) dA_{SL} \end{aligned} \qquad (83)$$

Taking the total differential of (78):

$$dA_{LV} = \pi(2h\,dh + 2r\,dr) \qquad (84)$$

but dh is related by dr by the requirement that the volume remain constant; taking the total differential of (79) and setting it to zero:

$$dV = 0 = V = \frac{\pi dh}{6}\left(h^2 + 3r^2\right) + \frac{\pi h}{6}(2h\,dh + 6r\,dr)$$

Solving for dh: $\quad dh = \dfrac{-2hr\,dr}{h^2 + r^2}$

Substituting this result into (84):

$$dA_{LV} = \frac{r^2 - h^2}{r^2 + h^2} 2\pi r\,dr$$

Substituting this result and (82) into (83):

$$dG = 0 = \gamma_{LV} \frac{r^2 - h^2}{r^2 + h^2} 2\pi r\,dr + \left(\gamma_{SL} - \gamma_{SV}\right) 2\pi r\,dr$$

After dividing through by the common factors:

$$\gamma_{LV} \underbrace{\frac{r^2 - h^2}{r^2 + h^2}}_{\cos\theta} + \left(\gamma_{SL} - \gamma_{SV}\right) = 0 \qquad (85)$$

We just need to show that the quotient equals cosθ. This can be shown using the geometry of the right triangle:

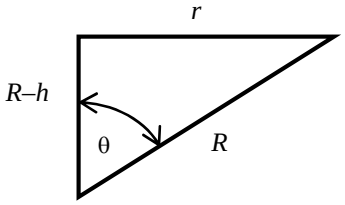

From Pathogorus' theorem:

$$R^2 = (R - h)^2 + r^2 = R^2 - 2Rh + h^2 + r^2$$

or $\qquad 2Rh = h^2 + r^2 \qquad (86)$

Now the cosine is ratio of the adjacent side to the hypotenuse:

$$\cos\theta = \frac{R - h}{R} = \frac{2Rh - 2h^2}{2Rh} \qquad (87)$$

where the second equation was obtained by multiplying the numerator and denominator by 2*h*. Substituting 2*Rh* from (86):

$$\cos\theta = \frac{\left(h^2 + r^2\right) - 2h^2}{h^2 + r^2} = \frac{r^2 - h^2}{r^2 + h^2}$$

With this substitution, (85) becomes Young's equation (76).

Lecture #12 begins here

Methods of Measuring Contact Angle

Ref: Adamson, p341

The contact angle ranks with surface tension as an important parameter in the characterization of liquid surfaces. However, from the analysis above, we see that the contact angle reflects not only properties of the L/V interface, but also of the S/V and S/L interface.

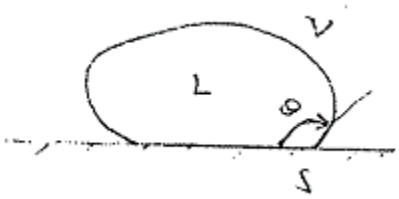

Sessile Drop - Photograph drop, then measure contact angle on enlargement.With clean,smooth, chemically homogeneous surfaces, and good optics, you can measure θ ±1º. Alternatively, telescopes are available with a goniometer eyepiece (from Greek *gonia*, meaning "angle").

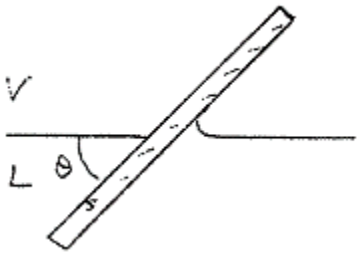

Tilted Plate - The angle of inclination of the plate is varied until liquid surface on one side of the plate remains flat right up to the plate. The angle of inclination of the plate can be measured directly with a protractor. A disadvantage of this technique is that you need a much larger volume of liquid and more space.

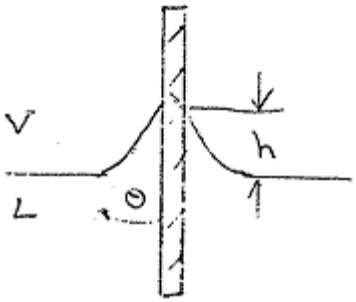

Wilhelmy plate - Although the angle can be measured directly, the rise height can often be measured more accurately. With proper illumination, the termination of the menicus can be made quite sharp. This height is related to the contact angle:

$$\sin\theta = 1 - \frac{\rho g h^2}{2\gamma}$$

Perhaps the most accurate measurement of contact angle has been made with this method (±0.1º).

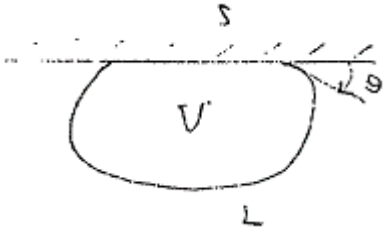

Sessile Bubble - has the advantage that gas rapidly reaches equilibrium with the liquid (recall that contact angle reflects equilibrium properties).

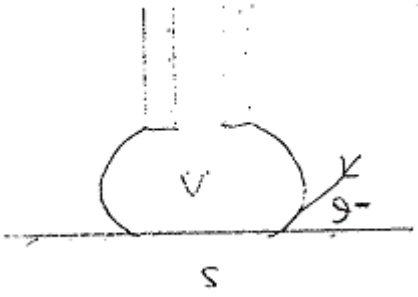

Captive Bubble - A bubble, formed at the tip of a pipette, is forced against the plate. The main advantage is that the volume of the bubble is easily varied.

Contact Angle Hysteresis

The experimental methods used to evaluate θ are not particularly difficult, but the results can be quite confusing. For example, one complication frequently observed is that the contact angle may

depend on whether the edge of a sessile drop was advancing or receding during the time just before the measurement was taken (even if the shape is constant at the time of the measurement). This is called contact angle *hysteresis*.

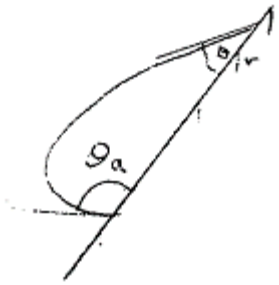

A familiar example is rain drop on a window pane, or any tilted plane. Explanations include:

- Contamination
- Roughness
- Surface inhomogeneity

All of which are likely to apply to a window pane.

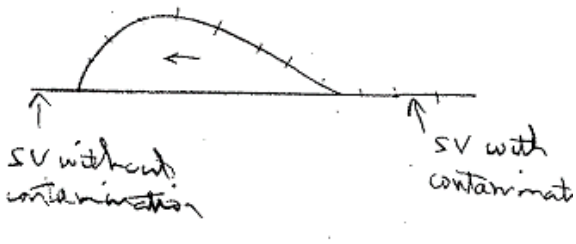

Contamination. If the liquid contains a surfactant which tends to adsorb at the L/V interface, motion of the drop down the plane will transfer the surfactant to the S/V interface behind the drop. This has the tendency to make γ_{SV} higher on the trailing side of the drop, giving rise to a smaller contact angle.

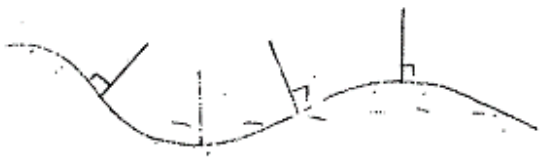

Roughness. Likewise, if the surface has microscopic roughness, the contact angle measured relative to an apparent flat surface will depend on position.

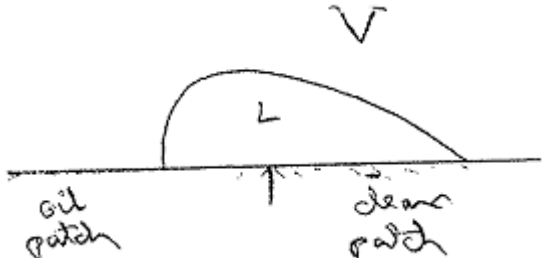

Heterogeneity. For example, part of the solid surface may contain patches of oil. If the drop straddles the boundary of this patch, the contact angle at the two sides of the drop will be different. The drop keeps moving down the plane until the net surface forces are large enough to overcome gravity and halt the downward acceleration. Generally this corresponds to a shape like that shown, in which the advancing angle is larger than the receding angle.

Although the difference in advancing and receding contact angles for clean, homogeneous, smooth surfaces tends to be within experimental error, it can be enormous. A particularly bad case is mercury on steel, in which a hysteresis of 154° has been reported. Most of the values reported are advancing contact angles.

Methods for Measuring Surface Tension

Capillary Rise

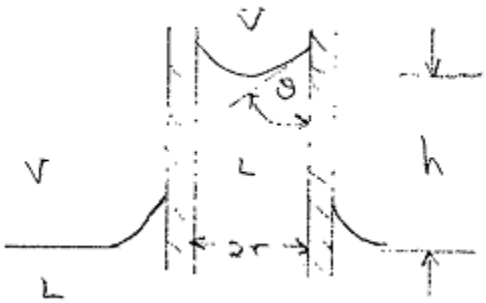

This technique was discussed earlier. One disadvantage with this technique is that, in order to deduce the surface tension from the measured rise height, you must know the contact angle.

ideal: $$\Delta\rho g h = \frac{2\gamma}{r}\cos\theta$$

Fortunately, most liquids completely wet glass, making a zero contact angle. This equation is "ideal" because it

- neglects the weight of the meniscus, and it
- neglects departure from spherical shape.

Corrections for both of these neglected effects can be calculated.

Wilhelmy Plate

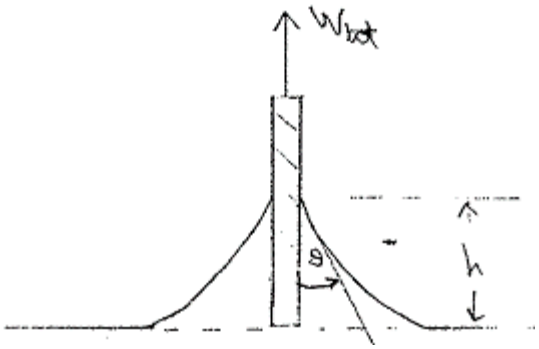

Suppose we slowly lower a vertical flat plate until it just comes in contact with the liquid. The fluid will pull down on the plate with a force which is in addition to the dry weight of the plate.

$$W_{tot} - W_{plate} = \Delta W = \gamma p \cos\theta$$

where p is the total length of the contact line (i.e. the perimeter of the cross section of the plate).

Using equations that describe the shape of the interface, one can also show that rise height is related to the surface tension and contact angle:

$$\left(\frac{h}{a}\right)^2 = 1 - \sin\theta$$

where a is the capillary constant defined by (75). Thus by measuring ΔW and h, one can deduce both γ and θ.

Modes of operation:

- Slowly raise liquid until contact is made
- With plate initially submerged, slowly increase force on plate until plate rising out of the liquid and breaks free of it.

With good technique W_{tot} measured in either mode is within 0.1%.

Drop-Weight Method

Suppose I form a liquid drop on the end of a pipette, then slowly add more liquid to the drop until finally it detaches from the pipette. To a first approximation, the weight of the drop at detachment is given by Tate's law (1864):

$$W = 2\pi r\,\gamma$$

This would be correct if, at the instant of detachment, the drop had the shape of a hemisphere, so that the surface tension acts in a purely vertical direction. In most liquids, the shape of the drop is not that of a hemisphere. Usually, the drop tends to "neck" just before detaching (as shown above). The fact that the surface of the drop is not tangent to the outer cylinder of the pipette makes the vertical component of the surface tension force less than $2\pi r\gamma$:

$$W = 2\pi r\gamma\, f\left(\frac{r}{V^{1/3}}\right)$$

where $V = W/\rho g$ is the volume of the detached drop and f is a correction factor which can be computed knowing the shape of the drop just before detachment.

Tensiometer (DuNouy Ring)

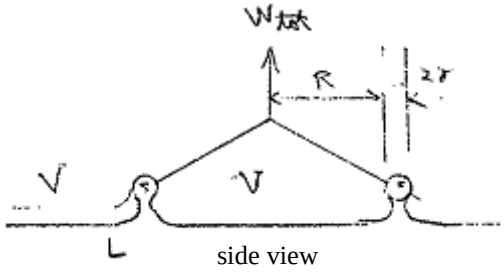

side view

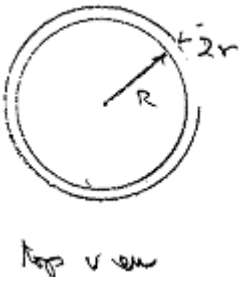

top view

One of the most common commercial instruments for measuring surface tension is the "Tensiometer," which is based on the principle of the DuNouy ring. It is similar to the Wilhelmy plate in the sense that ΔW is measured, but instead of a vertical plate, a ring is used.

Most commercial apparatuses of this type apply the force by means of a torsion wire. This has the advantage that it is easly to continuous and slowly increase the force by twisting the wire. So the idea is to start with the ring submerged and slowly increase the force until the ring detaches from the liquid. To a first approximation, this critical force exceeds the weight of the dry ring by

$$W_{tot} = W_{ring} + \gamma p \cos\theta$$

where p is the wetted perimeter, which equals twice the circumference of the ring if $r<<R$:

$$p = 2\,(2\pi R)$$

Usually a platinum ring is used. Since Pt is completely wet by most liquids

$$\cos\theta = 1$$

However, just because the contact angle is zero doesn't mean the surface tension force will be purely vertical. Just like the drop tends to neck just before detaching, the liquid hanging from the ring tends to neck just before detaching. This has the effect of decreasing the vertical component of the surface tension force by an amount dependent on the shape of the meniscus. The final result is

$$W_{tot} = W_{ring} + 4\pi R\gamma\, f\left(\frac{R^3}{V}, \frac{R}{r}\right)$$

where V is the meniscus volume.

Shapes of Bubbles and Drops

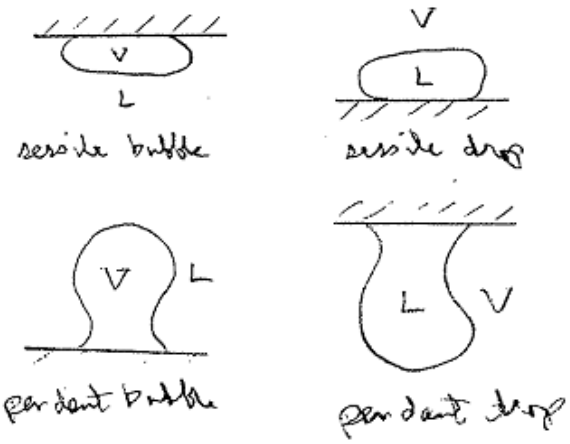

We have already pointed out that a small bubble or drop will tend to be spherical. But when the radius of the sphere becomes comparable to or larger than the capillary radius, the shape is nonspherical. By measuring how nonspherical the drop or bubble is, we can deduce the surface tension.

Sessile drops or bubbles or pendant drops or bubbles might be photographed and their shape determined. Interpretation of this shape requires a predictive model. Such a model was developed by Bashforth & Adams (1883).

Detergency and Work of Adhesion

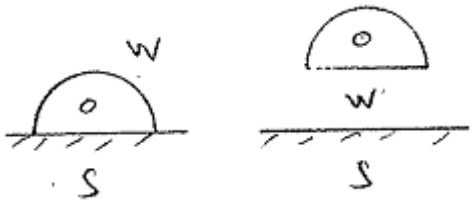

Consider a drop of oil adhering to a solid surface, completely surrounded by water. Generally speaking, it takes work to remove the drop from the solid surface. This work of adhesion is the difference in surface energies between the attached and detached drop. To detach the drop, we must add energy to form additional O/W and S/W interface, but some of this is recovered from the decrease in O/S:

$$W_{SOW} = \gamma_{OW} + \gamma_{SW} - \gamma_{SO}\ [=]\ \mathrm{J/m^2}$$

From Young's equation (76):

$$\gamma_{OW}\cos\theta = \gamma_{SW} - \gamma_{SO}$$

Substituting this into the previous equation:

$$W_{SOW} = \gamma_{OW}(1+\cos\theta) \qquad (2)$$

To make it easier to remove the soil by mechanical scrubbing, we must reduce the work of adhesion. This can be accomplished by adding chemicals called "detergents" which either reduce γ_{OW} or make $\cos\theta \rightarrow -1$ (completely non-wetting drop).

Spreading of L/L Interface

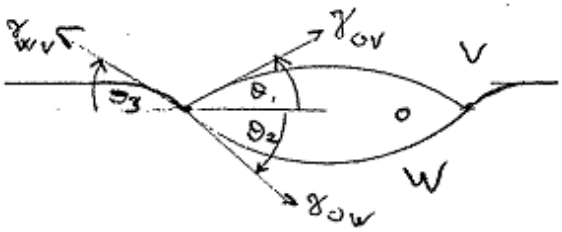

Suppose I have two immiscible liquids and I place a drop of one liquid on a pool of the more dense liquid. What will happen? There are three possible outcomes:

- form a lens
- spread to form monolayer
- spread to monolayer with excess in lenses

The choice among these depends of the relative values of the three interfacial tensions. A balance of horizontal components at the three-phase contact line yields (This same result can be obtained by minimization of surface free energy):

$$\gamma_{WV}\cos\theta_3 = \gamma_{OV}\cos\theta_1 + \gamma_{OW}\cos\theta_2$$

The left-hand side can be thought of as the tendency to spread while the right-hand side represents the tendency to contract. Suppose that:

$$\gamma_{WV} > \gamma_{OV} + \gamma_{OW}$$

No choice for the θ's will be able to satisfy the force balance -- the tendency to spread is just irresistible. The liquid will spread out as a thin film until it reaches the boundaries or until it becomes a monolayer.

If this inequality is not met, the liquid will contract to form a lens. Clearly, the difference in the left and right-hand sides is a measure of the tendency to spread. Thus:

$$S = \gamma_{WV} - (\gamma_{OV} + \gamma_{OW})$$

is called the ***spreading coefficient***. Some examples of various nonpolar liquids spreading on water:

Oil (O)	γ_{OV}	γ_{OW}	S
n-hexadecane	30.0	52.1	-9.3
n-octane	21.8	50.8	+0.2
n-octanol	27.5	8.5	36.8

On the basis of the value of the spreading coefficient, we can say that hexadecane will not spread on water while octanol will spread. Octane will just barely spread. Contamination tends to reduce the surface tension of water and thus it tends to reduce S and oppose spreading.

Lecture #13 begins here

Adsorption from Solution

Addition of a solute can have an important effect on the surface tension of the solution. Some examples are shown below in Fig. 7.14 from Hiemenz:

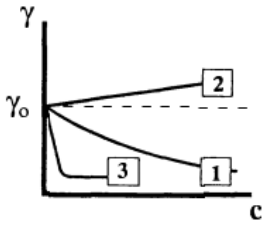

where curve 1 is typical for the addition of simple nonelectrolytes to water, curve 2 is for simple electrolytes (e.g. NaCl) and curve 3 is for amphipathic solutions (i.e. surfactants).

Thus the addition of solute can either increase or decrease the surface tension of the solution. As it turns out which effect applies to a given solute depends on whether that solute concentration is higher or lower at the interface between the liquid and gas.

Solute Concentration at Interface

We tend to think of the interface between liquid and its vapor as a discrete plane -- so that the concentration profile is discontinuous at the interface. Indeed, the interface remains sharp even under the best microscope using visible light. However, with the much higher magnifications obtainable with an electron microscope, the interface is fuzzy. This fuzziness is not connnected with the resolving power of the microscope, but rather it is an intrinsic quality of any interface.

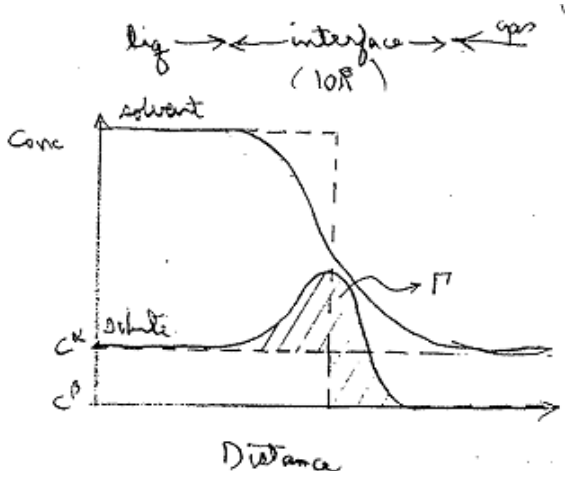

The concentration profile of the solvent varies continuously from one bulk value to another. Typically, the change in bulk concentrations occurs over a distance of about 10 Angstroms. The concentration of solute also varies continuously with distance across an interface. However, unlike the solvent profile – which is usually monotonic – the solute centration profile often has maximum value near the interface. Solutes which have this characteristic are called:

surfactant - a solute which has a higher concentration at the interface than in the bulk; a solute which lowers the surface tension of the solution.

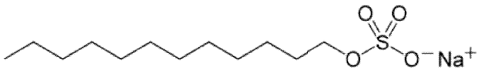

a sodium dodecyl sulfate molecule

The word "surfactant" is a contraction of "surface-active agent;" in particular, this word is formed from the underlined letters. Using the second part of this definition, sodium dodecylsulfate (SDS, molecular structure shown above) and ethanol act as surfactants in water, but NaC1 does not. As we shall soon see, SDS and ethanol also satisfy the first part of this definition.

adsorb - to accumulate at an interface (so that equilibrium concentration at interface is higher than bulk).

which is quite different from

absorb - to dissolve in the bulk (e.g. NH_3 absorbs in water.)

The quantity which measures the extent of adsorption is:

surface excess - amount of solute adsorbed per unit area

$$\Gamma \equiv \int_{-\infty}^{\infty} \left(C - C_{bulk}\right) dx$$

$$= \int_{-\infty}^{x_0} \left(C - C_{\alpha}\right) dx + \int_{x_0}^{\infty} \left(C - C_{\beta}\right) dx$$

where C_α and C_β refer to the bulk concentration of a particular species (either solvent or solute) in the phase corresponding to $x < x_0$ or to $x > x_0$, respectively, where x_0 denotes the location of the plane dividing the two phases.

Since C_{bulk} changes value at x_0, the numerical value of surface excess depends on where we choose to draw the dividing line between the two phases. The precise location of the dividing surface is *arbitrary*. One common choice is

Gibbs dividing surface – x_0 determined such that $\Gamma_{solvent} = 0$.

This turns out to be a particularly convenient choice because using this dividing surface, we can show that surface excess also has the following meaning:

$$\Gamma_i = -\left(\frac{\partial\gamma}{\partial\mu_i}\right)_{T,P} \qquad (88)$$

where μ_i is the chemical potential (partial molar Gibbs free energy) of component *i*.

Partial Proof: For a more complete derivation, see Hiemenz §7.7. Here I will just reproduce the final steps in the derivation so that you can see why Gibbs choice of a dividing surface is convenient.

First one divides the properties of the system into contributions from each of the bulk phases (denoted by superscripts α and β) and from the surface (denoted by superscript *s*):

$$G = G^{\alpha} + G^{\beta} + G^{s}$$

$$n_i = n_i^{\alpha} + n_i^{\beta} + n_i^{s}$$

where G is the Gibbs energy and n_i is the number of moles of component *i*. Recall the Gibbs-Duhem equation:

$$\sum_i n_i^k d\mu_i^k = 0$$

where $k = \alpha$ or β. This applies to either bulk phase for any constant *T,P* process. The analogous relationship for the surface "phase" turns out to be (see Hiemenz §7.7):

$$\sum_i n_i^s d\mu_i^s + A d\gamma = 0$$

Solving for dγ:♦

$$-d\gamma = \sum_i \Gamma_i d\mu_i$$

$$= \underbrace{\Gamma_{solvent}}_{0} d\mu_{solvent} + \Gamma_{solute} d\mu_{solute}$$

where $\Gamma_i \equiv n_i^s / A$

is call the ***surface excess*** of component *i* and it has units of moles per area. For a binary solution, we have only the solvent and the solute. Choosing the dividing surface such that $\Gamma_{solvent} = 0$ and solving the remainder for Γ_{solute} leads to (88) which is called ***Gibbs adsorption equation***.

For a thermodynamically ideal solution:

$$(d\mu_i)_{T,P} = RT d\ln C_i$$

Using this in (88):

$$\Gamma_i = -\frac{1}{RT}\left(\frac{\partial\gamma}{\partial\ln C_i}\right)_{T,P} \qquad (89)$$

Note that if surface tension is *decreased* by the addition of the solute, the solute must be adsorbed at the interface ($\Gamma > 0$). This is the case for most nonelectrolytes and surfactants. On the other hand, addition of a simple electrolyte like NaCl *increases* surface tension, which implies negative adsorption ($\Gamma < 0$). Negative adsorption of ions arises because of the strong electrostatic attraction between any ion and the water dipole.

Addition of many solutes results in a linear decrease in surface tension with ln(C) over a couple of decades of concentration. For example, the figure below (taken from p145 of Berg) shows the surface tension of alcohol-water mixtures.

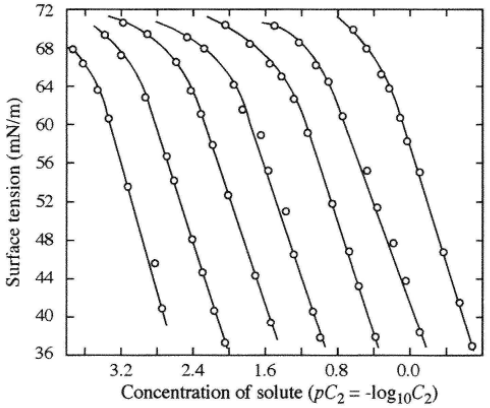

Fig. 3-19: Surface tension dependence on concentration for aqueous solutions of the normal alcohols ($C_2 - C_8$) at 25°C. Data from [Posner, A.M., Anderson, J.R. and Alexander, A.E., *J. Colloid Sci.*, **7**, 623 (1952).]

♦ We have dropped the superscript on μ_i because at equilibium, components will distribute themselves between the phases such that $\mu_i^{\alpha} = \mu_i^{\beta} = \mu_i^{s} = \mu_i$.

Example: calculate the surface excess corresponding to the linear regions of the data above.

Solution: each of the curves have a slope of

$$\frac{d\gamma}{d\log C} = \frac{-36\dfrac{\text{mN}}{\text{m}}}{1.2} = -30\frac{\text{mN}}{\text{m}}$$

or
$$\frac{d\gamma}{d\ln C} = \frac{d\gamma/d\log C}{2.303} = -13\frac{\text{mN}}{\text{m}}$$

(89) gives

$$\Gamma = \frac{-\left(-13\dfrac{\text{mN}}{\text{m}}\right)}{\left(8.315\dfrac{\text{J}}{\text{mol-K}}\right)(298\text{ K})} = 5.3\times10^{-6}\ \frac{\text{mol}}{\text{m}^2}$$

To see if this is reasonable, let's further calculate the surface area per adsorbed molecule:

$$\frac{1}{\Gamma N_A} = 32 \text{ Angstroms}^2$$

which is about 30% higher than the known cross-sectional area of a hydrocarbon chain. Notice also that the slope is the same for all chain lengths for the alcohols in the figure (C_2 through C_8).

These two observations suggest that the alcohols are adsorbing into a fairly compact monolayer with their hydrocarbon chains protruding normal to the air/water interface as shown in the cartoon below:

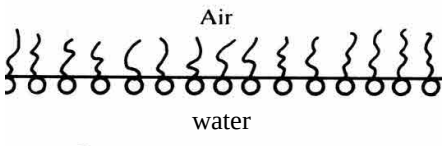

This would allow the polar –OH head group (indicated by the circles in the cartoon above) to remain in the water while the nonpolar hydrocarbon tails protrude into the air. This also explains why the slope becomes constant at high concentration: the adsorbed layer becomes saturated.

Langmuir Isotherm

Adsorption at solutes at the air-water interface generally follow a ***Langmuir adsorption isotherm***:

$$\Gamma(C) = \frac{\Gamma_{\max} C}{C_{sat} + C} \qquad (90)$$

where $\Gamma_{\max}$ is the surface excess of the saturated monolayer while C_{sat} is the solute concentration in the bulk solution roughly corresponding to the onset of the saturated monolayer. For the alcohols in the figure above, $\Gamma_{\max}$ = 5.3 μmol/m^2 for all while C_{sat} varies between 0.2 mM for octanol to 0.4 M for ethanol.

For $C \ll C_{sat}$, the Langmuir isotherm is approximated by

$$\Gamma \approx \frac{\Gamma_{\max}}{C_{sat}} C$$

and
$$L_{ads} \equiv \lim_{C\to 0} \frac{\Gamma}{C} = \frac{\Gamma_{\max}}{C_{sat}}$$

is called the ***adsorption length***. This represents the thickness of a layer of solution having concentration C which contains the same number of molecules Γ per unit area as adsorb. This parameter is a measure of the tendency for the solute to adsorb: a larger adsorption length means a stronger tendency to adsorb. For the alcohols, L_{ads} varies between 10 nm for ethanol to 20 μm for octanol. This can be rationalized by noting that the longer the nonpolar tail of the alcohol, the happier the molecule is at the interface where it can place its tail in air.

Eliminating Γ between (89) and (90):

$$-\frac{1}{RT}\frac{d\gamma}{d\ln C} = \frac{\Gamma_{\max} C}{C_{sat} + C}$$

or
$$d\gamma = -RT\Gamma_{\max}\frac{dC}{C_{sat} + C}$$
$$= -RT\Gamma_{\max} d\ln\left(C_{sat} + C\right)$$

Integrating from $C = 0$ and $\gamma = \gamma_0$ (pure water) to $C = C$ and $\gamma = \gamma$:

$$\int_{\gamma}^{\gamma_0} d\gamma = -RT\Gamma_{\max}\int_{C}^{0} d\ln\left(C_{sat} + C\right)$$
$$= RT\Gamma_{\max}\int_{0}^{C} d\ln\left(C_{sat} + C\right)$$

$$\gamma_0 - \gamma = RT\Gamma_{\max}\ln\left(\frac{C_{sat} + C}{C_{sat}}\right) \qquad (91)$$

which is called ***Szyszkowski's equation***.

Another example of how surface tension is affected by solute concentration is Fig. 7.15 from Hiemenz:

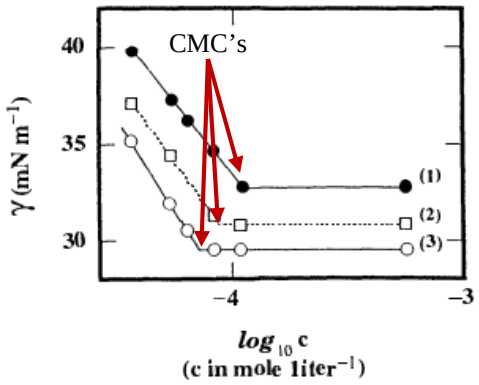

for the dodecylether of hexaethylene oxide [i.e. $H(CH_2)_{12}O(C_2H_2O)_6$] at three different temperature: curve 1 is 15ºC, curve 2 is 25ºC and curve 3 is 35ºC.

For any concentration of the solute (a surfactant), the surface tension decreases with temperature. This also occurs for pure water where we argued that, as we increase toward the critical temperature for water, all differences between liquid and vapor vanish. It was the difference in density of liquid and vapor which was cited as the reason why water molecules near the interface felt a net force pulling them into the liquid, which is the molecular origin of surface tension.

Like the corresponding data for the alcohols, this solute also displays a linear decrease in surface tension with the log of the concentration of solute. However, the three straight lines do not have the same slope: generally the slope is more negative for higher tempature, suggesting that Γ_{max} increases with temperature.

Micellization

One dramatic difference between Fig. 7.15 and the earlier figure with the alcohols is the leveling out of the surface tension at higher concentrations. This plateau is very typical of surfactant solutions.

Does this zero slope imply that $\Gamma = 0$ as suggested by Gibbs adsorption equation (89)? Such a sudden drop in Γ from Γ_{max} to zero is highly unlikely. Moreover, not only does surface tension show an abrupt change in behavior with concentration at this particular concentration, but several other properties as well:

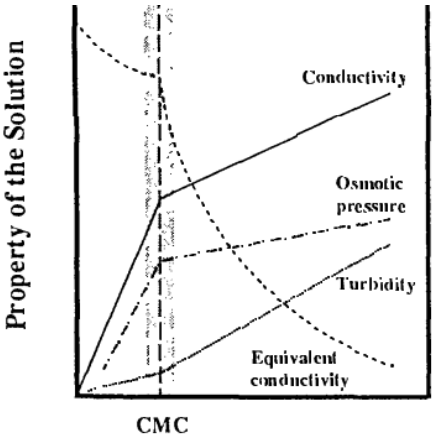

Aggregation of surfactant molecules into clusters provides a plausible explanation for all of these trends. These clusters are called:

micelles - aggregates of surfactant molecules

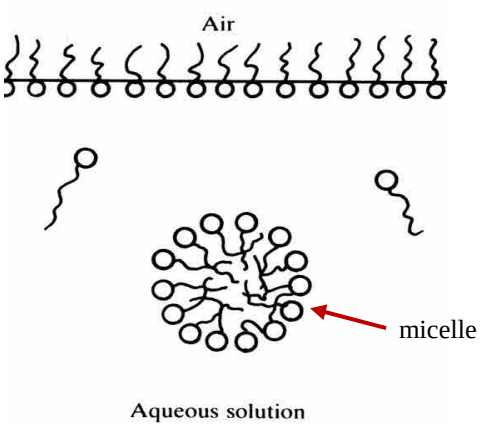

The solute concentration above which micelles form is called the ***critical micelle concentration*** or CMC. The process of micellization occurs with molecules which are

amphiphilic – soluble in both polar and non--polar sovents

Amphiphilic molecules are usually composed of a hydrocarbon chain (an alkane) attached to a polar group (e.g. –OH or $–SO_4$). The polar group is sometimes called the ***head*** while the hydrocarbon chain is called the ***tail***. Here is the structure for SDS (see page 46):

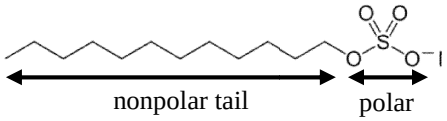

TABLE 8.1 Critical Micelle Concentration, Degree of Aggregation, and Effective Fractional Ionization for Several Surfactants With and Without Added Salt

Surfactant	Solution	Critical micelle concentration (mole liter^{-1})	Aggregation number n	Ratio of charge to aggregation number, z/n
Sodium dodecyl sulfate	Water	0.00810	80	0.18
	0.02 M NaCl	0.00382	94	0.14
	0.03 M NaCl	0.00309	100	0.13
	0.10 M NaCl	0.00139	112	0.12
	0.20 M NaCl	0.00083	118	0.14
	0.40 M NaCl	0.00052	126	0.13
Dodecylamine hydrochloride	Water	0.01310	56	0.14
	0.0157 M NaCl	0.01040	93	0.13
	0.0237 M NaCl	0.00925	101	0.12
	0.0460 M NaCl	0.00723	142	0.09
Decyl trimethyl ammonium bromide	Water	0.06800	36	0.25
	0.013 M NaCl	0.06340	38	0.26
Dodecyl trimethyl ammonium bromide	Water	0.01530	50	0.21
	0.013 M NaCl	0.01070	56	0.17
Tetradecyl trimethyl ammonium bromide	Water	0.00302	75	0.14
	0.013 M NaCl	0.00180	96	0.13

Source: J. N. Phillips, *Trans. Faraday Soc.*, **51**, 561 (1955).

Since the molecule has both polar and non-polar parts, it is soluble in both kinds of solvents.

In water, SDS forms spherical micelles with the tails on the inside and the heads ors the outside. In this way, the non-polar parts of the molecule are away from the polar solvent, forming a non-polar interior phase. In non-polar solvents, inverted micelles are formed, having the polar group on the inside. The number of molecules in a single micelle depends primarily on the length of the hydrocarbon chain: see Table 8.1 above.

Lecture #14 begins here

Any concentration of surfactant above the CMC goes into forming micelles – not into increasing the concentration of monomers. To clarify this point, let C denote the total concentration of surfactant added to a solution, which is distributed between monomer surfactant molecules and micelles:

$$[\text{micelles}] = \begin{cases} 0 & \text{for } C < CMC \\ \dfrac{C - CMC}{N} & \text{for } C > CMC \end{cases}$$

$$[\text{monomer}] = \begin{cases} C & \text{for } C < CMC \\ CMC & \text{for } C > CMC \end{cases}$$

$$C = [\text{monomer}] + N\,[\text{micelles}]$$

where N is the aggregation number (i.e. the number of surfactant molecules per micelle).

Returning to Fig. 7.15 on page 49: the reason for the plateau above the CMC is that C which appears in (90) and (91) is the monomer concentration – not the total concentration. Since the monomer concentration is constant above the CMC, so Γ and γ are constant above the CMC.

Solubilization

Surfactant solutions above the CMC can solubilize otherwise insoluble material. This is dramatically illustrated by certain organic dyes which are insoluble in water. Because of the low solubility, these dye solutions are practically colorless without SDS. Addition of SDS at concentrations above the CMC results in intensely colored solution. The dye, being more soluble in non-polar solvents, has been incorporated in the center of the micelle.

Surfactant Types

SDS is said to be an ***anionic*** surfactant. When it is dissolved in water, it dissociates into a sodium ion and a negatively charged (i.e. anionic) tail:

$$H(CH_2)_{12}SO_4^-Na^+ \rightarrow H(CH_2)_{12}SO_4^- + Na^+$$

Other anionic surfactants include sodium stearate:

$$H(CH_2)_{17}COO^-Na^+$$

An example of a ***cationic*** surfactant is hexadecyltrimethylammonium bromide (CTAB):♠

$$H(CH_2)_{16}N(CH_3)_3^+Br^-$$

Of course, the polar group need not be ionic. Perhaps the most common ***nonionic*** surfactants are the polyethylene oxides:

$$H(CH_2)_nC_6H_4(OCH_2CH_2)_mOH$$

which consists of a nonpolar alkane chain connected through a benzene ring to a polar polyethylene oxide chain. By varying the length of either chain, you can achieve a wide variety of properties. They are commercially available as the Brij® series (ICI America).

TABLE 8.5 Names and Structures of Some Typical Phospholipid Surfactants

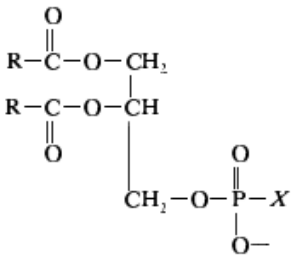

Name	X
Phosphatidic acid	$-OH$
Phosphatidylcholine	$-OCH_2CH_2\overset{+}{N}(CH_3)_3$
Phosphatidylethanolamine	$OCH_2CH_2NH_2$
Phosphatidylserine	$-OCH_2CCHNH_2$ (COOH)
Phosphatidylthreonine	$-OCH-CH-NH_2$ (CH_3, COOH)
Phosphatidylglycerol	$-OCH_2CHCH_2OH$ (OH)

♠ "Hexadecyl" is also called "cetyl" – hence the C in CTAB.

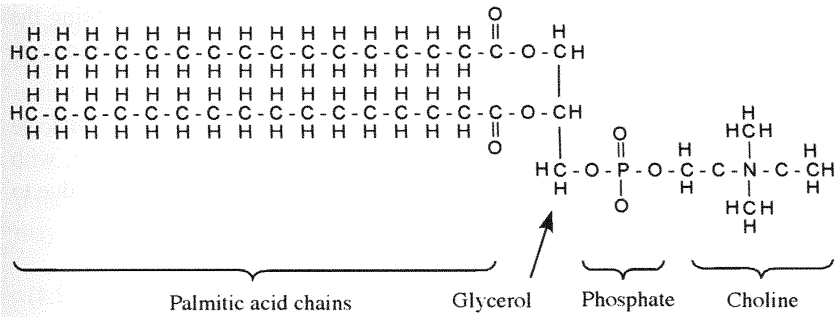

Fig. 2-6: Stylized diagram of a lung surfactant molecule: L-a, dipalmitoyl lecithin.

Phospholipids are an biologically important class of surfactants. They have two tails instead of one. They also tend to form bilayers which are the basis of all cell membranes. One of them (dipalmitoyl lecithin) is a lung surfactant which keeps the air sacs open in the lung by reducing surface tension; without them capillarity would make breathing almost impossible.

Micelle Shape

Spheres are not the only shapes which micelles can take.

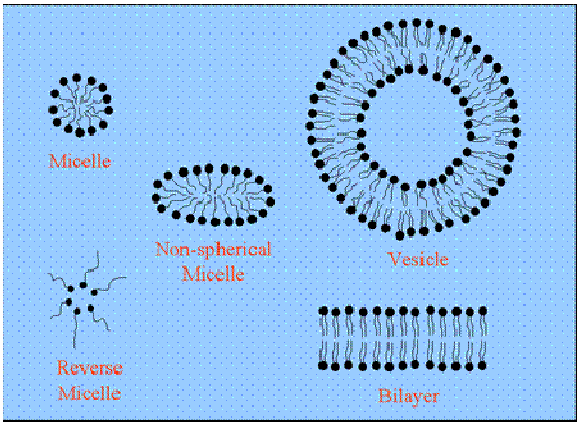

Other shapes include cylinders, lamellar bilayers and vesicles. Vesicles are also bilayer structures. Perhaps the most common occurance of this bilayer structure is in biological systems.

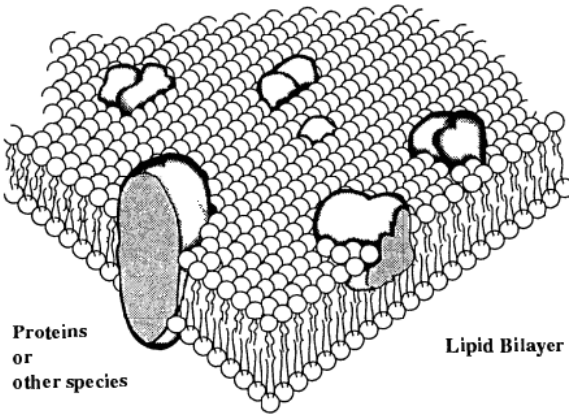

Lipid bilayers of phosphoglycerides are a very important part of nearly all biological membranes -- from cell walls to the lining of the gut. Their function in biology is to make transport of solutes through the membrane highly selective.

Packing Factor

The shape of the micelle depends largely on the architecture of the surfactant molecules: in particular, the size the headgroup relative to the size of the tail. This is quantified in a dimensionless number called the packing factor:

$$P \equiv \frac{v_t}{a_h \ell_t} = \frac{a_t}{a_h}$$

where v_t is the volume of the micelle core per surfactant molecule, a_t is the cross-sectional area of the headgroup and ℓ_t is the length of the tail. If we think of the tail as a cylinder then the ratio of its volume to its length would equal its cross-sectional area. Thus the packing factor can also be thought of as the ratio of the cross-section of the tail to the area of the headgroup.

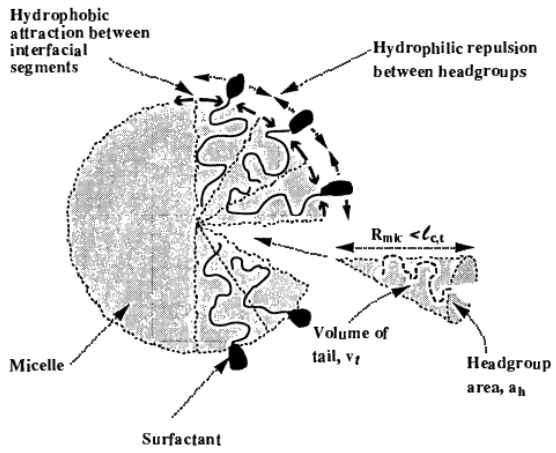

The area occupied by the headgroup depends on the balance between hydrophobic attraction between tail segments near the outer edge of the core and hydrophilic repulsion between the headgroups themselves (as suggested by the figure above).

For surfactants having alkane tails, the fully extended length and volume can be estimated from known structural properties of alkane molecules: normal alkanes have a C-C bond length of 0.154 nm and a bond angle of 109.5°. The terminal methyl group has a radius of 0.21 nm while the half length of the bond between the alkane and the polar head is 0.06 nm.

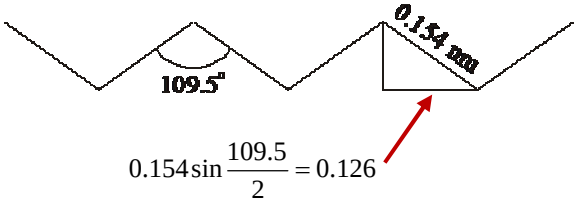

$$0.154 \sin\frac{109.5}{2} = 0.126$$

Using this information we can deduce a formula for the extended length of an *n*-carbon alkane chain:

$$\ell_t = [0.21 + 0.126(n-1) + 0.06]\ \text{nm}$$
$$= (0.144 + 0.126n)\ \text{nm}$$

This is close to what Tanford (1980) recommends:

$$\ell_t = (0.154 + 0.1265n)\ \text{nm}$$

and $\quad v_t = (27.4 + 26.9n)\times 10^{-3}\ \text{nm}^3$

Example: show that the packing factor must be less than 1/3 in order to get spherical micelles.

Solution: let R_s denote the radius of the core of the micelle. Dividing the volume of the core by the volume of the tail of one surfactant molecule yields the number of surfactant molecules (i.e. the aggregation number):

$$n_a = \frac{\frac{4\pi}{3}R_s^3}{v_t}$$

Dividing the surface area of the spherical micelle by the area per headgroup also yields the aggregation number:

$$n_a = \frac{4\pi R_s^2}{a_h}$$

Eliminating n_a between these two equations:

$$\frac{v_t}{a_h} = \frac{R_s}{3}$$

Dividing both sides by the length of the tail yields the packing factor:

$$P \equiv \frac{v_t}{a_h \ell_t} = \frac{R_s}{\ell_t}\frac{1}{3} \le \frac{1}{3}$$

Now the radius of the core must be less than the extended length of the hydrocarbon tail (otherwise you would have a vacuum at the center); in other words $R_s/\ell \le 1$.

Larger values of the packing factor leads to other shapes for micelles as shown in table 8.2:

TABLE 8.2 Packing Parameter and Its Relation to Shapes of Aggregates

Lipid	Critical packing parameter	Critical packing shape	Structures formed
Single-chained lipids (surfactants) with large head group areas: SDS in low salt	$<1/3$	Cone 	Spherical micelles 
Single-chained lipids with small head group areas: SDS and CTAB in high salt, nonionic lipids	1/3–1/2	Truncated cone 	Cylindrical micelles 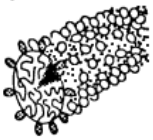
Double-chained lipids with large head group areas, fluid chains: phosphatidyl choline (lecithin), phosphatidyl serine, phosphatidyl glycerol, phosphatidyl inositol, phosphatidic acid, sphingomyelin, DGDG,[a] dihexadecyl phosphate, dialkyl dimethyl ammonium salts	1/2–1	Truncated cone 	Flexible bilayers, vesicles 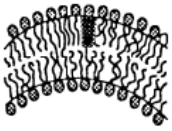
Double-chained lipids with small head group areas, anionic lipids in high salt, saturated frozen chains: phosphatidyl ethanolamine phosphatidyl serine + Ca^{2+}	~1	Cylinder 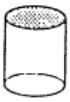	Planar bilayers 
Double-chained lipids with small head group areas, nonionic lipids, poly (cis) unsaturated chains, high T: unsaturated phosphatidyl ethanolamine, cardiolipin + Ca^{2+} phosphatidic acid + Ca^{2+} cholesterol, MGDG[b]	>1	Inverted truncated cone or wedge 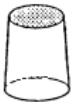	Inverted micelles 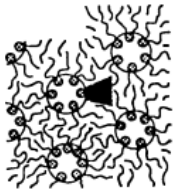

Lecture #15 begins here

Intermolecular Forces

Reading: Hiemenz Chapt. 10

Intermolecular forces are responsible for many macroscopic effects:

- departure from ideal-gas behavior
- phase changes: condensation and solidification
- surface tension of liquids
- instability of colloidal dispersions

van der Waals forces are so called because these are the forces J.D. van der Waals invoked in this Ph.D. thesis in 1873 to explain departures from ideal-gas behavior. It was his thesis that first derived the van der Waals equation of state for nonideal gas behavior.

van der Waals himself did not know precisely the origin or nature of these forces. He just proposed that intermolecular attractions existed and were the cause of departures from ideal-gas behavior. Today we know that there are several type of intermolecular interactions that are important:

- dipole — dipole
- dipole — induced dipole
- instantaneous dipole — induced dipole

Charge-Charge Interactions

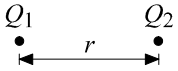

This is just the type of interaction described by Coulomb's law in its most simple form.

$$F = \frac{1}{4\pi\varepsilon}\frac{Q_1 Q_2}{r^2}$$

which is positive for repulsion (i.e. $Q_1Q_2 > 0$). The sign convention on interaction energy is such that repulsion also causes a positive potential energy $W(r)$ which requires

$$F(r) = -\frac{dW}{dr}$$

where $W(r)$ is the work required to bring charges from $r = \infty$ to $r = r$:

$$W(r) = -\int_{\infty}^{r} F(r')\,dr' = \int_{r}^{\infty} F(r')\,dr' = \frac{Q_1 Q_2}{4\pi\varepsilon r}$$

which is the work to bring charges together from $r' = \infty$. We know that like charges repel one another and produce

repulsion: $Q_1Q_2 > 0 \quad \rightarrow \quad W > 0$

Likewise, unlike charges attract:

attraction: $Q_1Q_2 < 0 \quad \rightarrow \quad W < 0$

This is the sign convention used for the interaction energy W here and in the expressions below.

Charge-Dipole

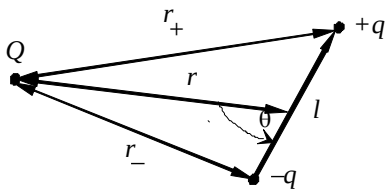

Here we have three charges in the system, rather than two. We can calculate the force on the monopole charge as the sum of the force from each of the two charges, then integrate out to infinity to obtain the potential. The result is

$$W(r) = -\frac{qQ}{4\pi\varepsilon}\left(\frac{1}{r_-} - \frac{1}{r_+}\right)$$

When $l << r$, we can approximate:

$$r_- \approx r - \tfrac{1}{2} l\cos\theta$$

$$r_+ \approx r + \tfrac{1}{2} l\cos\theta$$

Then $$W = -\frac{1}{4\pi\varepsilon}\frac{Qp}{r^2}\cos\theta \qquad (92)$$

where $$p = ql$$

is the dipole moment. Note that the decay of energy is more rapid with separation distance than for the interaction of two monopoles.

Dipole-Dipole

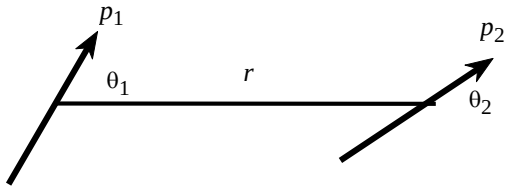

For each of the two point charges in the left dipole, we have two terms — one for each charge in the right dipole. For point dipoles, brought together at fixed orientation, the interaction energy is

$$W(r,\theta_1,\theta_2,\phi) = -\frac{p_1 p_2}{4\pi\varepsilon r^3}\left[2\cos\theta_1\cos\theta_2 - \sin\theta_1\sin\theta_2\cos\phi\right]$$

In the figure, we have shown the two dipole vectors lying in the same plane with the line between their centers. In general the three lines will lie in two different planes. ϕ is the angle between these two planes (not shown in figure).

Charge-Rotating Dipole

In calculating the above energies, we have assumed that the orientation of the dipoles was fixed. But the dipole moment of a water molecule, for example, undergoes rotary Brownian motion and can sample all orientations. Each orientation has associated with it some potential energy of interaction (with a monopole or another dipole) which determines the probability of finding that orientation.

$$P(r,\theta,\phi) \propto \exp\left[-\frac{W(r,\theta,\phi)}{kT}\right]$$

where orientation requires two angles (θ,ϕ) to specify. The proportionality constant is determined by normalization of the probability density:

$$\int P(r,\Omega)d\Omega = \int_0^{2\pi}\left\{\int_0^{\pi} P(r,\theta,\phi)\sin\theta\, d\theta\right\} d\phi = 1$$

where the integration is over all orientations and where Ω is a solid angle and shorthand for (θ,ϕ). We can now define an average interaction energy:

$$e^{-W_{av}/kT} = \left\langle e^{-W/kT}\right\rangle = \frac{\int e^{-W/kT} d\Omega}{\int d\Omega}$$

This average energy has the property that its Boltzmann factor is the same as the average of the Boltzmann factor over all orientations. In general, this average is a complicated function. Suppose $|W|$ is always small compared to kT. Then we can replace the exponential by its truncated Taylor series expansion:

$$e^{-W/kT} = 1 - \frac{W}{kT} + \frac{1}{2}\left(\frac{W}{kT}\right)^2 + \ldots$$

Next we integrate over all orientations (θ,ϕ) of the dipole:

$$\int e^{-W/kT} d\Omega = \int d\Omega - \frac{1}{kT}\int W d\Omega + \frac{1}{2}\frac{1}{(kT)^2}\int W^2 d\Omega + \ldots$$

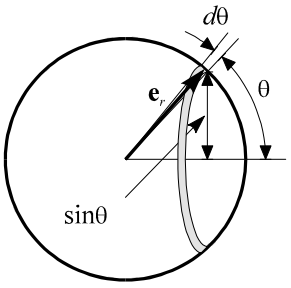

where $d\Omega = \sin\theta\, d\theta\, d\phi$ is an element of solid angle. Then the integrals over the solid angle can be computed as ...

$$\int d\Omega = \int_0^{2\pi} d\phi \int_0^{\pi} \sin\theta d\theta = 4\pi$$

Recall that for a ion interacting with a point dipole:

$$W = -\frac{1}{4\pi\varepsilon}\frac{Qp}{r^2}\cos\theta = W_o\cos\theta$$

where W_o is the part of W which is independent of orientation.

$$\int W\, d\Omega = W_o 2\pi \int_0^{\pi} \sin\theta\cos\theta d\theta = 0$$

The remaining integral is not zero, however, and evaluating it we obtain for $|W| < kT$:

$$W_{av} \approx -\frac{Q^2 p^2}{6(4\pi\varepsilon)^2 kTr^4}$$

Notice that for a freely rotating dipole, the interaction decays as r^{-4} instead of r^{-2}. This came from squaring the interaction energy. Also notice that the interaction energy is now ***temperature dependent***.

Free Dipole/Dipole

If both dipoles are free to undergo Brownian rotation and if the interaction energy is small so that their orientation is not strongly biased, then we can perform a similar analysis which leads to:

$$W_{av} \approx -\frac{p_1^2 p_2^2}{3(4\pi\varepsilon)^2 kTr^6} \qquad (93)$$

once again assuming $|W| < kT$. This result for W_{av} is sometimes called the ***Keesom interaction***. Again the orientation-average decays more rapidly with r that for fixed dipoles and the interaction is temperature dependent.

Charge-Neutral Atom

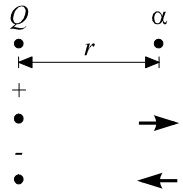

Suppose we have a neutral atom in the vicinity of point charge or an ion. The electric field "given off" by the ion will polarize the neutral atom, producing a dipole. If the ion is positive, the dipole will point away, resulting in attraction between the ion and the induced dipole.

If the ion is negative, the dipole will point toward the ion, resulting again in attraction. Now let's quantify this description. According to Coulomb's law, the force between two point charges is:

$$F = \frac{Qq}{4\pi\varepsilon r^2}$$

Thus the electric field given off by one of them, say Q, is

$$E = \frac{F}{q} = \frac{Q}{4\pi\varepsilon r^2}$$

The strength of the dipole induced by this electric field is

$$p = \alpha E = \frac{\alpha Q}{4\pi\varepsilon r^2} \qquad (94)$$

where α is the appropriate atomic polarizability (either electronic or orientational). Now we can compute the interaction energy between a point charge and a point dipole. For a fixed permanent dipole, this energy is given by (92):

$$W_{perm} = -\frac{1}{4\pi\varepsilon}\frac{Qp}{r^2}\cos\theta \qquad (95)$$

This is the work required to bring a permanent dipole from $r=\infty$ to $r=r$. In our case, the dipole moment is not independent of r, so this expression is not directly applicable. However, we can use this expression to calculate the force between the charge and the induced dipole at any separation (taking $\cos\theta = \pm 1$ so as to obtain the expected attraction):

$$F = -\frac{dW_{perm}}{dr} = -\frac{2}{4\pi\varepsilon}\frac{Qp}{r^3}$$

Substituting p from (94):

$$F = -\frac{2\alpha Q^2}{(4\pi\varepsilon)^2 r^5}$$

Finally, we compute the energy by integrating the force from ∞ to r:

$$W_{ind} = -\frac{\alpha Q^2}{2(4\pi\varepsilon)^2 r^4}$$

If we had substituted (94) directly into (95), we would obtain a result twice as large. Note that this expression for the interaction between a point charge and a neutral atom (induced dipole) decays more rapidly (r^{-4}) than the interaction of a point charge and a permanent dipole (r^{-2}).

Dipole-Neutral Atom

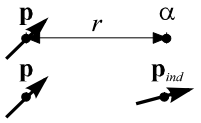

We just saw that a point charge can induce a dipole in a neutral atom in such a way that an attraction occurs between the two. In the same way a permanent dipole also generates an electric field which can induce a dipole in an otherwise neutral atom.

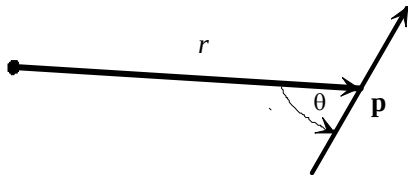

To quantify this description, we must first compute the electric field associated with the permanent dipole. Suppose we put a small test charge q in the vicinity of the dipole. What force does the test charge feel? For a point charge q interacting with a point dipole **p**, we found the energy is given by (92):

$$W = -\frac{1}{4\pi\varepsilon}\frac{qp}{r^2}\cos\theta$$

The corresponding electric field is

$$\mathbf{E} = -\frac{1}{q}\nabla W = -\frac{1}{q}\left(\mathbf{e}_r \frac{\partial W}{\partial r} + \frac{\mathbf{e}_\theta}{r}\frac{\partial W}{\partial \theta}\right)$$

Since W depends on θ as well as r, the electric field is not purely radial as in the charge-neutral atom interaction. After performing the differentiation, we obtain:

$$\mathbf{E} = -\frac{p}{4\pi\varepsilon r^3}\left(2\mathbf{e}_r \cos\theta + \mathbf{e}_\theta \sin\theta\right) \qquad (96)$$

This electric field induces a dipole moment in the neutral atom:

$$\mathbf{p}_{ind} = \alpha\mathbf{E} = -\frac{\alpha p}{4\pi\varepsilon r^3}\left(2\mathbf{e}_r \cos\theta + \mathbf{e}_\theta \sin\theta\right) \qquad (97)$$

Next we can compute the interaction between the permanent dipole $\mathbf{p}$ and the induced dipole $\mathbf{p}_{ind}$. Recall that we previously computed the potential energy of interaction for two *fixed dipoles*. The result was a complicated function of the three angles needed. That result can be expressed more compactly using vector notation:

$$W_{perm} = -\mathbf{p}_2 \cdot \mathbf{E}_1 = -\mathbf{p}_1 \cdot \mathbf{E}_2 \qquad (98)$$

where $\mathbf{E}_i$ is the electric field produced by permanent dipole $\mathbf{p}_i$. Substituting (96) and (97) into (98) gives:

$$W_{perm} = -\alpha\mathbf{E}\cdot\mathbf{E} = -\alpha E^2$$

Of course, in calculating the energy in (98), we assume that the dipole moments are independent of separation distance, whereas our induced dipole depends on separation. Proceeding as in the previous section, we could show that interaction energy is halved as a result of the varying strength of the induced dipole:

$$W_{ind} = -\frac{\alpha}{2}E^2$$

From (96):

$$E = \sqrt{E_r^2 + E_\theta^2} = \frac{p}{4\pi\varepsilon r^3}\sqrt{(2\cos\theta)^2 + \sin^2\theta}$$

$$= \frac{p}{4\pi\varepsilon r^3}\sqrt{1 + 3\cos^2\theta}$$

Finally $$W_{ind} = -\frac{\alpha p^2}{(4\pi\varepsilon)^2 r^6}\left(1 + 3\cos^2\theta\right)$$

Free Rotating Dipole - Neutral Atom

If we now let the dipole undergo rotary Brownian motion and sample different orientations, the "thermodynamic average" over the orientations is:

$$W = -\frac{\alpha_e p^2}{(4\pi\varepsilon)^2 r^6} \qquad (99)$$

which is sometimes called the ***Debye energy***. Note that if we substitute the expression orientational polarization ($\alpha = p^2/3kT$), this result reduces to Keesom energy (93) due to the interaction of freely rotating dipoles. The Debye energy refers to the contribution from electronic polarization, so we add a subscript "*e*" to remind us.

Neutral Atom - Neutral Atom (Dispersion Forces)

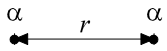

Consider the interaction of two neutral atoms — say two hydrogen atoms — which have no charge and no permanent dipole. As we shall now see, an attractive force still arises between them. To correctly calculate this force, we would need to use quantum mechanics. But we can get an intuitive feeling for the origin and strength of the force by applying classical mechanics to the Bohr picture of a hydrogen atom:

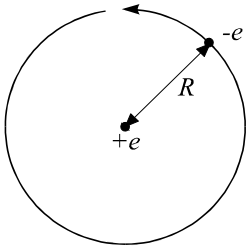

The Bohr atom is an electron orbiting a proton. Suppose the radius of the orbit is R. Then, at any instant of time, there exists a temporary dipole moment:

$$p = eR$$

This instantaneous dipole induces a dipole in a neighboring hydrogen atom. The interaction can be estimated by substituting this dipole moment into (99):

$$W = -\frac{\alpha(eR)^2}{(4\pi\varepsilon)^2 r^6} \qquad (100)$$

The electronic polarizability of a Bohr atom is given by (36):

$$\alpha = 4\pi\varepsilon R^3 \qquad (101)$$

Finally, the Bohr radius can also be related to the frequency of the orbit (ν). In classical mechanics, the orbit radius is dictated by a balance of the electrostatic attractive force and the centrifugal force

$$\underbrace{\frac{e^2}{4\pi\varepsilon R^2}}_{\text{electrostatic}} = \underbrace{\frac{mv^2}{R}}_{\text{centrifugal}} = \frac{2h\nu}{R}$$

where the second equation was obtained by equating the kinetic energy of the electron $(1/2)mv^2$ with the ***ionization potential*** $h\nu$; h is Planck's constant and ν is the frequency. Equating these two forces yields another expression for the Bohr radius:

$$R = \frac{e^2}{2(4\pi\varepsilon)h\nu} \qquad (102)$$

(100), (101) and (102) can be combined to give:

$$W \overset{(99)}{=} -\frac{\alpha(eR)^2}{(4\pi\varepsilon)^2 r^6} \overset{(100)}{=} -\frac{\frac{\alpha^2}{(4\pi\varepsilon R^3)}(eR)^2}{(4\pi\varepsilon)^2 r^6}$$

$$= -\frac{\alpha^2 \frac{e^2}{(4\pi\varepsilon R)}}{(4\pi\varepsilon)^2 r^6} \overset{(101)}{=} -\frac{\alpha^2(2h\nu)}{(4\pi\varepsilon)^2 r^6}$$

which is within a multiplicative factor (3/8) of the rigorous expression derived by London (1937) using quantum electrodynamics:

$$W = -\frac{3\alpha^2 h\nu}{4(4\pi\varepsilon)^2 r^6}$$

for the interaction of two identical atoms. For different atoms, the corresponding result is

$$W(r) = -\frac{3}{2}\frac{\alpha_{e1}\alpha_{e2}}{(4\pi\varepsilon)^2 r^6}\frac{h\nu_1\nu_2}{\nu_1+\nu_2} \qquad (103)$$

Van der Waals Forces

Consider an un-ionized gas -- one composed of polar molecules, but having no monopole charge. What are the forces which might act between such molecules? First, we have the interaction of freely rotating dipoles (Keeson energy) given by (93):

$$W_{orient} \approx -\frac{p_1^2 p_2^2}{3(4\pi\varepsilon)^2 kTr^6}$$

Next we have a freely rotating dipole causing *electronic* polarization of the other molecule (Debye energy) given by (99):

$$W_{ind} = -\frac{\alpha_{e1}p_2^2 + \alpha_{e2}p_1^2}{(4\pi\varepsilon)^2 r^6}$$

Finally, we have the dispersion energy resulting from an instantaneous dipole in one molecule causing an electron polarization in a neighboring molecule (London energy) given by (103):

$$W(r) = -\frac{3}{2}\frac{\alpha_{e1}\alpha_{e2}}{(4\pi\varepsilon)^2 r^6}\frac{h\nu_1\nu_2}{\nu_1+\nu_2}$$

Notice that each of these forces is proportional to r^{-6}. Their collective effect is called the ***van der Waals interaction***:

$$W_{vdw}(r) = -\frac{C_{vdw}}{r^6} = -\frac{C_{orient}+C_{ind}+C_{disp}}{r^6}$$

These are the forces which cause a departure from the ideal gas law as first considered by van der Waals in 1873, although he did not know the origin of the forces nor the functional form of the distance dependence. Recall that his celebrated equation of state is given by:

$$\left(P + \frac{a}{V^2}\right)(V-b) = RT$$

The constant *"a"* is associated with molecular attractions

$$a = \frac{2\pi N_A^2 C_{vdw}}{3\sigma^3}$$

while b is associated with the excluded volume occupied by the gas molecules:

$$b = (2/3)\pi N_A \sigma^3$$

where $\sigma \equiv R_1 + R_2$

is the ***collision diameter***.

Lecture #16 begins here

Retardation

We said that the dispersion component of van der Waals forces arises from the instantaneous dipole moment which any atom has as a result of the separation of electron and protons. This instantaneous dipole, in turn, induces a dipole moment in a neighboring atom. These two dipoles interact, leading to a time-average interaction which

is attractive although the time-average of the instantaneous dipole (or of the induced dipole) is zero.

In the Bohr model of the hydrogen atom which we used to derive the inverse 6^{th} power law, we treated the instantaneous and induced dipole as if they were frozen in time -- or at least quasistatic. Actually the electric field arising from the instantaneous dipole is fluctating at high frequency ν, so that the time over which it may be considered constant is very short.

$$\text{dipole life time} << 2\pi/\nu$$

Yet it takes a finite amount of time for the electric field to propagate to the second atom:

$$\text{travel time} = r/c$$

If the travel time is not short compared to the dipole life time, the primary dipole will change before its effect propagates to the second atom. This results in a weakening of the van der Waals interaction which is called the retardation effect:

if $r \ll \lambda$: $W_{vdw} \propto r^{-6}$

if $r \gg \lambda$: $W_{vdw} \propto r^{-7}$

where $\lambda = 2\pi c/\nu$

is the wavelength of radiation e mminating from the fluctuation dipole.

Van der Waals Forces between Macroscopic Bodies

Hamaker's Superposition Principle

In 1937, H.C. Hamaker estimated the attraction between macroscopic bodies (e.g. colloidal particles) by assuming that the interatomic interactions could be linearly superimposed:

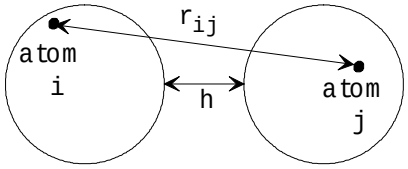

$$\phi_A = \sum_i \sum_j -\frac{C}{r_{ij}^6}$$

To make this sum tractable, let's partition the volume of these bodies into pieces dV_1 and dV_2 which are small enough so that r_{ij} is the same for all pairs of atoms in the two differential volumes. Then we just multiply the contribution for one pair of atoms by the number of such pairs in the two differential volumes:

$$\text{no. of pairs} = \underbrace{(dn_1)}_{dM/m}(dn_2) = \frac{\rho dV_1}{m}\frac{\rho dV_2}{m}$$

where m is the mass of one atom and ρ/m is the no. of atoms/vol.

$$\phi_A = -C\left(\frac{\rho}{m}\right)^2 \int_{V_1}\int_{V_2} \frac{1}{r^6}\, dV_1 dV_2$$

For the case of two spheres of radius a:

$$\phi_A(h) = -\frac{A}{12}\left[\frac{1}{s(s+2)} + \frac{1}{(s+1)^2} + 2\ln\frac{s(s+2)}{(s+1)^2}\right]$$

where $s = \dfrac{h}{2a}$ and $A = \left(\dfrac{\pi\rho}{m}\right)^2 C$ (104)

is called ***Hamaker's constant***.

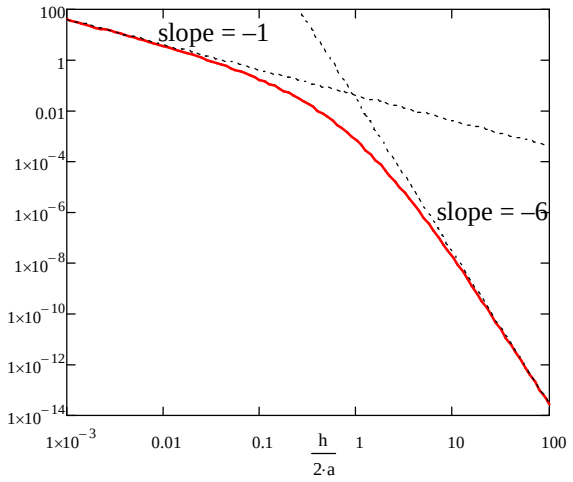

The potential has the following asymptotic behavior:

for $h \ll a$: $\phi_A = -\dfrac{A}{12}\dfrac{a}{h}$

for $h \gg a$: $\phi_A = -\dfrac{16A}{9}\left(\dfrac{a}{h}\right)^6$

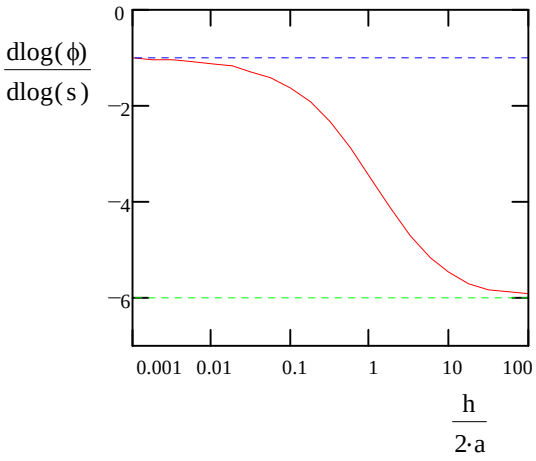

Notice that the attractive energy decays like h^{-1} when $h \ll a$ and like h^{-6} when $h \gg a$. The more rapid decay at large separations has the same exponent as between two atoms [see (103)]. This change in exponent is due to geometry only (retardation is not included in this result).

The results for several other geometries are summarized in the following table (taken from Hunter, Foundations, Vol I).

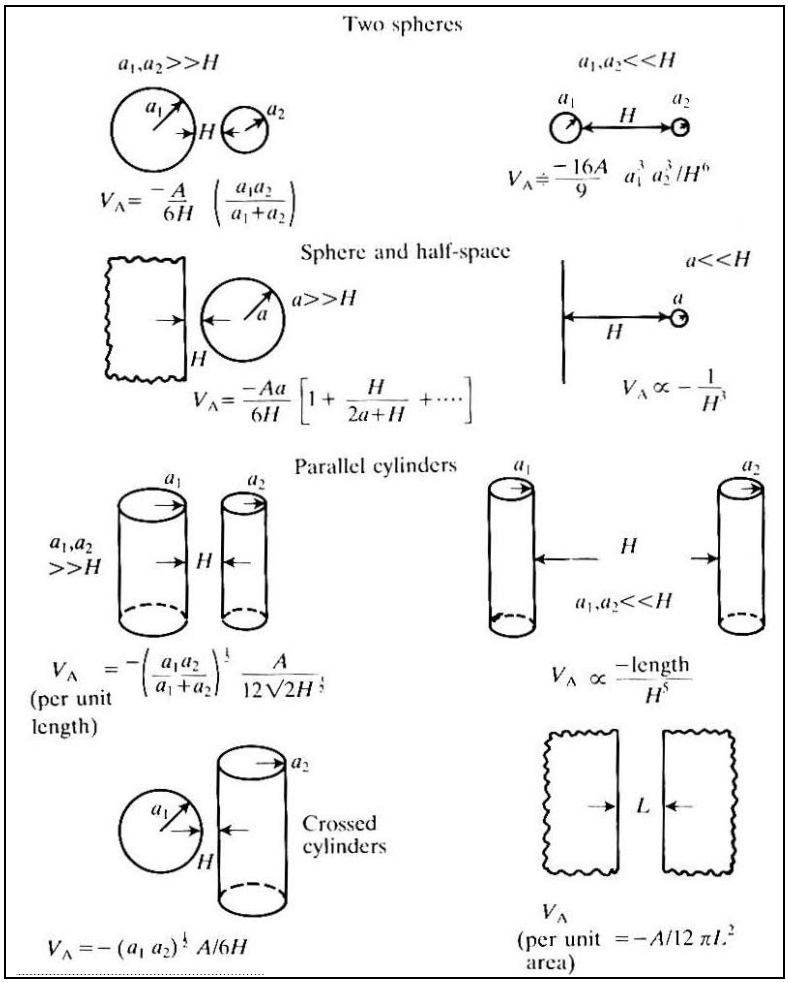

Hamaker's superposition of atomic or molecular interactions gives the correct dependence on the geometry but the proportionality constant A is not accurately predicted by (104) – even when the two bodies are separated by vacuum. When another media separates the bodies, their interaction is more complicated: the net interaction might even be repulsive. While repulsive interactions can be predicted in the framework of Hamaker's superposition theory, the assumption of pairwise additivity of intermolecular forces is inherently incorrect: the interaction involves the simultaneous interaction between many molecules.

Lifshitz's Continuum Theory

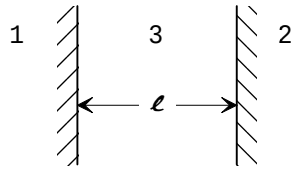

Instead of treating every atom as a discrete and independent oscillator, Lifshitz theory treats the three materials as continua. From Lifshitz theory, the interaction energy per unit area between two half spaces, composed of materials 1 and 2, separated by thickness l of material 3, is (Hunter, p210)

$$\phi_A(l)=-\frac{A_{132}(l)}{12\pi l^2}$$

This is also the expression we would get from Hamaker's superposition theory for this geometry. The main difference in Lifshitz's theory is that A_{132} depends on properties of the *continuum* — rather than properties of the individual atoms — and A_{132} will also depend on the separation distance l.

Here are the general expressions which can be used to evaluate the Hamaker constant:

$$A_{132} = -\frac{3}{2}kT\sum_{n=0}^{\infty}{}'\int_{r_n}^{\infty} x\left[\ln\left(1-\Delta_{13}\Delta_{23}e^{-x}\right) + \ln\left(1-\bar{\Delta}_{13}\bar{\Delta}_{23}e^{-x}\right)\right]dx$$

$$\Delta_{jk} = \frac{\varepsilon_j s_k - \varepsilon_k s_j}{\varepsilon_j s_k + \varepsilon_k s_j} \qquad \bar{\Delta}_{jk} = \frac{s_k - s_j}{s_k + s_j}$$

$$s_k^2 = x^2 + \left(\frac{2\xi_n l}{c}\right)^2 (\varepsilon_k - \varepsilon_3) \qquad r_n = \frac{2\xi_n l\sqrt{\varepsilon_3}}{c}$$

$$\xi_n = \frac{2\pi nkT}{h} \qquad \varepsilon_k = \varepsilon_k\left(i\xi_n\right)$$

where c = 3.00×10^8 m/s is the speed of light in vacuum and h = 1.0545×10^{-34} J-s is Planck's constant divided by 2π. The prime (′) on the sum denotes that the first term is to be multiplied by 1/2. The material properties enter this equation through $\varepsilon_k(i\xi_n)$. This is the dielectric permittivity of the material (k=1,2,3) except that it has to be evaluated at a purely imaginary frequency. This probably appears to be quite artificial, but it is a consequence of representing *real* quantities by *complex* numbers.

Below are results showing how the Hamaker constant depends on separation distance for two polystyrene half-spaces, separated by water.♥

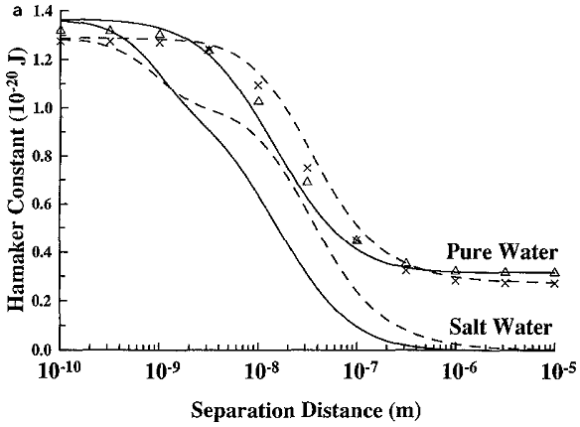

Owing to the complexity of the expressions above, it's hard to see how A depends on the properties of the materials. The expressions simplify somewhat if we look at the unretarded limit: in other words, if we let $l \to 0$:♣

$$A_{132}(0) = -\frac{3}{2}kT\sum_{n=0}^{\infty}{}'\underbrace{\int_0^{\infty} x\ln\left(1-\Delta_{13}^0\Delta_{23}^0e^{-x}\right)dx}_{-\mathrm{Li}_3\left(\Delta_{13}^0\Delta_{23}^0\right)\approx-\Delta_{13}^0\Delta_{23}^0}$$

where $$\Delta_{jk}^0(\xi_n) = \frac{\varepsilon_j(i\xi_n) - \varepsilon_k(i\xi_n)}{\varepsilon_j(i\xi_n) + \varepsilon_k(i\xi_n)}$$

Since the Δ^0's no longer depend on x, we can evaluate the integral once and for all. When $\left|\Delta_{13}^0\Delta_{23}^0\right| \ll 1$, the following simple result is a good approximation (max error is 20%):

$$A_{132}(0) \approx \frac{3}{2}kT\sum_{n=0}^{\infty}{}'\Delta_{13}^0\Delta_{23}^0$$

The table below summarizes the contributions of various terms to the sum

Relative Contributions to Nonretarded Hamaker Constant for Polystyrene–Water–Polystyrene

Spectral region	n	Percentage contribution
Static	0	23
Infrared	1–11	13
Visible	12–24	15
Ultravoilet	25–∞	49

Material Properties and Frequency Dependence

The only material property which appears in the previous section is the dielectric permittivity ε, which is the continuum property (of the medium separating the point charges) which appears in Coulomb's law [see (37) on page 20]. This property reflects how the medium becomes polarized by an electric field. The analogous property for atoms and molecules is the polarizability α. ε and α for the same material are related by the Clausius Mossoti relation (38).

It turns out that the ability to polarize a material by applying an electric field depends on the frequency of that electric field. The largest polarization occurs at zero frequency. As the frequency becomes very high, the molecules don't have time to respond. The following simple

♥ taken from Prieve & Russel, *J. Colloid Interface Sci.***125,** 1 (1988). A reprint is available on Blackboard.

♣ $\mathrm{Li}_n(z)$ is the polylog function with index n. $\mathrm{Li}_3(z)$ is the trilog function.

harmonic oscillator model provides insights into the frequency dependence.

Harmonic Oscillator Model

The direct proportionality between the dipole moment of a H atom and the electric field generating it [see (35) on page 19] is very much analogous to a linear Hookean spring whose displacement from its equilibrium position is proportional to the applied force. Let's now explore this analogy a little further to see what it says about the dynamics for an oscillating force.

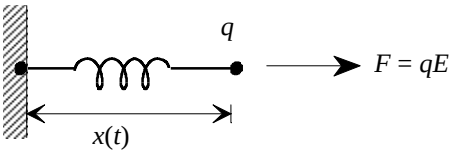

Let k = spring const

restoring force = kx

Suppose the electron has mass m. Then the dynamics of the electron are governed by Newton's law of the motion:

$$ma = \Sigma F$$

$$m\frac{d^2x}{dt^2} = qE - kx \qquad (105)$$

Now let's try to predict the response of the electron if the electric field oscillates with time:

$$E(t) = E_0\cos(\omega t) \qquad (106)$$

(106) into (105) gives:

$$m\frac{d^2x}{dt^2} + kx = qE_0\cos(\omega t)$$

The general solution of this equation for $\omega \neq \omega_o$ is given by:

$$x(t) = A\sin(\omega_o t) + B\cos(\omega_o t) + C\cos(\omega t) \quad (107)$$

where $$C(\omega) = \frac{qE_0}{m(\omega_o^2 - \omega^2)} \qquad (108)$$

and $$\omega_o = \sqrt{\frac{k}{m}}$$

is called the ***natural frequency*** (a.k.a. ***resonance frequency***). This is the frequency with which the electron would oscillate back and forth if there was no electric field forcing it. This is the frequency of oscillation which would result if you initially displaced the spring away from equilibrium and then just let it go without touching the spring again.

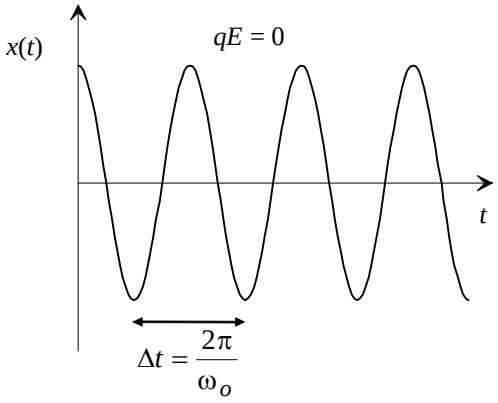

Now let's return to the response described by (107) when a sinusoidal force is applied with a frequency different from the natural one. Let's focus attention on the particular solution, because the values of the integration constants A and B will depend on the initial conditions, whereas the particular solution is more universal: it is independent of the initial conditions. Indeed, there exists one set of initial conditions in which A=B=0.

Special Case: ω=0 ($E = E_0$)

In this case the particular solution is a constant:

$$C(0) = \frac{qE_0}{m\omega_o^2} = \frac{qE_0}{k}$$

We can use this as a gauge to judge the amplitude of the response as a function of frequency. (108) can be rewritten as

$$\frac{C(\omega)}{C(0)} = \frac{\omega_o^2}{\omega_o^2 - \omega^2} \qquad (109)$$

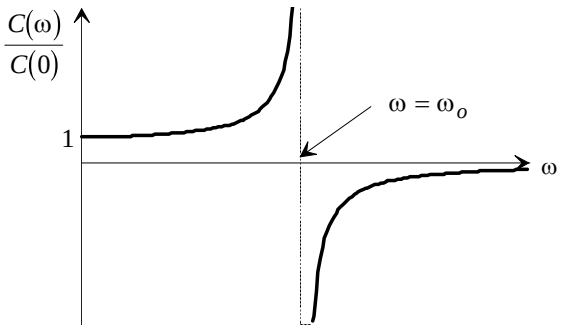

Notice that as the frequency increases from zero to the natural frequency the amplitude of the response increases to infinity, then reverses sign. However, above the natural frequency, the amplitude decays to zero as the frequency becomes much greater than the natural value.

Driving a system at it's natural frequency is clearly special. Let's see if we can understand what is happening. It turns out that if $\omega=\omega_o$, (107) is not the general solution. Instead, the general solution is:

$$x(t) = A\sin(\omega_o t) + B\cos(\omega_o t) + Dt\sin(\omega_o t) \quad (110)$$

where $D = qE_0\omega_o/2k$

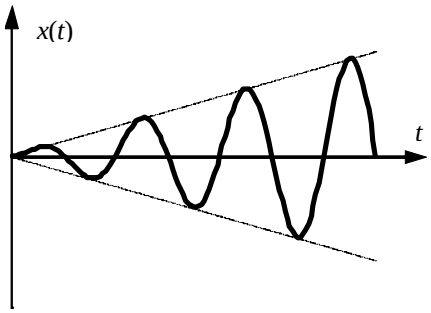

Notice that this particular solution oscillates, but the amplitude grows with time.

There is a simple physical explanation. Suppose the system is already oscillating at its natural frequency when we start to drive it at the same frequency. Even without any driving force, the system would oscillate with constant amplitude. With a oscillating driving force of the same frequency, we pull the electron further from the center with each cycle than it would otherwise move. In effect, the electron cloud is absorbing energy. Indeed this natural frequency corresponds to an ***absorption peak*** on a spectrogram. Of course, atoms and molecules generally possess many electrons and they also display multiple absorption peaks in their spectra.

The dipole moment induced by the oscillating electric field is proportional to the displacement $x(t)$ of the electron cloud:

$$p(t) = qx(t) = \alpha E(t) \quad (111)$$

Substituting (107) with A=B=0:

$$\alpha(\omega) = \frac{q^2}{m(\omega_o^2-\omega^2)} \quad (112)$$

Damped Harmonic Oscillator Model

There is one additional feature we can add to this simple-harmonic oscillator model to make it more realistic: friction. Any real mechanical oscillator would have irreversible losses of energy owing to viscous drag on the object moving back and forth. Likewise, an oscillating electon cloud around a hydrogen atom would radiate energy in all direction: this radiated energy also represents an irreversible loss. We can model the effect of such losses by adding a viscous drag force to (105):

$$\underbrace{m\frac{d^2x}{dt^2}}_{\text{inertia}} = \underbrace{qE(t)}_{\text{external force}} - \underbrace{kx}_{\text{spring restoring force}} - \underbrace{f\frac{dx}{dt}}_{\text{viscous drag}} \quad (113)$$

where $f = 6\pi\mu a$

A particular to solution to this refined model for $E(t) = E_0\cos\omega t$ is:

$$x(t) = C(\omega)\cos\omega t + S(\omega)\sin\omega t \quad (114)$$

where $$C(\omega) = \frac{\overbrace{qE_0}^{C(0)}}{k}\frac{\left(\omega_0^2-\omega^2\right)\omega_0^2}{\left(\omega_0^2-\omega^2\right)^2+\left(\frac{f}{m}\right)^2\omega^2}$$

and $$S(\omega) = \frac{qE_0}{k}\frac{\frac{f}{m}\omega\omega_0^2}{\left(\omega_0^2-\omega^2\right)^2+\left(\frac{f}{m}\right)^2\omega^2}$$

Notice that for f=0, this equation for $C(\omega)$ reduces to (109), which was singular at $\omega = \omega_0$. But when $f\neq 0$ neither of these expressions is singular.

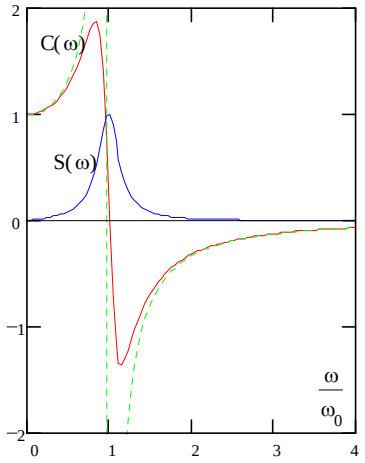

The solid curves in the figure above shows how C and S depend on ω for one particular value of f. Notice that damping significantly attenuates C compared to its singular behavior predicted from (109) (dotted curve).

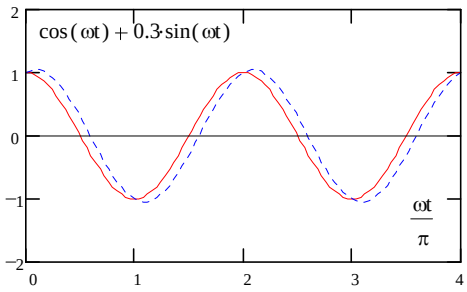

Another very important difference compared to (107) is the appearance of the sine term in (114). The sum of a sine and a cosine of the same frequency produces a cosine wave of a different amplitude which is shifted in phase (see figure above).

Lecture #17 begins here

All of this type of behavior can be represented more compactly using complex numbers. For example, instead of representing the driving force by a real function♥

$$E(t) = E_0 \exp(i\omega t) \qquad (115)$$

The particular solution to (113) becomes:

$$x(t) = \underbrace{\frac{qE_0}{m\left(\omega_0^2 - \omega^2\right) + i\omega f}}_{re^{i\theta}} e^{i\omega t} = re^{i(\omega t+\theta)} \qquad (116)$$

If we took the real parts of (115) and (116) for the case of no damping (i.e. f = 0), we would obtain (106) through (108). The real advantage of using the complex exponential form of the time dependence in (115) is that 1) differentiation w.r.t. t is easier and 2) the application of trig identities to calculate the phase angle is replaced by a conversion of the final complex number into polar form. Once r and θ are calculated, the real part of (116) is easy:

$$x(t) = \mathrm{Re}\left\{re^{i(\omega t+\theta)}\right\} = r\cos(\omega t + \theta)$$

which should be compared to (115). Clearly θ is the phase angle for $x(t)$ relative to $E(t)$.

Complex Polarizability and Permittivity

Using (111) and (116) we can deduce the complex polarizability♠

$$\alpha(\omega) = \frac{q^2}{m\left(\omega_o^2 - \omega^2\right) - i\omega f}$$

Using the mathematical principles of analytic continuation, the definition of this function can be extended to complex values of its argument ω. In particular, notice that for purely imaginary frequencies (i.e. ω = $i\xi$), the polarizability is a purely real function which decays monotonically with frequency:

$$\alpha(i\xi) = \frac{q^2}{m\left(\omega_o^2 + \xi^2\right) + \xi f}$$

In particular, the singularity at $\xi = \omega_0$ has disappeared. The plot below compares α(ω) and α(iω) for the undamped case (i.e. f=0).

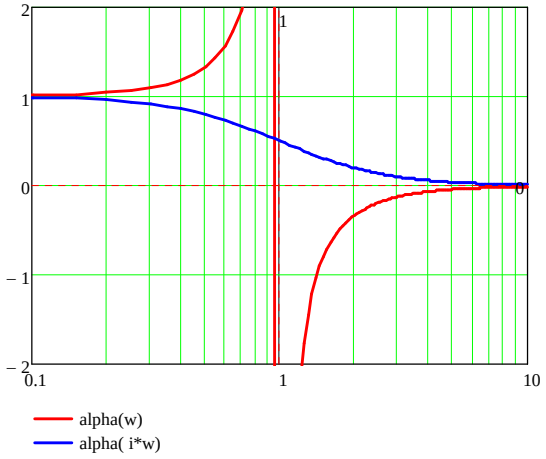

For this reason, imaginary frequencies offer a convenient alternative for curve fitting of experimental results, which will be summarized below. The Kramers-Kronig relationship of analytic-continuation theory allows experimental data taken at real frequencies to be mapped into purely imaginary frequencies.

For gases (which have $\varepsilon/\varepsilon_0 \approx 1$), the Clausius Mossoti relation (38) gives

♥Recall Euler's formula for complex exponentials:

$$e^{i\theta} = \cos\theta + i\sin\theta$$

♠The appearance of $-i\omega f$ [instead of $+i\omega f$ in (116)] in the denominator of the following expression is not a typo: it results if exp($+i\omega t$) in (115) is replaced by exp($-i\omega t$).

$$\varepsilon(i\xi)-\varepsilon_0=\frac{Nq^2}{m\left(\omega_o^2+\xi^2\right)+\xi f}$$

These expressions for $\alpha(\omega)$ and $\varepsilon(\omega)$ (which display a single absorption peak at $\omega=\omega_0$) were developed for a simple atom like H. More generally, atoms and molecules possess many electrons and they also display multiple absorption peaks in their spectra. In addition, condensed media (e.g. liquid water) are not sufficiently dilute so that this approximation to the Clausius Mossoti relation applies. Nonetheless, the permittivity spectra of nearly any material can be fit to a semi-empirical function having the following form:

$$\frac{\varepsilon(i\xi)}{\varepsilon_0}=1+\frac{g_0}{\xi^2}+\frac{h_0}{f_0+\xi}+\sum_j\frac{g_j}{\xi^2+f_j\xi+\omega_j^2} \quad (117)$$

where the first term following unity is the contribution from free electrons (present only in metals), the second term in the contribution from the orientation of a permanent dipole (present only for polar liquids like water) and the remaining terms are contributions from absorptions peaks j in the IR or UV. For example, Parsegian & Weiss♦ fit experimental results for water using the permanent-dipole term, 5 IR peaks and 6 UV peaks (a total of 35 fitting constants). Their results for $\varepsilon(i\xi)/\varepsilon_0$ is shown as the $\times$'s in the figure below:

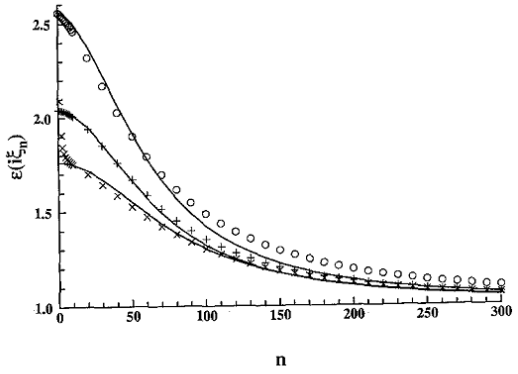

FIG. 2. A comparison of the dielectric spectrum deduced from approximation [2.5] and Table I (—) with the more complete representation of [2.2] (10) for polystyrene (○), tetradecane (+), and water (×). The zero-frequency dielectric constant of water is not shown (ε_0 = 79.69).

where $$\xi_n=\frac{2\pi nkT}{h}$$

and $h = 1.0545\times10^{-34}$ J-s is Planck's constant divided by 2π. The pluses and circles also show comparable data for tetradecane and polystyrene. To obtain the complete spectra requires combining data from several experiments covering various subsets of the spectra (microwave, IR, visible or UV). The solid curves are simpler approximations to the spectra which are discussed in the next section.

Cauchy Plot

Full characterization of the permittivity spectra $\varepsilon(i\xi)$ requires a lot of experimental data and effort. This has generally hindered the use of Lifshitz theory for van der Waals forces. A glimmer of hope was offered in the work of Hough & White♠ who suggested that an adequate representation of the permittivity spectra can be obtained from a single undamped (i.e. f=0) absorption peak in the UV. In other words, (117) can be approximated by

$$\frac{\varepsilon(i\xi)}{\varepsilon_0}=1+\frac{g_{UV}}{\xi^2+\omega_{UV}^2}$$

In the absence of absorption, $\varepsilon/\varepsilon_0 = n^2$, where n is the fractive index of the material [recall (37)]. In terms of purely real frequencies, this corresponds to

$$\frac{\varepsilon(\omega)}{\varepsilon_0}=n^2(\omega)=1+\frac{g_{UV}}{\omega_{UV}^2-\omega^2}$$

Note that as long as ω is in the visible portion of the spectra (i.e. $\omega_{vis} < \omega_{UV}$), this function is well behaved. This relationship can be rearranged to obtain

$$n^2(\omega)-1=C+\left[n^2(\omega)-1\right]\left(\frac{\omega}{\omega_{UV}^2}\right)^2$$

A plot of n^2–1 vs $(n^2–1)\omega^2$ is called a ***Cauchy plot***. The slope equals ω_{UV}^{-2} while the intercept equals

$$C=\frac{g_{UV}}{\omega_{UV}^2}$$

Cauchy plots for polystyrene (triangles), tetradecane (squares) and water (circles) are shown below (the units on the x-axis is 10^{30} Hz^2):

♦ *J. Colloid Interface Sci.* **81**, 285 (1981).

♠ *Adv. Colloid Interface Sci.* **14**, 3 (1980).

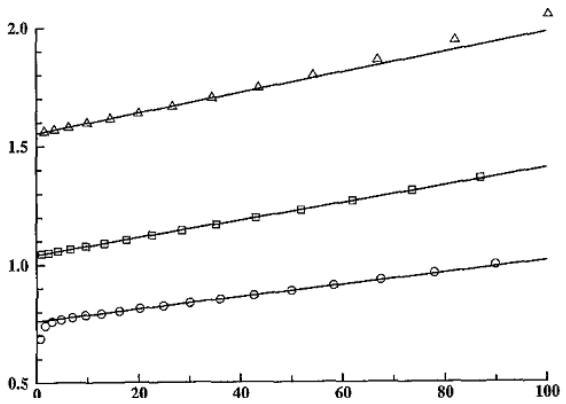

Using this simplified characterization of the spectra, the solid curves of $\varepsilon(i\xi_n)$ vs n were obtained (see figure just before last one).

Theory vs. Experiment

Below are direct force measurements between crossed cylinders of mica (about 1 cm in diameter) in air.

The dotted line shows the corresponding theory for nonretarded van der Waals forces. The agreement is quite good for separations below about 7 nm. At larger separations, retardation causes the force to decay more rapidly with further increases in separation.

At larger separations yet, the forces are much smaller. The figure below shows the severely retarded vdW interaction between a 6 μm sphere of polystyrene interacting with a glass microscope slide, separated by dilute aqueous salt solutions having various concentrations.♣ The two dashed curves represent two different approximations (for the geometry) which use Lifshitz theory to predict the retarded interaction across half-spaces. Deviations between theory and experiment for separations below about 70 nm are due to roughness on both surfaces (which is not a problem in the previous figure employing mica which is atomically smooth).

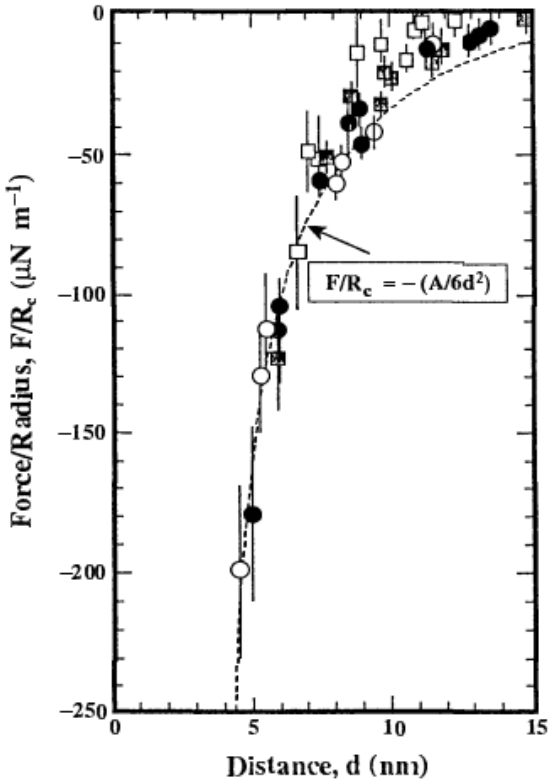

FIG. 10.7 Direct measurements of van der Waals dispersion forces. The measurements correspond to the force between two flat (mica) surfaces separated by a distance d. The line shown is the theoretical expression for unretarded van der Waals force. The figure shows that the unretarded expression describes the measurements sufficiently accurately for d about 6.5 nm or less. (Redrawn with permission of J. N. Israelachvili and G. E. Adams, *J. Chem. Soc., Faraday Trans. 1*, **78**, 975 (1978).)

♣ Bevan & Prieve, *Langmuir* **15**, 7925 (1999).

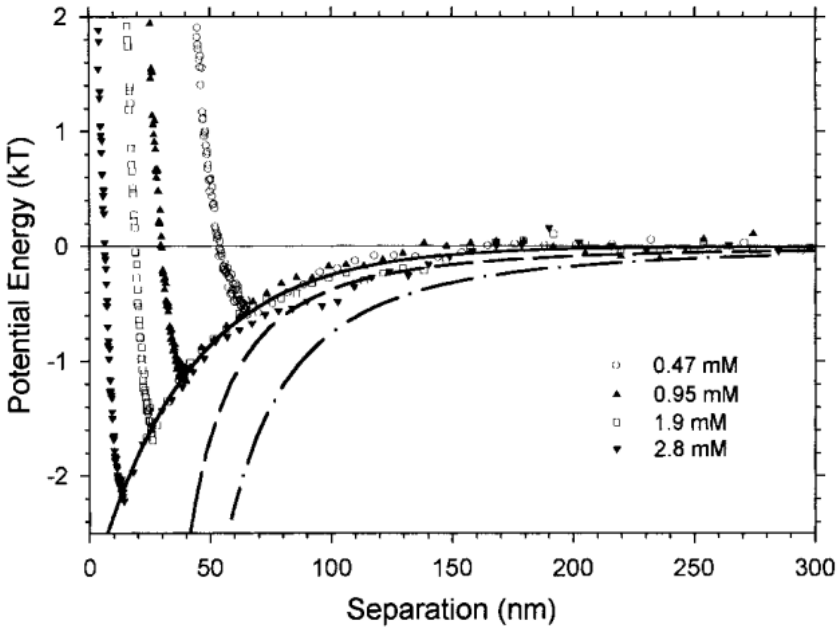

Figure 1. Profiles of the colloid interactions between the same 6 μm PS sphere and a glass slide in solutions having different ionic strengths. The solid line is an empirical fit given by eq 5, the dashed line shows the van der Waals interaction predicted from the Lifshitz–Derjaguin equation (eq 3), and the dot–dash line shows the van der Waals interaction predicted from the Lifshitz–Hamaker equation (eq 4).

Lecture #18 begins here

Lecture #19 begins here

The Electric Double Layer

Whereas van der Waals attraction between droplets or particles is responsible for the thermodynamic tendency of a dispersion to be unstable and flocculate, electrostatic repulsion between particles of like sign can reduce the rate of flocculation to near zero and impart kinetic stability to the colloidal state. Before we consider the interaction of two charged interfaces, we will first study a single charge interface and how its charge can be measured.

Origin of Charge

Nearly all particles, bubbles or drops in water are charged. We know this because when you apply an electric field across water containing a particle, bubble or drop, you can observe it to move. An example is the red blood cell experiment below.

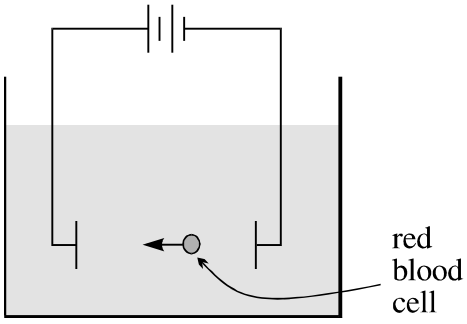

The surface of the blood cell or other particle acquires charge by a number of mechanisms:

- adsorption of ions (e.g. SDS and $FeOH^{+2}$)
- dissolution of ions from ionic solids (e.g. AgI)
- dissociation of acidic or basic sites on interface:

$$—COOH \rightarrow —COO^- + H^+$$

$$—NH_2 + H^+ \rightarrow —NH_3^+$$

Electrostatic Forces in Water vs. Coulomb's Law

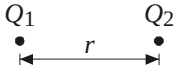

Coulomb's law (see page 20) states that two point charges Q_1 and Q_2, separated by a distance r, experience an electrostatic force given by

$$F = \frac{1}{4\pi\varepsilon}\frac{Q_1 Q_2}{r^2}$$

where the proportionality constant ε is called the ***electric permittivity*** which is a property of the medium separating the charges.

Electrostatic interactions across water are more complicated than across simple dielectrics like air or oil because water always contains ions which are also charged. In response to the charge on the interacting particles, these ions are rearranged: oppositely charged ions (called "counterions") are attracted to the particle while like ions of the same sign of charge (called "co-ions") are repelled.

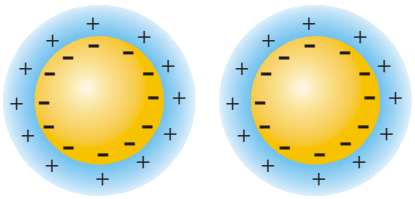

At equilibrium, a diffuse cloud of counterions surrounds each charged particle. Since the cloud's charge is always of opposite sign to the particle itself, from a distance, the particle appears to be electrically neutral (equal numbers of opposite charges in the diffuse cloud and on the particle). No electrostatic force is felt between two such particles in water until they get close enough for their clouds to overlap. Then the electrostatic repulsion decays exponentially with r :

$$F \propto e^{-\kappa r}$$

where $1/\kappa$ is the thickness of the charge cloud, also known as the Debye length.

The resulting severe weakening of the electrostatic forces is called ***Debye screening***: the cloud essentially hides the bare charge borne by the particles until they get very close together.

Gouy-Chapman Model of Double Layer

Let's try to quantify this description. In particular, we would like to know how thick this cloud of counterions is. Because of the charge on the interface, ions feel a electrostatic force. The force per unit charge is called the ***electric field***:

$\mathbf{E}(\mathbf{x})$ = electric field (force/charge)

Like gravity, this vector field is ***conservative***, thus there must exist a scalar potential $\psi(\mathbf{x})$ such that:

$$\mathbf{E} = -\nabla\psi \qquad (118)$$

Like the gravitational potential, the minus sign is included by convention. ψ is called the ***electrostatic potential***.

ψ [=] volts (energy/charge)

Boltzmann's Equation:Transport Derivation

The flux of ions will have contributions from diffusion and electro–migration of ions driven by the electric field:

$$\mathbf{N}_i = -D_i \nabla c_i + \mathbf{v}_i c_i \qquad (119)$$

where D_i is the diffusion coefficient of ion species i, c_i is the number of ions per unit volume and $\mathbf{v}_i$ is the velocity of an individual ion. This might be the velocity of the fluid in cases in which the ions are entrained in flowing fluid. In stagnant fluid, $\mathbf{v}_i$ is the terminal velocity of any ion induced by the electric field **E**. Recalling the electric field is force per unit charge, we can calculate the force on any ion by multiplying the electric field by the charge on that ion:

$$z_i e \mathbf{E} \qquad (120)$$

Stokes law (16) can be used to estimate* the mobility of that ion (velocity induced per unit applied force):

$$m_i = \frac{1}{f_i} = \frac{1}{6\pi\mu a_i} \qquad (121)$$

where μ is the viscosity of the solution a_i is the (apparent) hydrodynamic radius and f_i is the friction coefficient defined in (16). Multiplying the mobility – given by (121) – by the force – given by (120) – yields the velocity $\mathbf{v}_i$ in (119). Also substituting (118) leads to

$$\mathbf{N}_i = -D_i \nabla c_i - z_i e m_i c_i \nabla \psi$$

A combination of (15) and (23) yields

$$D_i = m_i kT$$

which is sometimes call ***Einstein's equation***. Using this to eliminate m_i, the flux becomes

$$\mathbf{N}_i = -D_i \left(\nabla c_i + c_i \frac{z_i e}{kT} \nabla \psi \right) \qquad (122)$$

which is called the ***Nernst-Planck equation***.

Let's now restrict attention to a uniformly charged surface.

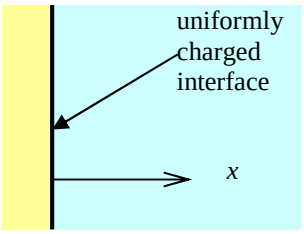

Then any electric field will act purely normal to the surface and we expect the electrostatic potential and the ion concentration to depend only on the normal distance from the charged surface (say x) and we expect that the ionic concentration will approach the bulk value $c_{i\infty}$ at some distance from the charged interface. For this to happen, the electrostatic potential must tend to some constant (say $\psi \to 0$ as $x \to \infty$) or $\mathbf{E} \to \mathbf{0}$:

$$\text{as } x \to \infty: \qquad c_i \to c_{i\infty},\ \psi \to 0 \qquad (123)$$

Continuity of species mass requires

$$\frac{\partial c_i}{\partial t} + \nabla \cdot \mathbf{N}_i = 0$$

For steady state, the partial time derivative is zero. For diffusion in one direction, this yields

$$\frac{dN_{ix}}{dx} = 0 \quad \text{or} \quad N_{ix} = \text{const} = 0$$

If no adsorption or reaction of ions occurs at the wall (x=0) and the wall is otherwise inpenetrable to ions, the flux must vanish at the wall; then continuity requires it to vanish for all x. (122) becomes

$$0 = -D_i \left(\frac{dc_i}{dx} + c_i \frac{z_i e}{kT} \frac{d\psi}{dx} \right)$$

After dividing out the D_i, we have a separable, first-order ODE:

$$\int_{c_{i\infty}}^{c_i(x)} \frac{dc_i}{c_i} = -\frac{z_i e}{kT} \int_0^{\psi(x)} d\psi$$

After applying bc (123), we have

$$c_i(x) = c_{i\infty} \exp\left[-\frac{z_i e \psi(x)}{kT} \right] \qquad (124)$$

which is called ***Boltzmann's equation***. So if I knew the $\psi(y)$, I could calculate the concentration profile. But alas $\psi(y)$ is still unknown. I need another

* We say "estimate" because Stokes law is a continuum theory which applies when the particle is large compared to the size of individual water molecules. The ions in the current problem are not much larger than the water molecules. Nonetheless, the radius calculated from (121), which is called the ***hydrodynamic radius***, is usually within a factor of two of the true radius.

equation. The extra equation is provided by ***Coulomb's law*** of electrostatics. If I knew the distribution of charges within a system, I could calculate the force on them using Columb's law.

In continuum mechanics, the distribution of charges is given by the ***space charge density***. Just like we define the mass per volume to be the density of the fluid, we can define:

$\rho_e(\mathbf{x},t)$ = local charge density (charge/volume)

For a continuum, Coulomb's law can be written either as Gauss's law (in differential form)

$$\nabla\cdot\mathbf{E}=\frac{\rho_e}{\varepsilon} \tag{125}$$

or ***Poisson's equation***:♦

$$\nabla^2\psi=-\frac{\rho_e}{\varepsilon} \tag{126}$$

where ε is the electric permittivity♣ of the medium between the ions (e.g. the water):

$$\varepsilon_{\text{vacuum}}=1.113\times10^{-10}\ \frac{\text{Coul}^2}{\text{N-m}^2}$$

$$\varepsilon_{\text{water}}=78\ \varepsilon_{\text{vacuum}}$$

The charge density of the fluid arises from the charge born by each ion. Adding up the charges from each species *i*, then substituting Boltzman's equation, gives

$$\begin{aligned}\rho_e(x)&=\sum_i z_i e c_i(x)\\&=\sum_i z_i e c_{i\infty}\exp\left[-\frac{z_i e\psi(x)}{kT}\right]\end{aligned} \tag{127}$$

Substituting this into (126) yields

$$\nabla^2\psi=-\frac{e}{\varepsilon}\sum_i z_i c_{i\infty}\exp\left[-\frac{z_i e\psi(x)}{kT}\right] \tag{128}$$

which is called the ***Poisson-Boltzmann Equation***.

♦ For a derivation of Gauss's and Poisson's equations from Coulomb's law, see Electrostatics of Continuous Media.pdf at Blackboard.

♣ This is the value after 4π has been factored out as in the representation of Coulomb's law appearing on page 20. This is called the "rationalized" value: by factoring out 4π in Coulomb's law, 4π does not appear in Gauss's law or Poisson's equation.

Special Case #1: small potentials. If the potentials are small enough, then we can linearize the exponential:

$$\exp\left[-\frac{z_i e\psi(x)}{kT}\right]=1-\frac{z_i e\psi(x)}{kT}+\ldots$$

Truncating the series after the second term, (127) yields

$$\rho_e=\sum_i z_i e c_i=e\left\{\underbrace{\sum_i z_i c_{i\infty}}_{0}-\frac{e\psi(x)}{kT}\underbrace{\sum_i z_i^2 c_{i\infty}}_{2I}\right\}$$

Now the first sum vanishes because the bulk solution must be electrically neutral. This leaves

$$\rho_e(x)=-\frac{2Ie^2}{kT}\psi(x) \tag{129}$$

and substituting into (128) yields

$$\nabla^2\psi=\underbrace{\frac{2e^2I}{\varepsilon kT}}_{\kappa^2}\psi=\kappa^2\psi \tag{130}$$

where $$I\equiv\frac{1}{2}\sum_i z_i^2 c_{i\infty}$$

is called the ***ionic strength*** of the bulk solution. In the case of a symmetric univalent electrolyte (e.g. NaCl), the ionic strength is also the bulk concentration of salt. The remaining collection of constants is lumped to κ^2 where κ is called the ***Debye parameter***. (130) is called the ***linearized Poisson-Boltzmann equation***. If $\psi = \psi(x)$ this equation reduces to

$$\frac{d^2\psi}{dx^2}=\kappa^2\psi \tag{131}$$

Integrating this ODE subject to:

$$\Psi=\Psi_0 \text{ at } x=0$$

and $$\Psi=0 \text{ at } x=\infty$$

yields $$\psi(x)=\psi_0\exp(-\kappa x) \tag{132}$$

and the linearlized form of Boltzmann's equation (124) yields

$$c_\pm(x)=c_\infty\left(1\mp\frac{ze\psi_0}{kT}e^{-\kappa x}\right)$$

The linearized form for the space charge density (127) is

$$\rho_e(x) = -\frac{2Ie^2}{kT}\psi(x) = -\frac{2Ie^2}{kT}\psi_0 e^{-\kappa x} \quad (133)$$

Integrating over the entire solution:

$$\int_0^\infty \rho_e(x)\,dx = -\frac{2Ie^2}{kT}\psi_0 \int_0^\infty e^{-\kappa x}dx = -\frac{2Ie^2}{\kappa kT}\psi_0$$

Global electroneutrality requires:

$$\sigma + \underbrace{\int_0^\infty \rho_e(x)\,dx}_{\sigma_d} = 0 \quad (134)$$

σ = surface charge density (charge/area)

σ_d = charge density of diffuse cloud

Substituting this integral into (134) yields the surface charge density

$$\sigma = -\int_0^\infty \rho_e(x)\,dx = \underbrace{\frac{2Ie^2}{\kappa kT}}_{\kappa\varepsilon}\psi_0 = \kappa\varepsilon\psi_0$$

Notice that the surface charge density σ and the surface potential ψ_0 have the same sign (since all the other symbols in the equation are positive). Of course the electrolyte solution must have a net charge opposite in sign to that born by the surface itself.

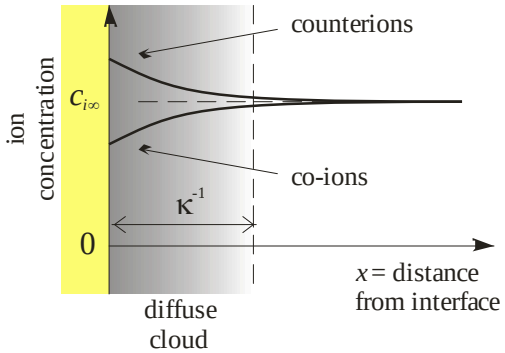

Clearly κ is associated with the thickness of the diffuse cloud. κ^{-1} is called the ***Debye length***:

$\kappa^{-1} = 10^{-9}$ m = 1nm for $c_\infty = 10^{-1}$ M

$\kappa^{-1} = 10^{-6}$ m = 1μm for $c_\infty = 10^{-7}$ M

This provides some idea of the thickness of the charge cloud.

Special Case #2: symmetric binary electrolyte, which means there are only two different species of ions and they have the same magnitude of charge:

$$z_+ = -z_- = z$$

$$c_{+\infty} = c_{-\infty} = c_\infty$$

Then Boltzmann's equation can be used to calculate the charge density:

$$\begin{aligned}\rho_e(x) &= z_+ e c_{+\infty}\exp\left(-\frac{z_+ e\psi}{kT}\right) \\ &\quad + z_- e c_{-\infty}\exp\left(-\frac{z_- e\psi}{kT}\right) \\ &= zec_\infty\left[\exp\left(-\frac{ze\psi}{kT}\right) - \exp\left(+\frac{ze\psi}{kT}\right)\right] \\ &= -2zec_\infty \sinh\left(\frac{ze\psi}{kT}\right)\end{aligned} \quad (135)$$

Substituting this into Poisson's equation, we get:

$$\frac{d^2\psi}{dx^2} = \frac{2ec_\infty}{\varepsilon}\sinh\left(\frac{ze\psi}{kT}\right)$$

The argument of the sinh must be dimensionless, so let's use this combination to define a new dimensionless potential

$$\Psi \equiv \frac{ze\psi}{kT}$$

We can make the ψ on the left-hand side dimensionless by multiplying both sides by ze/kT. Then we have

$$\frac{d^2\Psi}{dx^2} = \kappa^2 \sinh\Psi \quad (136)$$

where $$\kappa^2 = \frac{2z^2e^2c_\infty}{\varepsilon kT}[=]\frac{1}{\mathrm{m}^2}$$

This is a nonlinear ODE. Despite its innoccuous appearance, it is much more difficult to solve than linear equations. However, a particular solution is possible:

$$\tanh\left[\frac{\Psi(x)}{4}\right] = \tanh\left(\frac{\Psi_0}{4}\right)e^{-\kappa x} \quad (137)$$

which is called the ***Gouy-Chapman model*** for the double layer. Of particular interest is relationship between the surface potential ψ_0 and the surface charge density σ. Substituting (135) into (134):

$$\begin{aligned}\sigma &= -\int_0^\infty \rho_e(x)\,dx \\ &= 2zec_\infty \int_0^\infty \sinh[\Psi(x)]\,dx\end{aligned}$$

Substituting $\sinh\Psi$ from (136) and κ^{-2}:

$$\sigma = 2zec_\infty \kappa^{-2} \int_0^\infty \frac{d^2\Psi}{dx^2} dx$$

$$= \underbrace{2zec_\infty \kappa^{-2}}_{\frac{\varepsilon kT}{ze}} \left(\underbrace{\left.\frac{d\Psi}{dx}\right|_{x=\infty}}_{0} - \left.\frac{d\Psi}{dx}\right|_{x=0} \right)$$

$$= -\frac{\varepsilon kT}{ze} \left.\frac{d\Psi}{dx}\right|_{x=0}$$

Finally we calculate an expression for the wall derivative from (137):

$$\sigma = \sqrt{8c_\infty \varepsilon kT}\, \sinh\left(\frac{ze\psi_0}{2kT}\right) \qquad (138)$$

which is called the ***Gouy-Chapman Equation*** in honor of the two men who first solved the Poisson-Boltzmann equation in this 1D case: Gouy (1910) and Chapman (1913). By contrast, the solution to the linearized PBE in spherical geometry was reported by Debye & Huckel in 1923 as part of their general theory for the activity of strong electrolytes.

For comparison between these two special cases, we evaluate (132) and (137) for $z = 1$, $\kappa y = 0$ to 2 and $\Psi_0 = 1$, 2, 4, 7 and 10. The results are shown below:

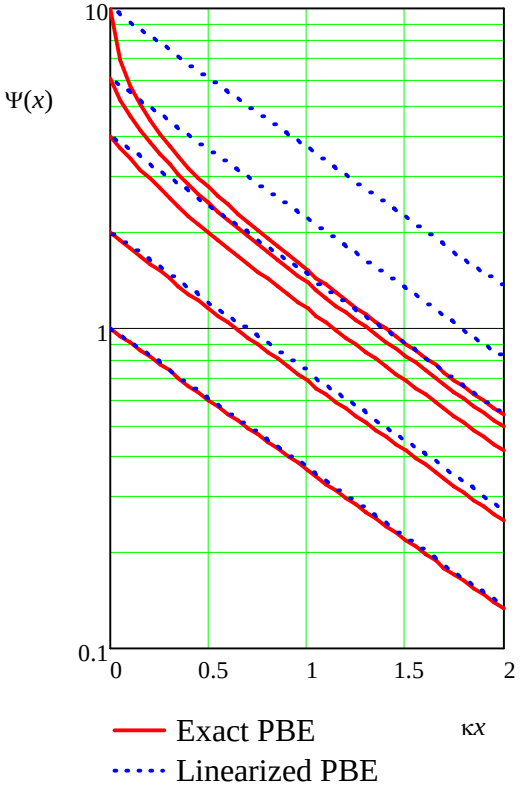

By making the x-axis logarithmic, we make predictions of (132) linear, while those of (137) are not linear, except for the smaller surface potentials Ψ_0 or at large x. Notice that for large x, red curves always become linear with a slope the same as all the blue curves.

In the limit $x\to\infty$, (137) predicts that $|\Psi_0| \to 0$ so that eventually $|\Psi_0|$ becomes small enough so that tanh can be linearized. Under these conditions, (137) predicts

$$\lim_{x\to\infty} \Psi(x) = \underbrace{4\tanh\left(\frac{\Psi_0}{4}\right)}_{\Psi_{0,app}} e^{-\kappa x} \qquad (139)$$

where the pre-exponential factor is the apparent surface potential which yields the same y-dependence as in the linearized model of (132).

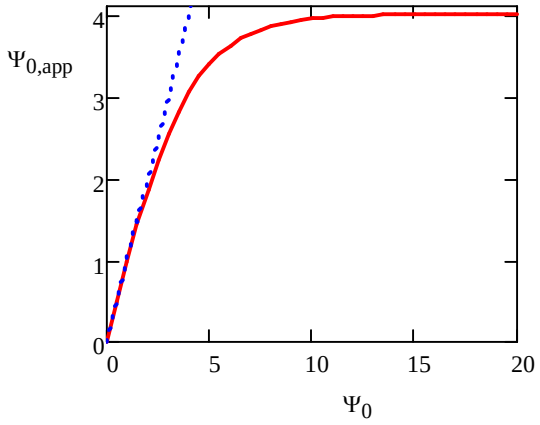

Note that this apparent surface potential exhibits of plateau of 4 as the true surface potential increases.

Some Limitations

While the Gouy-Chapman model of the diffuse part of the double-layer is generally accepted, there are some difficulties which will be brought out in the following example.

Assume that the surface charge arises from the dissociation of acid sites on the surface. A large charge density on the surface would correspond to elemental charges placed at a spacing of molecular dimensions, say

$$\sigma = \frac{e}{(0.5\text{ nm})^2} = 0.641\text{ Coul/m}^2$$

Let's calculate the surface concentration of counterions when the bulk concentration is

$$c_\infty = 0.1\text{ mol/dm}^3$$

The Gouy-Chapman equation (138) predicts

$$\frac{ze\psi_0}{2kT} = 3.546$$

or $$\psi_0 = 182 \text{ mV}$$

To see if this is reasonable, let's now calculate the maximum concentration of counterions, which occurs in the solution closest to the charged plane. Boltzmann's equation (124)

$$c_-(0) = c_\infty e^{2\times 3.546} = 116 \text{ M}$$

which is absurdly high. This concentration would correspond to an average spacing between ions in solution of only 0.25nm, which is about half the hydrated diameter of most ions. Indeed the solubility of common salts in water is usually limited to about 5 M.

Although we have obtained an absurd answer from the model in this case, this case is somewhat extreme in that the surface charge density is very large, particularly for this high ionic strength. In most cases, the Gouy-Chapman model of the double-layer gives reasonable results. Nonetheless, this absurdity motivated several refinements to the Gouy-Chapman model.

Lecture #20 begins here

Stern Model

In 1924, O. Stern introduced a correction to the Gouy-Chapman model of the double layer in an attempt to avoid the absurdly high counterion concentration which are sometimes predicted for high surface charge densities.

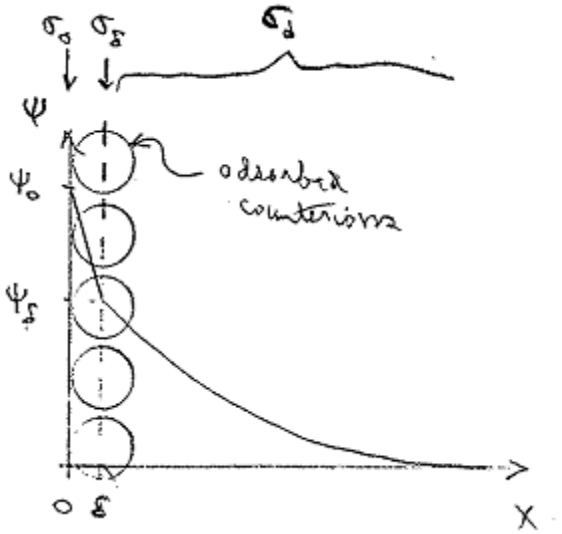

Stern reasoned that, when the concentration of counterions next to the surface becomes large, some of these counterions will adsorb on the surface to reduce the surface charge. This layer of adsorbed counterions is now called the:

Stern layer - layer of (partially dehydrated) counterions which physically adsorb onto surface.

Adsorption of counterions tends to reduce the absolute magnitude of surface charge remaining in the diffuse part of the double-layer which moderates the tendency to predict absurdly higher concentrations. Stern's work was published only a few years after Langmuir's work on adsorption of gas molecules onto a solid surface. The quantitative models of Stern and Langmuir are very similar.

Charge Regulation

In the 1920's, research centered on the Hg/water interface and silver halides in water. Today, fundamental studies are often done using polymer latexes, since these particles are nearly perfect spheres and can be made with very narrow size distributions. Moreover, you can tailor the surface chemistry to suit your needs.

Latexes usually acquire their surface charge through the dissociation of acid or basic sites.

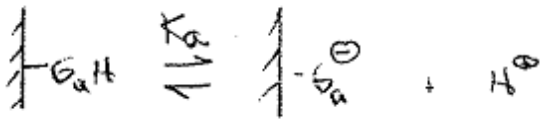

This is a reversible reaction. If the site is a weak acid, then if [H+] next to the surface is large, then H+ will be forced to reassociate with the surface, again reducing the surface charge due to the dissociated sites. Most weak acids have a pKa which would prevent the free [H+] from reaching 116 M.

charge regulation - σ_0 is determined by dissociation equilibria of surface sites.

This term was coined by Ninham & Parsegian in 1971.

Although there might still be room for improvement in accounting for the charging mechanism for a particular type of colloid, there is general agreement that the Gouy-Chapman model correctly represents the structure of the diffuse cloud, given the surface charge density.

Double-Layer Repulsion

Before discussing the forces acting on charged surfaces, let's discuss the forces acting on fluid elements inside the counterion cloud.

Hydrostatic Pressure Inside Double Layer

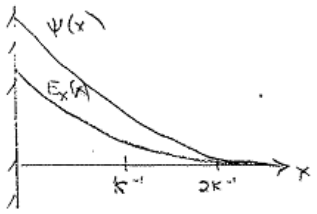

According to the Gouy-Chapman theory, there is a voltage drop across the diffuse part of the double layer. This means that there must be an electric field inside the double layer. This electric field represents the force/charge acting on charges inside the counterion cloud:

$$E(x) = -\frac{d\psi}{dx} = \frac{\text{force}}{\text{charge}} \qquad (140)$$

This represents the force acting on ions in the fluid. Consider a small element of fluid inside the counterion cloud.

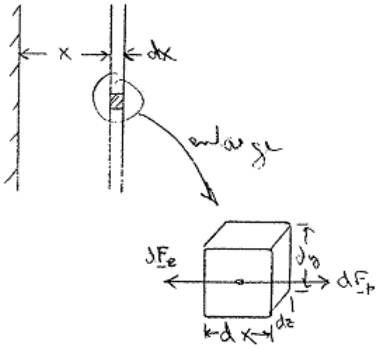

The electrical force acting on this fluid is:

$$dF_e = \rho(x)\, E(x)\, dx\, dy\, dz \qquad (141)$$

In general the fluid will always bear a charge which is opposite in sign to that on the wall. So the charge fluid elements will always be pulled toward the wall. This is like the gravitational force which acts on water in a lake or pond which pulls the water toward the earth. Gravity causes the hydrostatic pressure to rise as you go deeper into the lake. At equilibrium, this electrical force is opposed by hydrostatic pressure rise:

$$dF_p = [p(x) - p(x+dx)]\, dy\, dz$$

or

$$dF_p = -(dp/dx)\, dx\, dy\, dz \qquad (142)$$

At mechanical equilibrium, the net force on the fluid element must vanish:

$$dF_e + dF_p = 0$$

Substituting (141) and (142) and dividing by *dxdydz*:

$$\frac{dp}{dx} = \rho E(x) \qquad (143)$$

Pressure in terms of Ion Concentrations or Potential

Substituting (140) and multiplying through by *dx*:

$$dp = -\rho\, d\psi$$

Next we substitute ρ from (127) and Boltzmann's equation:

$$dp = -d\psi \sum_i z_i e c_i(y)$$

$$= -d\psi \sum_i z_i e c_{i\infty} \exp\left[-\frac{z_i e \psi(y)}{kT}\right]$$

In preparation for integrating this expression, note that each term of the sum has the form

$$a\, e^{-b\psi}\, d\psi = -a/b\, d(e^{-b\psi})$$

With this substitution, we have

$$dp = kT \sum_i c_{i\infty} d \exp\left(-\frac{z_i e\psi}{kT}\right) = kT \sum_i dc_i$$

With the help of Boltzmann's equation (124), the individual terms of the sum can be seen to be dc_i, which was used in the second equation above. Integrating from $x=\infty$ (where $p=p_\infty$ and $c_i=c_{i\infty}$) to $x=x$:

$$\int_{p_\infty}^{p(x)} dp = kT \sum_i \int_{c_{i\infty}}^{c_i(x)} dc_i \qquad (144)$$

and the pressure can be written as:

$$p(x) - p_\infty = kT\left[\sum_i c_i(x) - \sum_i c_{i\infty}\right] \qquad (145)$$

Thus $p - p_\infty$ is sometimes called the ***osmotic pressure*** since the above equation is just ***van't Hoff's law*** for the osmotic pressure for a ideal solution of multiple ions. Finally, we can relate the pressure to the electrostatic potential using Boltzmann's equation (124):

$$p(x) - p_\infty = kT \sum_i c_{i\infty} \left\{\exp\left[-\frac{z_i e\psi(x)}{kT}\right] - 1\right\} \qquad (146)$$

Pressure in terms of Electric Field

For one-dimensional problems, Gauss's law (125) can be written as $dE/dx = \rho/\varepsilon$. Then (143) becomes

$$\frac{dp}{dx} = \varepsilon E(x)\frac{dE}{dx} = \frac{\varepsilon}{2}\frac{dE^2}{dx}$$

Integrating between $x=\infty$ (where $p=p_\infty$ and $E=0$) to $x=x$:

$$p(x) - p_\infty = \tfrac{1}{2}\varepsilon E^2(x) - 0 \qquad (147)$$

or

$$\underbrace{\underbrace{p(x)}_{\text{hydrostatic pressure}} \quad \underbrace{-\tfrac{1}{2}\varepsilon E^2(x)}_{\text{Maxwell stress}}}_{\text{Total Stress}} = \underbrace{p_\infty}_{\text{a constant}} \qquad (148)$$

The 2nd term on the left-hand side is the electrical force per unit area; it has the same units as pressure and is called the ***Maxwell stress*** (the minus sign is part of the Maxwell stress). By contrast, ρE represents the electric force per unit volume. By adding the Maxwell stress to the hydrostatic pressure, we obtain the total force per unit area acting normal to and inward on any x=const surface of our system.

Let's illustrate how the Maxwell stress can be used. In deriving (143), we performed a force balance on a system whose size was differential in the x-direction. This was required because pressure is a surface force (force = pressure×area) whereas ρE is a body force (force = ρE×volume). Now that we have the electric force as a stress (force = area×stress) instead of a body force, we can easily perform force balances on systems which are not differential in x. For example, consider the slice of fluid held between parallel planes are $x=x_1$ and $x=x_2$.

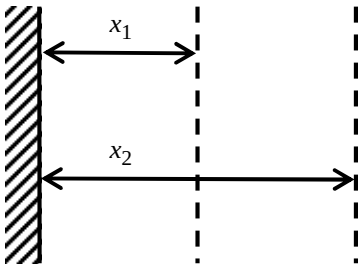

A x-force balance on this slice of fluid requires that the inward force acting the left face (force acts in +x direction) must equal the inward force acting on the right face (force acts in –x direction):

$$\underbrace{p(x_1) - \tfrac{1}{2}\varepsilon E^2(x_1)}_{p_\infty} = \underbrace{p(x_2) - \tfrac{1}{2}\varepsilon E^2(x_2)}_{p_\infty} \qquad (149)$$

This result is consistent with (148), which states that the total stress equals a constant (p_∞) independent of x. Using the Maxwell stress allowed us to write this force balance on a macroscopic system directly – without having to integrate (143).

In the text between (141) and (142) we argue that the pressure force on fluid elements always acts in the $+x$ direction, regardless of the sign of the surface charge. This implies that $p(x) \ge p_\infty$ which is apparent from (147) but not from (145). To see that (145) also implies $p(x) \ge p_\infty$, let's look at a couple of special cases:

Special Case #1: For a symmetric binary electrolyte, there are just two terms in this sum: one for the cation (+) and one for the anion (-). (146) yields:

$$\begin{aligned} p(x) - p_\infty &= kTc_\infty\left(e^{y} - 1 + e^{-y} - 1\right) \\ &= 2kTc_\infty\left(\cosh y - 1\right) \ge 0 \end{aligned}$$

where $y = ze\psi(x)/kT$

Since the cosh function has a minimum value of 1, this pressure difference is greater than or equal to zero.

Unfortunately, the potential profile $\psi(x)$ given by (137) is not so simple that we can visualize the shape of the pressure profile. Note, however, that the pressure is always higher inside the counterion cloud than outside the cloud. To get a simpler expression whose shape we can visualize, we continue to:

Special Case #2. In the special case in which the potential is small enough to make the Debye approximation:

$$\left|y(x)\right| \equiv \left|\frac{e\psi(x)}{kT}\right| \ll 1$$

then (146) yields:

$$p - p_\infty = kT\sum_i c_{i\infty}\left(e^{-z_i y} - 1\right)$$

Expanding the exponential in a Taylors series:

$$p - p_\infty = kT\sum_i c_{i\infty}\left[\cancel{1} + \left(-z_i y\right) + \tfrac{1}{2}\left(-z_i y\right)^2 + \ldots - \cancel{1}\right]$$

$$p - p_\infty = \underbrace{-kTy\sum_i z_i c_{i\infty}}_{0} + \underbrace{kTy^2\,\tfrac{1}{2}\sum_i z_i^2 c_{i\infty}}_{I} + \ldots$$

Now the first sum must vanish owing to electroneutrality of the bulk solution. The second sum is just the ionic strength of the solution (I) leaving:

$$p(x) - p_\infty = IkT\, y^2$$

Owing to the exponent of "2" on y (which can be + or –), we again concluded that $p(x) \geq p_\infty$ as previously argued. Substituting the definitions of y and κ:

$$p(x) - p_\infty = \frac{IkTe^2}{(kT)^2}\left[\psi(x)\right]^2 = \frac{1}{2}\kappa^2\varepsilon\left[\psi(x)\right]^2 \quad (150)$$

where the last step involves:

$$\frac{IkTe^2}{(kT)^2} = \frac{Ie^2}{kT} = \frac{\varepsilon}{2}\times\underbrace{\frac{2Ie^2}{\varepsilon kT}}_{\kappa^2} = \frac{1}{2}\kappa^2\varepsilon$$

Substituting $\psi(x)$ from (132):

$$p(x) - p_\infty = \frac{1}{2}\kappa^2\varepsilon\psi_0^2 e^{-2\kappa x}$$

From the "2" in the exponent, we see that the pressure decays more rapidly to its bulk value than either potential or ion concentrations.

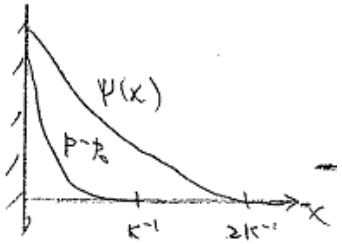

Lecture #21 begins here

Overlap of Two Double Layers

Suppose we have two flat plates immersed in the same electrolyte solution and we bring them close together so that their double layers begin to overlap.

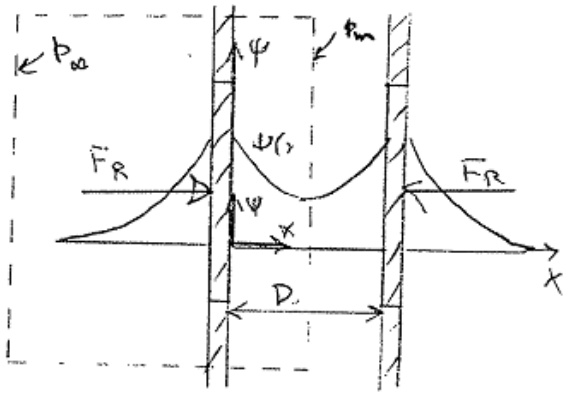

If the plates are identical, they will repel each other. To calculate the repulsion, consider the forces acting on the system indicated by dotted lines above. For convenience, we chose a system consisting of a unit area of plate surface, with one boundary located at some arbitrary x located between the two plates and the second vertical boundary located well outside the counterion cloud (say at $x = -\infty$). Besides the surface forces of pressure and Maxwell stress acting on either vertical surface, we also have the external force which we must apply to keep the plates from moving apart:

$$P_{DL} = \frac{F_R}{A} = \frac{\text{dbl repul}}{\text{area}}$$

A horizontal force balance gives

$$P_{DL} + p_\infty = p(x) - \tfrac{1}{2}\varepsilon E^2(x)$$

Thus the total stress is independent of x – just as in (149). However, unlike in (149), that total stress is not equal to p_∞. To evaluate the double-layer pressure P_{DL} from the equation above, we can choose to evaluate the total stress at the most convenient value of x.

If the two plates bear identical charge densities, symmetry dictates that the electrostatic potential profile $\psi(x)$ will experience a minimum at the mid-plane between the total plates: let's denote this location as $x = x_m$. If $\psi(x)$ has a min at $x = x_m$, then $E(x) = -d\psi/dx$ must vanish at $x = x_m$: $E(x_m) = 0$. Then the Maxwell stress also vanishes as $x = x_m$, leaving only the hydrostatic pressure $p(x_m) = p_m$. Our force balance then yields the double-layer repulsion as

$$P_{DL} = p_m - p_\infty \quad (151)$$

So all we need to do is evaluate the pressure at the midplane between the two plates.

Although it was derived for a single plate, (145) also applies to the two-plate problem. To prove this, we note that (144) can be generalized to vector form and converted into a contour integral:

$$\int_{\mathbb{C}} \underbrace{\nabla p \cdot d\mathbf{r}}_{dp} = kT\sum_i \int_{\mathbb{C}} \underbrace{\nabla c_i \cdot d\mathbf{r}}_{dc_i}$$

where $\mathbb{C}$ is any open contour and $d\mathbf{r}$ is a vector displacement of differential length. We choose an arbitrary contour $\mathbb{C}$ connecting some point far outside the region between the plates (where the pressure is p_∞ and the concentrations are $c_{i\infty}$) – then passes around the top edge of the plate into the region between the plates – ending up at a second point on

the mid-plane having pressure p_m and concentrations c_{im}.♥ The result is

$$p(x_m) - p_\infty = kT\left[\sum_i c_i(x_m) - \sum_i c_{i\infty}\right]$$

Substituting Boltzmann's equation (124) and (151)

$$P_{DL} = kT\sum_i c_{i\infty}\left[\exp\left(-\frac{z_i e\psi_m}{kT}\right) - 1\right]$$

Note that if the plates are widely separated (i.e. $D \to \infty$), the solution at the midplane can be expected to have the same composition as the bulk (i.e. $c_{im} \to c_{i\infty}$) and $\psi_m \to 0$, so that the above equation predicts $P_{DL} \to 0$ as $D \to \infty$, which is reasonable.

If D is a few Debye lengths, then ψ_m is not yet zero, but it is small enough so that the exponentials in (152) can be linearized [as in the right-hand side of (150)]. This leads to

$$\lim_{\psi_m \to 0} P_{DL} = \frac{1}{2}\kappa^2 \varepsilon \psi_m^2$$

Finally, we can make the quantities in this expression dimensionless

$$\lim_{\psi_m \to 0} P_{DL} = \frac{1}{2}\frac{2Ie^2}{\varepsilon kT}\varepsilon\left(\frac{kT}{e}\right)^2\left(\frac{e\psi_m}{kT}\right)^2$$

$$= IkT\left(\frac{e\psi_m}{kT}\right)^2$$

or

$$\lim_{\psi_m \to 0} \frac{P_{DL}}{IkT} = \left(\frac{e\psi_m}{kT}\right)^2 \qquad (152)$$

Note that IkT is an osmotic pressure (as might be given by van't Hoff's law), so it has the same units as P_{DL}.

Debye Approximation

What remains is to solve the Poisson-Boltzmann equation to calculate ψ_m. There are two approximations which yield simple analytical expressions for the potential profile and the double-layer force. First, we can once again assume that the potential is everywhere small enough to linearize the Poisson-Boltzmann equation

$$|\psi_0| \ll \frac{kT}{e}$$

where ψ_0 denotes the surface potential of the inner surface of either plate. Using the Debye approximation, the Poisson-Boltzmann equation becomes (131):

$$\frac{d^2\psi}{dx^2} = \kappa^2\psi$$

Integrating this ODE subject to:

$$\Psi = \Psi_0 \text{ at } x=0$$

and

$$\frac{d\psi}{dx} = 0 \text{ at } x=x_m$$

The particular solution is:

$$\frac{\psi(x)}{\psi_0} = \cosh \kappa x - \tanh \kappa x_m \sinh \kappa x$$

In particular, we are interested in the potential at the mid-plane:

$$\psi_m = \psi_0 \operatorname{sech} \kappa x_m$$

which will then be used in (152). Thus the double-layer force per unit area between two plates separated by a distance D (i.e. $x_m = D/2$) is given by

$$\lim_{\psi_0 \to 0} \frac{P_{DL}}{IkT} = \left(\frac{e\psi_0}{kT}\right)^2 \operatorname{sech}^2 \frac{\kappa D}{2} \qquad (153)$$

where

$$\operatorname{sech} u \equiv \frac{1}{\cosh u} = \frac{2}{e^u - e^{-u}}$$

To see more clearly the functional form of the decay in the double-layer force with distance, consider the limit $D \to \infty$:

$$\lim_{u \to +\infty} \operatorname{sech} u = \frac{2}{e^u - \cancel{e^{-u}}} = 2e^{-u}$$

and

$$\lim_{u \to +\infty} \operatorname{sech}^2 u = 4e^{-2u}$$

Then (153) becomes

♥ A subtle requirement revealed by this proof is that this contour (between the solution outside and the solution between the plates) must exist completely inside the solution. In particular the contour $\mathbb{C}$ cannot pass through the plate because the differential form of (144) does not apply inside a rigid solid. In effect, the final expression for p_m assumes the electrolyte solution between the plates is in electrochemical equilibrium with the solution outside. For this to happen, there must exist a path allowing ions to diffuse between the two regions.

$$\lim_{\substack{D\to\infty \\ \psi_0\to 0}} \frac{P_{DL}}{IkT} = 4\left(\frac{e\psi_0}{kT}\right)^2 e^{-\kappa D} \qquad (154)$$

Notice that this is the exponential decay mentioned in the introduction of this topic on page 70.

Linear Superposition Approx.

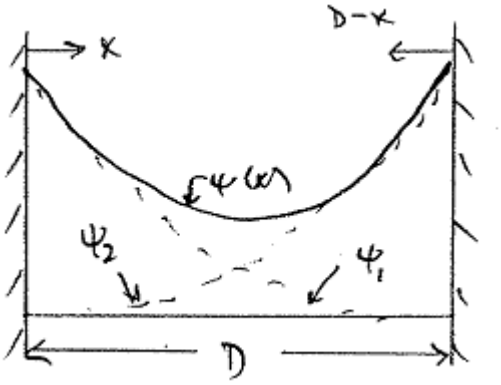

When two parallel plates are widely spaced, say $\kappa D >> 2$, the potential profile next to each of them is essentially that next to an isolated plate.

Thus, using our previous analysis of an single plate (137), the profile next to the left plate (#1) is:

$$\tanh\left[\frac{ze\psi_1(x)}{4kT}\right] = \gamma e^{-\kappa x} \qquad (155)$$

where $$\gamma \equiv \tanh\frac{ze\psi_0}{4kT}$$

while the profile next to the right plate (#2) is obtained by replacing x by (the distance from the right plate) $D–x$:

$$\tanh\left[\frac{ze\psi_2(x)}{4kT}\right] = \gamma e^{-\kappa(D-x)} \qquad (156)$$

Remember that (137) was for a z-z electrolyte. That restriction still applies here, although there is no need for the surface potential ψ_0 to be small. By saying that the potential profile next to either surface is essentially that for an isolated double layer, we mean that one surface doesn't "see" the other surface. When this is true, the total potential profile can be represented as the sum of the undisturbed profiles:

$$\psi(x) = \psi_1(x) + \psi_2(x)$$

In particular, we are interested in the potential at the midplane:

$$\psi_m = \psi_1\left(\frac{D}{2}\right) + \psi_2\left(\frac{D}{2}\right)$$

Since the potential profiles decay exponentially with distance, if we are more than a Debye length away from either surface, the potential will be small enough so that we can linearize the tanh function on the left-hand sides of (155) and (156) [see (139)]:

$$\tanh\left[\frac{ze\psi_1(x)}{4kT}\right] \approx \frac{ze\psi_1(x)}{4kT} = \gamma e^{-\kappa x}$$

or $$\psi_1(x) \approx \frac{4kT}{ze}\gamma e^{-\kappa x}$$

Similarly $$\psi_2(x) \approx \frac{4kT}{ze}\gamma e^{-\kappa(D-x)}$$

Thus $$\psi_1\left(\frac{D}{2}\right) \approx \psi_2\left(\frac{D}{2}\right) \approx \frac{4kT}{ze}\gamma e^{-\kappa D/2}$$

and our mid-plane potential becomes

$$\frac{ze\psi_m}{kT} \approx 8\gamma e^{-\kappa D/2}$$

Substituting this and $I = z^2 c_\infty$ into (152):

$$\lim_{D\to\infty} \frac{P_{DL}}{c_\infty kT} = \left(\frac{ze\psi_m}{kT}\right)^2 = 64\gamma^2 e^{-\kappa D} \qquad (157)$$

If the surface potential ψ_0 is small enough then

$$\gamma^2 \approx \left(\frac{ze\psi_0}{4kT}\right)^2$$

and our double-layer repulsion becomes

$$\lim_{\substack{D\to\infty \\ \psi_0\to 0}} \frac{P_{DL}}{c_\infty kT} = 4\left(\frac{ze\psi_0}{kT}\right)^2 e^{-\kappa D}$$

which is identical with (154) (recall $I = z^2 c_\infty$), as it should be if we haven't made a mistake.

Double-Layer Repulsion between Spheres: Derjaguin's Approximation

Calculating the double-layer force between nonplanar bodies (e.g. two spheres) is generally much more difficult than for parallel plates because the Poisson-Boltzmann equation is no longer ordinary. But when the radius of curvature of the bodies is much larger than the Debye length, the double layers are nearly planar in the region of minimum separation, where most of the interaction arises.

Recognizing this, Derjaguin suggested that the force could be estimated by replacing the curved surface with a series of terraces, which are plane, parallel, disks or annuli (as shown in the figure in the upper right corner of page). Let these surface elements have areas A_1, A_2, A_3 … and be separated by D_1, D_2, D_3 … If $P_{DL}(D_i)$ is the double-layer force per unit area between two infinite parallel plates separated by D_i, then $P_{DL}(D_i)A_i$ is the contribution to double-layer repulsion between the two spheres from the i^{th} terrace. Summing the contributions from each terrace gives the total double-layer force between the two spheres:

$$F_R = \sum_i P_{DL}\left(D_i\right) A_i$$

In the limit of a large number of very small terraces, the sum can be replaced by the integral

$$F_R = \int P_{DL}\left(D\right) dA \qquad (158)$$

Consider the interaction between an annulus having radii x and $x+dx$; let two of these be separated by a distance D: the area of the annulus is

$$dA = 2\pi x\, dx$$

and the contribution to the force between the spheres is

$$dF_R = P_{DL}(D)\, 2\pi x\, dx$$

Next we need to relate D to x. Let's do this for two spheres having unequal radii a_1 and a_2.

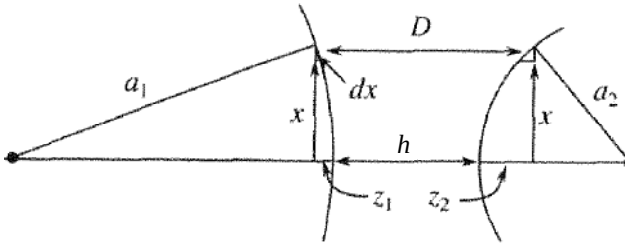

From the geometry above

$$D = h + z_1 + z_2 \qquad (159)$$

In turn, the z's can be related by x using Pathagorus' thereom:

$$\cancel{a_1^2} = x^2 + \left(a_1 - z_1\right)^2 = x^2 + \cancel{a_1^2} - 2a_1 z_1 + \underbrace{z_1^2}_{\text{neglect}}$$

leaving $$z_1 \approx \frac{x^2}{2a_1}$$

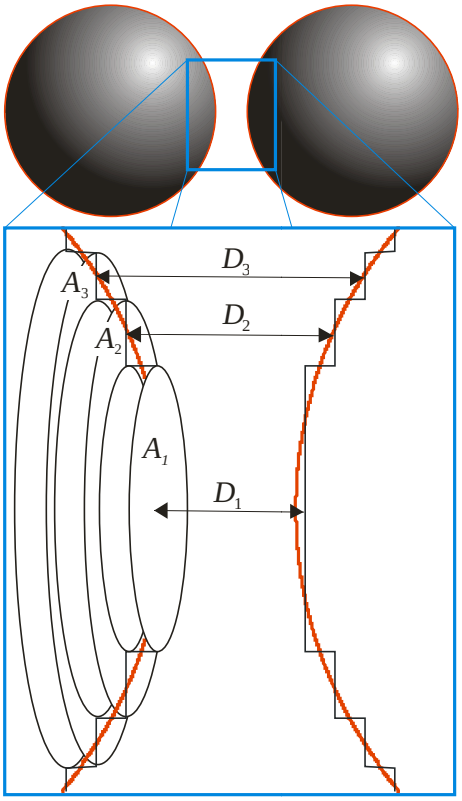

Similarly $$z_2 \approx \frac{x^2}{2a_2}$$

Substituting into (159)

$$D = h + \left(\frac{1}{a_1} + \frac{1}{a_2}\right)\frac{x^2}{2}$$

so $$dD = \left(\frac{1}{a_1} + \frac{1}{a_2}\right) x\, dx$$

and

$$dA = 2\pi x\, dx = 2\pi\left(\frac{1}{a_1} + \frac{1}{a_2}\right)^{-1} dD = 2\pi \frac{a_1 a_2}{a_1 + a_2} dD$$

(158) becomes♠

$$F_R\left(h\right) = 2\pi \frac{a_1 a_2}{a_1 + a_2} \int_h^\infty P_{DL}\left(D\right) dD$$

♠You might expect the upper limit to be the largest reasonable value of D (= $h + a_1 + a_2$). Since P_{DL} decays exponentially fast with D, P_{DL} vanishes long before D reaches such a large value. Thus we can replace this "reasonable" upper bound with ∞ (which greatly simplifies the final result) without incurring any significant error.

which is called ***Derjaguin's approximation***.

In colloid stability, we are really interested in the potential energy resulting from the double-layer interaction between particles. This is the work required to bring two spheres together:

$$\phi_R(h) = \int_h^\infty F_R(h')\,dh'$$

For example, if we use the resulting expression from the linear superposition aproximation [i.e. (157)], the interaction between two identical spheres of radius *a* is given by

$$\phi_R(h) = \frac{64\pi a c_\infty kT}{\kappa^2}\gamma^2 e^{-\kappa h}$$

Notice that both the force between two spheres, as well as the potential energy between two spheres, scales as the radius *a* of the spheres. Notice also the exponential decay with separation distance.

More Rigorous Approach

The 1-D analysis leading to the double-layer force between parallel plates cannot be directly generalized to give a rigorous method for calculating double-layer forces between arbitrary shapes. In this section, we show the general method, which necessarily involves vectors and tensors.

When two identical bodies bearing counterion clouds are brought sufficiently close to one another that their clouds overlap, then electrostatic repulsion occurs.

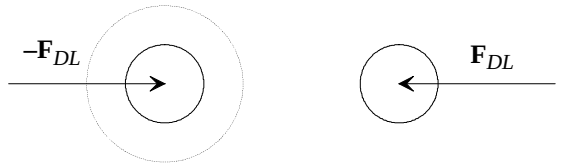

Then I would have to apply a force $\mathbf{F}_{DL}$ to keep them from moving apart. How large is this force?

To answer this question is difficult. Although $\psi(\mathbf{x})$ was known already in 1913, it took another 25 years before the force was calculated — even in the simplest geometry of parallel planes. Of course, today we enjoy the benefits of standing on the shoulders of giants. From this perspective, the answer appears simple.

We start by applying a force balance to some system (indicated by the dotted line in the schematic above). As our system, let's choose a region which completely encloses only one of the two bodies. Recognizing that this system might experience pressure forces and electrostatic body forces, our force balance becomes:

$$\mathbf{F}_{DL} + \mathbf{F}_e + \mathbf{F}_p = \mathbf{0} \qquad (160)$$

So the problem reduces to finding the electrical and pressure forces. These can be written as surface or volume integrals:

$$\mathbf{F}_p = -\int_S p\mathbf{n}\,da \qquad (161)$$

$$\mathbf{F}_e = \int_V \rho\mathbf{E}\,dV \qquad (162)$$

In principle, if $\psi(\mathbf{x})$ is known, we can calculate $\rho(\mathbf{x})$ from Poisson's equation and $\mathbf{E}(\mathbf{x})$ from the gradient. This purely computational problem can be greatly simplified if I can convert this volume integral into a surface integral. Unfortunately, this volume integral does not have the form needed to apply the Divergence Theorem — at least, not yet.

Recall the differential form of Gauss's law:

$$\nabla\cdot\mathbf{E} = \frac{\rho}{\varepsilon}$$

Thus the integrand of (162) can be written as:

$$\rho\mathbf{E} = \varepsilon(\nabla\cdot\mathbf{E})\mathbf{E} = \nabla\cdot\underline{\underline{\mathbf{T}}}$$

where $$\underline{\underline{\mathbf{T}}} \equiv \varepsilon\left(\mathbf{EE} - \tfrac{1}{2}E^2\underline{\underline{\mathbf{I}}}\right)$$

is called the ***Maxwell stress tensor***, **EE** is a dyadic product and $\underline{\underline{\mathbf{I}}}$ is the unit tensor.

Reference - Jackson, pp193f.

So (162) can be rewritten as:

$$\mathbf{F}_e = \int_V \nabla\cdot\mathbf{T}\,dV = \int_S \mathbf{n}\cdot\mathbf{T}\,da$$

where the second equation results from application of the Divergence Theorem. This result can be added to (161). Since the limit of integration of the two integrals is the same, we can just add the integrands:

$$\mathbf{F}_e + \mathbf{F}_p = \int_S [\mathbf{n}\cdot\underline{\underline{\mathbf{T}}} - p\mathbf{n}]\,da$$

Substituting this result into (160):

$$\mathbf{F}_{DL} = -(\mathbf{F}_e + \mathbf{F}_p) = -\int_S [\mathbf{n}\cdot\underline{\underline{\mathbf{T}}} - p\mathbf{n}]\,da \qquad (163)$$

where *S* can be any closed surface entirely containing just one of the two interacting bodies. Although the integral of a uniform hydrostatic pressure over an open surface yields a net force, the integral over a closed surface must vanish:

$$\int_S \mathbf{n}p_\infty\,da = 0 \qquad (164)$$

Subtracting (164) from (163):

$$\mathbf{F}_{DL} = \int_S [\mathbf{n}(p-p_\infty) - \mathbf{n}\cdot\underline{\underline{\mathbf{T}}}]\, da \qquad (165)$$

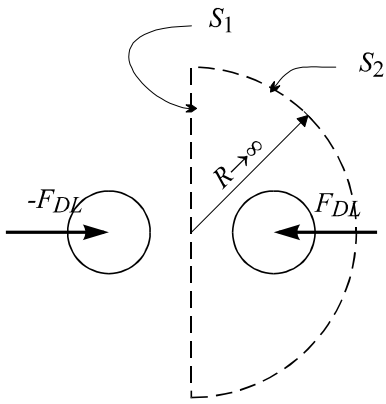

Some choices of S are more convenient than other. For example, if we choose a hemisphere of radius $R\to\infty$, the contribution to the integral from much of this surface will vanish. To show this, we need to recognize that far from either particle the electrostatic potential will decay as:

as $R\to\infty$: $\psi \to Ae^{-\kappa R}$ on S_2

This means that the electric field also decays exponentially $\mathbf{E} = -\nabla\psi$:

as $R\to\infty$: $E \to Be^{-\kappa R}$

The ion concentrations decay to their bulk values exponentially:

as $R\to\infty$: $c_i - c_{io} = c_{io}\,[\exp(-z_i\psi/kT) - 1]$

$= O(\psi) \to C_i\, e^{-\kappa R}$

and the hydrostatic pressure will decay exponentially:

as $R\to\infty$: $p-p_\infty = kT\,\Sigma_i\,(c_i - c_{io}) \to De^{-\kappa R}$ (166)

The Maxwell stress behaves like E^2:

as $R\to\infty$: $\underline{\underline{\mathbf{T}}} = O(E^2) \to Fe^{-2\kappa R}$ (167)

Adding contribution from (166) and (167), the integrand in (165) behaves like

as $R\to\infty$: $\mathbf{n}(p-p_\infty) - \mathbf{n}\cdot\underline{\underline{\mathbf{T}}} \to Ge^{-\kappa R}$

For a particular element of solid angle $d\Omega$, the area element will tend to become large as $R\to\infty$:

$$da = R^2\, d\Omega$$

However this is not nearly as fast an increase as the integrand decreases:

$[\mathbf{n}(p-p_\infty) - \mathbf{n}\cdot\underline{\underline{\mathbf{T}}}]\, da \to G\,R^2 e^{-\kappa R}\, d\Omega \to 0$ on S_2

Now the contribution from S_2 vanishes, leaving only the contribution from the open plane surface.

$$\mathbf{F}_{DL} = \int_{S_1}\left[\mathbf{n}\left(p-p_\infty\right) - \mathbf{n}\cdot\underline{\underline{\mathbf{T}}}\right] da$$

where S_1 is any infinite plane passing between the two bodies.

Application to Flat Plates

As an example, let's try to calculate the electrostatic interaction of two large parallel plates.

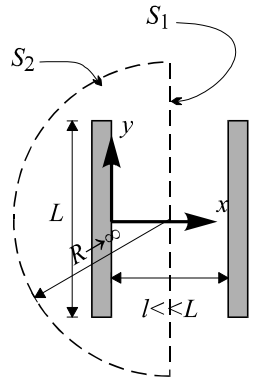

Let S_1 be a plane parallel to the plates which is located somewhere in between them. Let x be measured normal to this surface. If the dimensions of the plates are sufficiently large compared to the distance separating them, and the plates are uniformly charged, then away from the ends of the plates:

$l<<L$: $\psi = \psi(x)$

Thus $E_x = -d\psi/dx$

$E_y = E_z = 0$

If we are computing the force which must be applied to hold the *left* plate stationary, then $\mathbf{n}$ (which is the outward normal) will be

$$\underline{n} = \underline{e}_x$$

$$\underline{n}\cdot\underline{\underline{\mathbf{T}}} = (\varepsilon/4\pi)[\underline{n}\cdot(\underline{E}\underline{E}) - (1/2)(\underline{n}\cdot\underline{\underline{\mathbf{I}}})E^2]$$

$$= (\varepsilon/4\pi)[(\underline{n}\cdot\underline{E})E_x\underline{e}_x - (1/2)E_x^2\underline{e}_x]$$

$$= (\varepsilon/8\pi)E_x^2\underline{e}_x = (\varepsilon/8\pi)(d\psi/dx)^2\underline{e}_x$$

Since this is uniform over the entire surface, the integral is easy to compute:

$$\int_{S1} \underline{n} \cdot \underline{\underline{T}}\, da = (\varepsilon/8\pi)(d\psi/dx)^2 \underline{e}_x \int_{S1} da$$

$$= (\varepsilon/8\pi)(d\psi/dx)^2 \underline{e}_x A_1$$

where A_1 is the total area of the plate. The other term is also easy to compute:

$$\int_{S1} \underline{n}(p-p_\infty)da = \int_{S1} \underline{e}_x(p-p_\infty)da = (p-p_\infty)\underline{e}_x A_1$$

Substituting into our formula for computing the double-layer force:

$$\underline{F}_{DL} = [(p-p_\infty) - (\varepsilon/8\pi)(d\psi/dx)^2]A_1 \underline{e}_x$$

Clearly, there is only an x-component to this force which is proportional to the area of the plate. The double-layer force per unit area is

$$p_{DL} \equiv F_{DLx}/A_1 = (p-p_\infty) - (\varepsilon/8\pi)(d\psi/dx)^2 \qquad (168)$$

Lecture #22 begins here

Flocculation

There is an irresistible tendency for flocculation to occur in most lyophobic systems:

interfacial tension -- a contribution to the free energy of a two-phase system that is proportional to the interfacial area

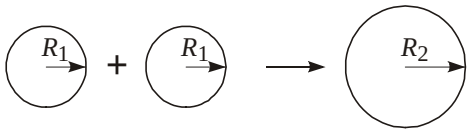

Since interfacial tensions are always positive, the free energy of any such system can be reduced by reducing the area. For example, consider two spherical oil droplets which coalesce together to form one larger sphere:

$$V_2 = 2V_1 \rightarrow \frac{R_2}{R_1} = 2^{1/3} = 1.26$$

then $$\frac{A_2}{2A_1} = 2^{-1/3} = 0.79$$

Thus there is a 21% reduction in area as a result of coalescence of two drops. This represents a thermodynamic tendency for flocculation to occur.

Rapid Brownian Flocculation

In a stagnant fluid, particles undergo Brownian motion, which from time to time results in a collision between two particles. Let's suppose that every collision between two singlets results in the formation of a doublet -- i.e. the particles stick together for some reason. Then the rate of flocculation is simply the rate of Brownian collisions.

Reference: Kruyt, pp278-82

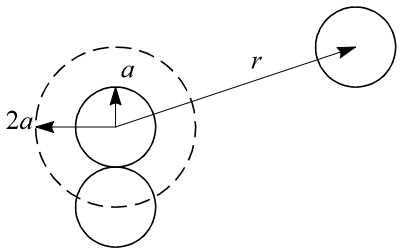

Smoluchowski (1916) calculated this rate by computing the rate of diffusion of particles to a sphere fixed at the center of the coordinate system. In spherical coordinates, the radial flux is given by Fick's law as:

$$J_r = \text{particles/m}^2\text{-s} = -D\frac{dc}{dr} \qquad (169)$$

At steady state, there can be no accumulation of particles in any spherical shell, so the rate of transport (flux times area) must be the same for all spherical shells:

$$\frac{d}{dr}\left(4\pi r^2 J_r\right) = 0 \qquad (170)$$

Substituting Fick's law for the radial flux:

$$\frac{d}{dr}\left(r^2\frac{dc}{dr}\right) = 0$$

which can be easily integrated to obtain the general solution for the concentration profile. We will need two boundary conditions to obtain the particular solution to or this second-order ordinary differential equation.

as $r\rightarrow\infty$: $\quad c \rightarrow c_\infty \qquad (171)$

at r=2a: $\quad c = 0 \qquad (172)$

This second boundary condition can be rationalized as follows. By c we mean the concentration of particles *free to undergo B.M.* c=0 at r=2a because particles at that position stick to the central particle and are no longer free to undergo B.M.

Integrating $$c(r) = c_\infty\left(1-\frac{2a}{r}\right)$$

The rate of collisions with the stationary target sphere is

$$-4\pi r^2 J_r = 8\pi D a c_\infty \qquad (173)$$

If the target sphere is allowed to also undergo B.M. with the same diffusion coefficient, what will be the collision rate? It turns out to be twice as large.♣

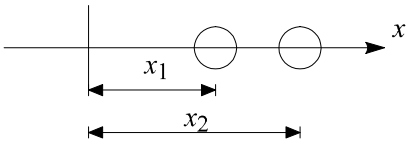

To show this, consider two Brownian particles which at time zero are located at the origin. At a later time t we know their mean square locations from Einstein's equation:

♣ See Exam #1, Prob. 1d for 06-712 during Spring 2010.

$$\langle x_1^2 \rangle = 2D_1 t$$

$$\langle x_2^2 \rangle = 2D_2 t$$

Thus we can also compute how the relative distance between the two changes with time:

$$\langle (x_2-x_1)^2 \rangle = \langle x_2^2 - 2x_2x_1 + x_1^2 \rangle$$

$$= \langle x_2^2 \rangle - 2\langle x_2x_1 \rangle + \langle x_1^2 \rangle$$

But $\langle x_2x_1 \rangle = 0$ because either particle is equally likely to be on either side of the origin. In other words, the probability of x_2x_1 being positive or negative is the same so that the average is zero. This leaves:

$$\langle (x_2-x_1)^2 \rangle = \langle x_2^2 \rangle + \langle x_1^2 \rangle = 2(D_1+D_2)t$$

For identical particles $D_1=D_2$ and the relative Brownian motion between two moving particles is twice as large as that when one is held stationary ($D_1=0$).

Generalizing (1), we replace D by $2D$. For a single target particle:

$$\text{no. of collisions/time} = 16\pi Dac_\infty \qquad (174)$$

To get the rate of collision per unit volume, we multiply by the number of targets per unit volume, c_∞:

$$\text{no. collision/vol-time} = 16\pi Dac_\infty^2 = b_{11} \qquad (175)$$

This determines the rate at which singlets combine to form doublets. Not surprisingly then, flocculation is a second-order reaction.

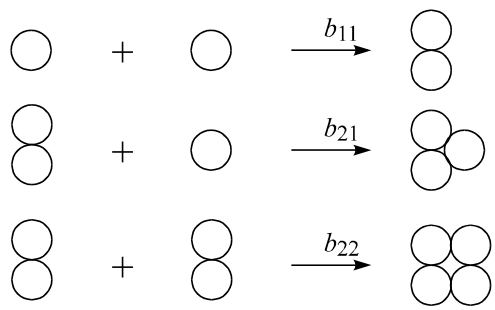

The resulting doublet may combine with a singlet or another doublet to form a triplet or quadruplet, which might then further combine to form larger aggregates. To describe the kinetics of aggregation we have to be able to predict the of collisions between each type of aggregate and any other.

Smoluchowski computed the rate of these collisions by treating any size aggregate as a sphere. To compute the rate of collisions between spheres of radii a_i and a_j, we start with (175) and replace:

$$2a \rightarrow a_i + a_j$$

$$2D \rightarrow D_i + D_j$$

$$c_\infty^2 \rightarrow c_i c_j$$

Thus (175) becomes:

$$b_{ij} = 4\pi (D_i+D_j)(a_i+a_j)c_ic_j$$

The the diffusion coefficient of any size sphere is inversely proportional to its radius. Bigger spheres have less mobility and a smaller diffusion coefficient:

$$D_i = m_i kT = \frac{kT}{6\pi\mu a_i}$$

which is called the ***Stokes-Einstein*** equation. Substituting it into the expression for the collision rate, we have:

$$b_{ij} = \frac{2kT}{3\mu}\left(\frac{1}{a_i}+\frac{1}{a_j}\right)\left(a_i + a_j\right)c_i c_j \qquad (176)$$

Kinetics of Flocculation

With the rate of each type of encounter known, we can now try to predict how the concentration of any type of aggregate will evolve with time. A mass balance on any species gives:

{rate of accum} = {rate of formation} – {rate of depletion}

Let's take a particular species, say quintuplets (k=5). Particles of size 5 are formed by the combination of 1+4 or 2+3, where particles of size 5 are depleted by combining with particles of any size:

$$\frac{dc_5}{dt} = b_{14} + b_{23} - (b_{51}+b_{52}+\ldots+b_{5\infty})$$

The corresponding mass balance for species of any size is:

$$\text{for } k\geq 2: \qquad \frac{dc_k}{dt} = \frac{1}{2}\sum_{\substack{i=1 \\ j=k-i}}^{i=k-1} b_{ij} - \sum_{i=1}^{\infty} b_{ik} \qquad (177)$$

The factor of 1/2 in front of the sum is to avoid double counting the same type of collision (for example, i,j = 1,k-1 and k-1,1).

Now (176) can be substituted into (177) to obtain a set of O.D.E. is the concentrations. One additional approximation by Smoluchowski allowed an analytical solution to this infinite set:

$$\left(\frac{1}{a_i}+\frac{1}{a_j}\right)\left(a_i+a_j\right)\approx 4 \qquad (178)$$

Note that this is true when $i=j$. It's also approximately true if a_i and a_j are approximately the same. Thus (176) becomes:

$$b_{ij}=\frac{8kT}{3\mu}c_i c_j \qquad (179)$$

Substituting (179) into (177):

$$\frac{dc_k}{dt}=\frac{8kT}{3\mu}\left\{\frac{1}{2}\sum_{\substack{i=1\\ j=k-i}}^{i=k-1} c_i c_j - c_k\sum_{i=1}^{\infty} c_i\right\}$$

Now this set of O.D.E.'s can be solved analytically once we have specified some initial conditions. Let's suppose we start with all singlets of some known concentration:

for k=1: $c_1(0)=c_o$

for k=2,3,.. $c_k(0)=0$

The particular solution to this initial-value problem is given by:

$$c_k(t)=\frac{\left(t/\tau\right)^{k-1}}{\left(1+t/\tau\right)^{k+1}}c_0$$

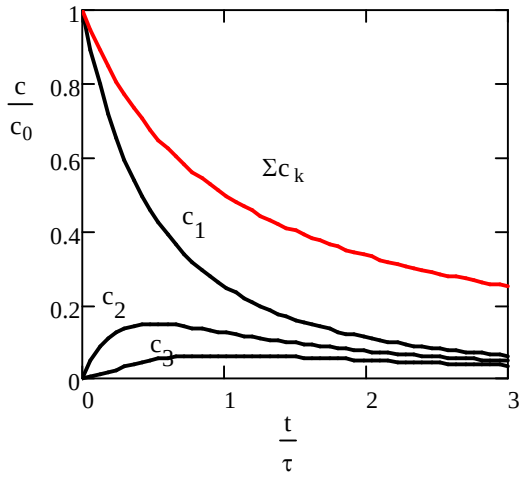

where τ is called the ***flocculation time***:

$$\tau=\frac{3\mu}{4kTc_0}\approx\frac{2\times10^{11}\ \text{s/cm}^3}{c_0}$$

when c_o is the initial number of singlets per unit volume. The number was computed the viscosity of water at room temperature.

The total concentration of particles, irrespective of their size can also be easily computed:

$$c\equiv\sum_{k=1}^{\infty}c_k=\frac{c_0}{1+\frac{t}{\tau}} \qquad (180)$$

This time dependence is characteristic of a second-order reaction. τ represents the half life of the particles concentration: the total particle concentration, c, is reduce by flocculation to half its initial value at t=τ.

EXAMPLE: compute the flocculation time for 1 **M** solution of AgI which precipitates to form 30 nm particles.

Solution: c_o = 4x10^{14} particles/cm^3

τ = 0.5 ms

Thus flocculation would occur in the blink of an eye. To study flocculation, we have to slow it down, say by starting with a much more dilute sol.

Experimental Verification

Since the availability of monodisperse latexes in the 1950's, there have been many experimental measurements of flocculation rates. One such study is that of Swift & Friedlander [*J. Colloid Sci.* **19**, 621 (1964)], whose used a Coulter counter to measure the concentration of flocs of various sizes at different times. Some are their results are plotted below.

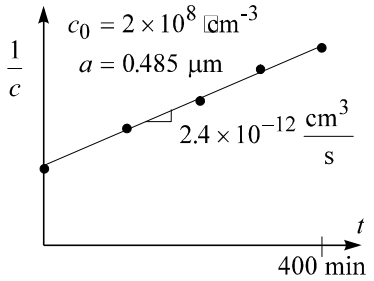

Eq. (180) can be linearized by taking the reciprocal of both sides:

$$\frac{1}{c(t)}=\frac{1}{c_0}+\frac{1}{c_0\tau}t$$

The slope of this plot should be

$$\frac{1}{c_0\tau} = \frac{1}{2\times10^{11}\ \mathrm{s/cm^3}} = 5\times10^{-12}\ \frac{\mathrm{cm^3}}{\mathrm{s}}$$

which should be independent of particle concentration or size. The experimentally determined slope is low by a factor of two. This can be attributed to the following effects which were neglected by Smoluchowski:

- van der Waals attraction is not completely negligible
- $D=D(r)$, for $r<3a$, $D<D(\infty)$ owing to the decreased mobility of either particle when it approaches a solid surface.

Lecture #23 begins here

Considering van der Waals attraction would increase the rate, since migration in the force field is a second transport mechanism which acts in parallel with diffusion. The second effect would decrease the rate since the diffusion coefficient is reduced. The ratio of the actual rate of flocculation to the Smoluchowski rate is called the ***stability ratio***.

$$W \equiv \frac{\text{Smoluchowski's rate}}{\text{actual rate}} \qquad (181)$$

which is usually greater than unity. Below are some more recent data obtained at CMU by Bob Ofoli (PhD Thesis, 1994) using small-angle light scattering.

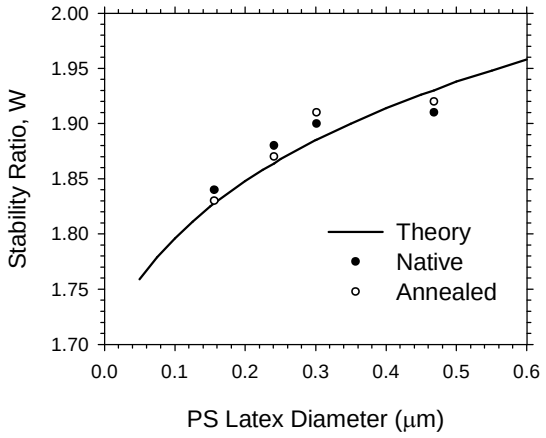

This shows quite good agreement between experiment and theory for rapid flocculation, which has been reported by others. The needed refinements to the theory will now be described.

Slow Brownian Flocculation

Repulsive forces between the particles can significantly slow the rate of flocculation. This can be seen in the sketch below showing experimental data taken by Bob Ofoli on polystyrene latex particles having a diameter of 0.154 μm. At low salt concentrations, the stability ratio can easily reach 1000: meaning the rate is only 0.1% of the rate predicted by Smoluchowski's equation. It has long be recognized that electrostatic repulsion between like charged particles can reduce the rate of flocculation to practically zero.

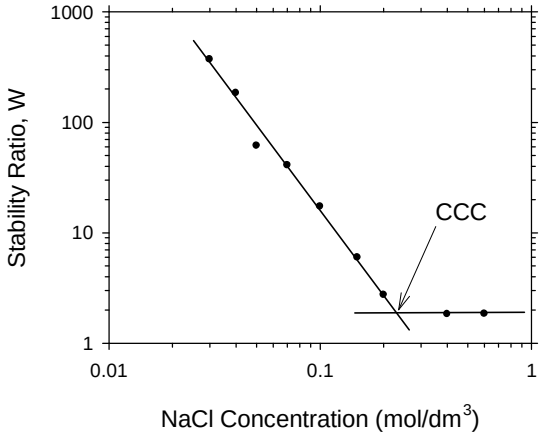

Forces of interaction between particles affect the rate by causing migration in the force field. ***Fuchs*** (1934) modified Smoluchowski's analysis to include migration in the force field. (169) becomes:

$$J_r = \underbrace{-D\frac{dc}{dr}}_{\text{diffusion}} + \underbrace{\frac{mFc}{}}_{\text{migration}} = -D\frac{dc}{dr} + \frac{D}{kT}\left(-\frac{d\phi}{dr}\right)c$$

$$= -D\left(\frac{dc}{dr} + \frac{c}{kT}\frac{d\phi}{dr}\right)$$

where we have substituted the Nernst-Einstein equation for m and we have assumed a conservative force field, so that $F = -d\phi/dr$. Hydrodynamic interactions are taken into account differently from van der Waals attraction or double-layer repulsion. The latter forces do not depend on the speed with which the particle is moving through the viscous fluid, whereas hydrodynamic drag is proportional to speed. ***Spielman*** (1970) showed that the hydrodynamic forces can be accounted for by reducing the diffusion coefficient (or mobility) by a factor which depends on the separation distance between the two spheres: in effect, replacing D (a constant) by $D(r)$:

$$J_r = -D(r)\left(\frac{dc}{dr} + \frac{c}{kT}\frac{d\phi}{dr}\right) \qquad (182)$$

Substituting (182) into (170) and integrating, subject to boundary conditions (171) and (172), leads eventually to the following expression for the stability ratio defined by (181):

$$W = 2aD(\infty)\int_{2a}^{\infty} \frac{e^{\phi(r)/kT}}{D(r)r^2}dr \qquad (183)$$

If we substitute $\phi(r) = 0$ and $D(r) = D(\infty)$, this reduces to $W = 1$, which means the rate of flocculation is just what Smoluchowski calculated. Because $D(r) \le D(\infty)$, hydrodynamic interactions causes $W \ge 1$, which is what we found experimentally.

Including double-layer repulsion in the theory can result in much larger stability ratios owing to significantly positive values of $\phi(r)$. The plot below shows predictions of van der Waals attraction (blue curve) and the total of van der Waals and double-layer repulsion for several different concentration of a simple 1-1 salt.

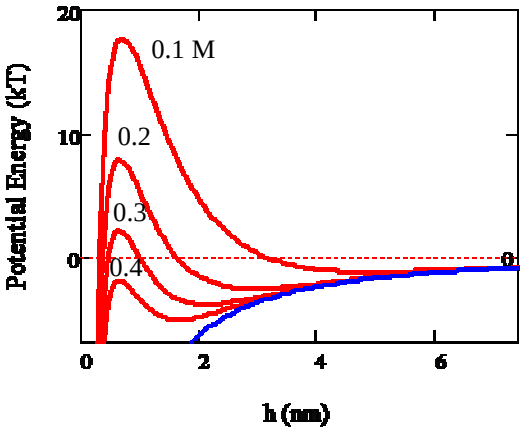

In particular, notice that each curve has a maximum and that maximum is getting smaller with ionic strength.

Below are corresponding predictions of the stability ratios made by Ofoli for slow flocculation:

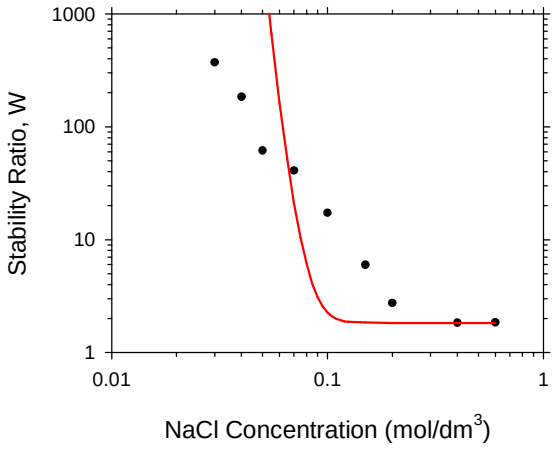

Although qualitative features of the experimental data are predicted (the existence of a CCC, the linear relationship between logW and logC), the quantitative agreement between theory and experiment leaves a lot to be desired.

When the potential energy profile has a maximum $\phi_{max} >> kT$, then the rate is exquisitely sensitive to ϕ_{max}, which represents an energy barrier that the particles must overcome in order to stick to one another. In this limit, a Taylor-series approximation to $\phi(r)$ around $r = r_{max}$ yields an approximation to (183):♠

$$W \approx \frac{2a}{r_{max}^2}\frac{D(\infty)}{D(r_{max})}\sqrt{\frac{2\pi kT}{-\phi''(r_{max})}}\exp\frac{\phi(r_{max})}{kT}$$

where r_{max} is the value of r at which $\phi(r)$ is maximum and $\phi'' = d^2\phi/dr^2$. This exponential sensitivity to the height of the barrier which makes this prediction very sensitive to everything. At least two different sources of error exist which might explain the departure between theory and experiment above for slow flocculation:

- surface roughness of particles
- polydispersity of charge on particles

Rapid Flocculation by Shear

Besides diffusion, another familiar mechanism for transport is ***convection***. Suppose now, that the particles are completely non-Brownian, but that the fluid in which the particles are dispersed moves. Of course, if the velocity of the fluid were uniform everywhere, the relative position of the particles would remain underchanged -- no flocculation would

♠ adapted from a similar expression derived in *AIChE J.*, vol. 276, p274 (1976).

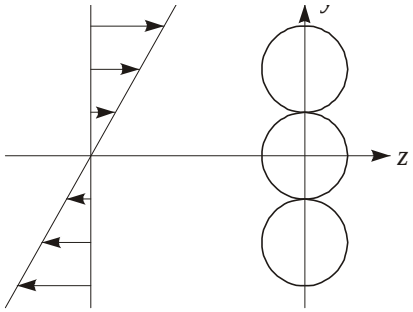

"side view"

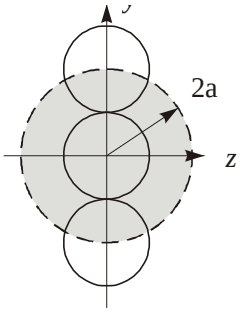

"end view"

occur. Thus it is necessary for the fluid velocity to vary from point to point so that the particles can move relative to one another. The first analysis of this problem was again done by Smoluchowski (1916):

Reference: Kruyt, pp289-92.

Assumptions:

- identical non-Brownian spheres of radius a, uniformly distributed throughout fluid
- fluid undergoes simple linear shear flow
- ignore hydrodynamic interactions (particles move with the same velocity as "undisturbed" fluid at their center)

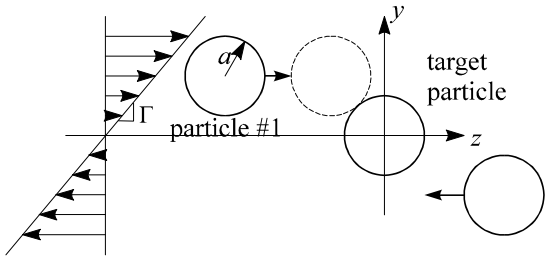

"side view"

As before, let's focus our attention on one target sphere. If we choose our reference frame to move along with the particle, then it appears stationary, particles above move to the right, while particles below move to the left. The velocity of these particles relative our stationary target is:

$$v_z = \Gamma y \qquad (184)$$

As a result of these different speeds, particles can overtake one another and collisions result. Indeed, you can see from the figure below that any particle whose projection onto the *y*-*z* plane lies within one collision diameter of the center of our target, will eventually collide with our target.

In other words, if particle center is located at:

$$(x,y,z) \text{ and } yz<0$$

Then a collision with target will eventually occur if

$$(x^2+y^2)^{1/2} \equiv r \le 2a$$

The rate of collisions with the target is then the net rate they are moving through this tube of radius 2*a* (since all particles in this tube eventually collide with target). Of course, the velocity of the particles varies with *y*. To get rate we must integrate the particle flux over the cross section of the tube:

$$\text{flux} = \left[v_z\left(y\right)\right] c \ [=] \frac{\text{particles}}{\text{cm}^2\text{-s}}$$

where *c* is the number of particles per unit volume (which is assumed to be independent of position).

$$\text{rate} = \iint_{\text{disk}} \left|v_z\left(y\right)\right| c \, dy \, dx \ [=] \frac{\text{particles}}{\text{s}} \qquad (185)$$

The absolute value signs were added because motion in either direction results in a "positive" collision. Noting that *c*=const and substituting (184), (185) becomes:

$$\text{collisions/s} = (64/3)\Gamma a^3 c \qquad (186)$$

This is the result for a single target. Multiplying by the number of targets per unit volume gives the collision frequency per unit volume:

$$\text{collisions/cm}^3\text{-s} = (64/3)\Gamma a^3 c^2$$

Of course, this is the collision frequency between identical particles. To complete the analysis Smoluchowski, generalizes this using:

$$(2a)^3 \rightarrow (a_i+a_j)^3$$

$$c^2 \rightarrow c_i c_j$$

to obtain the collision frequency between spherical flocs of arbitrary size:

$$b_{ij} = (8/3)\Gamma(a_i+a_j)^3 c_i c_j \qquad (187)$$

Using this collision frequency, we can re-analyze the flocculation kinetics according the species mass balance we already developed, namely (177):

$$\frac{dc_k}{dt} = \frac{1}{2}\sum_{\substack{i=1\\ j=k-i}}^{i=k-1} b_{ij} - \sum_{i=1}^{\infty} b_{ik}$$

To obtain an analytical solution to this difficult problem, Smoluchowski made an assumption which is analogous to (178), which is valid when a_i is not too much different from a_j. In this case, Smoluchowski assumed:

$$\sum_{i=1}^{\infty} b_{ik} = \frac{8}{3}\Gamma c_k \sum_{i=1}^{\infty} \underbrace{\left(a_i + a_k\right)}_{\approx 2a_i}^3 c_i \approx \frac{16}{\pi}\Gamma c_k \underbrace{\sum_{i=1}^{\infty}\left(\frac{4}{3}\pi {a_i}^3\right)c_i}_{\phi}$$

which is also valid when a_k is not too much different from a_i. A similar approximation can be made for the other sum in (177). Ultimately, the analysis leads to

$$\frac{dc}{dt} = -\frac{4}{\pi}\Gamma\phi c$$

where $c = \Sigma c_k$ is the total particle concentration. Because the total volume of particles does not change upon flocculation, ϕ is a constant and we see that shear-induced flocculation is a first-order process, unlike Brownian flocculation. Integration yields:

$$c(t) = c_o \exp(-t/\tau)$$

where $\tau = \pi/4\Gamma\phi$

is now the flocculation time.*

Brownian versus Shear-Induced Flocculation

Which is faster: Brownian or shear-induced flocculation? To answer this question, let's compare the collision frequencies for the encounter of identical particles. This is at least applicable during the initial phase when the sol consists of primarily singlets. Dividing (186) by (174):

$$\frac{\text{Shear}}{\text{Brownian}} = \frac{\frac{64}{3}\Gamma a^3 c}{16\pi Dac} = \frac{4\Gamma a^2}{3\pi D} = \frac{8\mu a^3\Gamma}{kT}$$

where we have substituting the Stokes-Einstein equation for D. Clearly shear is more important for larger particles and high shear rates, but is independent of particle concentration. In his review in Kruyt's book, Overbeek writes

> *Everyone, who has ever carried out a coagulation, has seen that coagulation is promoted by agitation of the sol. The agitation, which seems to have little or no influence in the first stages of coagulation, is very effective when the aggregation has already proceeded for some time.*

Why?

Experimental Confirmation of Shear-Induced Rates

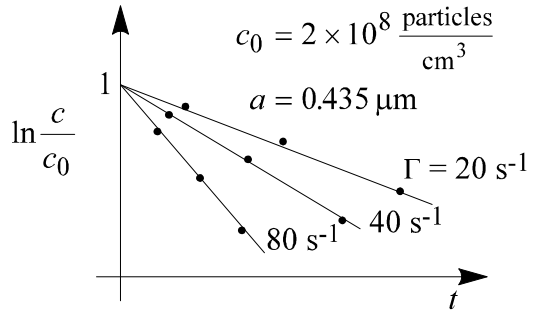

Swift & Friedlander also measured flocculation rates under conditions in which shear-induced flocculation dominates. A Couette apparatus was used to produce nearly uniform shear. Samples were obtained every few minutes and analyzed with a Coulter counter. The results shown at right confirm that the kinetics are ***first-order*** with respect to the particle concentration and that the rate constant is proportional to the ***shear rate***.

Origin on Charge

Nearly all solids in contact with a polar solvent bear a charge. The clearest evidence for this is electrophoretic migration of solid particles in an electric field.

Solids can acquire charge by any of several mechanisms:

* Homework: Repeat the analysis for extensional flow.

Homework: Replacing Γ by dv_z/dr, determine the rate of flocculation in a long tube in which Poiseuille flow occurs. Show that the extent of flocculation in the outlet of the tube is independent of flowrate.

- ***adsorption of ions*** (surfactants like SDS, hydrolysis products of heavy metal cations like $FeOH^{+2}$

- ***dissolution of ions*** from ionic solids, like AgI

For example, the solubility product for AgI is

$$K_{sp} = [Ag^+][I^-] = 7.5x10^{-17}M^2$$

If $[Ag^+] = [I^-] = \sqrt{K_{sp}}$, then the surface will be negatively charged because the smaller and more mobile Ag^+ has a greater tendency to leave the lattice for the solution than I^-. To have no charge on the surface we need to have a greater concentration of silver ions:

$$[Ag^+][I^-] = (3.0x10^{-6}M)(2.5x10^{-11}M) = K_{sp}$$

$[Ag^+] < 3.0x10^{-6}M \rightarrow$ negative charge on solid

$[Ag^+] > 3.0x10^{-6}M \rightarrow$ positive charge on solid

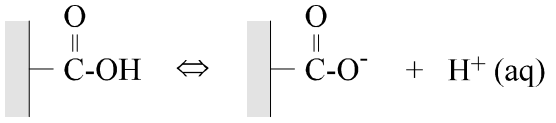

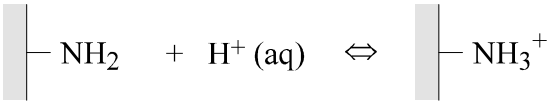

- ***dissociation of acid*** or basic sites. This is particularly common for biological surfaces which are usually composed of proteins containing carboxyl and amines

Most minerals also acquire their surface charge in this manner.

Of course, you would expect that changing the concentration of a potential determining ion — like Ag^+ in the case of AgI sols or H^+ in the case of biological surfaces — to have a profound effect because the surface potential and presumably the surface charge is changed. Indeed, as you approach the concentration of a potential determining ion for which the charge vanishes, the sol becomes unstable and flocculates. This concentration is called:

point of zero charge — concentration of a potential-determining ion at which surface charge vanishes

This concentration is often expressed like pH -- minus the base-10 logarithm of the concentration in moles per liter. For example, a AgI sol has the following PZC:

PZC of AgI:$[Ag^+]=3.0x10^{-6}M$ or pAg=5.5

At least as early as 1903, Freundlich observed that when other salts are added to an electrostatically stabilized dispersion of particles, they too can cause flocculation. Salts which do not contain potential-determining ions are called

indifferent electrolyte -- a salt, acid or base whose ions are not "potential determining"

Unlike potential determining ions, which destabilize only near a particular concentration, indifferent electrolyte cause rapid flocculation for all concentrations above some minimum value called the

critical coagulation concentration (*ccc*) -- minimum concentration of "indifferent" electrolyte required to destabilize a dispersion

The *ccc* was measured for a various indifferent electrolytes and was found to be about the same for all monovalent salts (KCl, NaCl, etc.). However, divalent salts have a much lower *ccc*, while trivalent salt have a even lower *ccc*:

$$ccc = 100:1.6:0.05 \text{ for } z = 1:2:3$$

This dependence on the valence of the salt (more specifically, on the charge number of the counterions, for unsymmetric electrolytes) is called the:

Shulze-Hardy Rule -- the *ccc* depends strongly on the charge number of the counterion

This was observed before 1900. It was generally assumed that even indifferent electrolytes adsorbed on the surface and reduced the charge, thereby destabilizing the sol. Then makes sense in that the higher the valance, the less electrolyte is needed to neutralize the surface charge. This was called the ***Freundlich adsorption theory*** after H. Freundlich who suggested it in 1903.

if ions adsorbed: $ccc \propto z^{-1}$

observed: $ccc \propto z^{-6}$

We now know that the *ccc* is associated with ***Debye screening*** of the electrostatic interactions between particles (due to the compression of the double layer by added salt) rather than changes in the charge on the surfaces. By the end of the 1930's, Freundlich's adsorption theory was abandoned by colloid scientists in favor of Debye screening.

During the next few weeks, we are going to delve into the theory to electrostatic interactions across an aqueous electrolyte solution, which turns out to be

very different from the interactions across vacuum or a simple dielectric material, owing to the presence of mobile charges in the water. But first, we need to review some basic ideas from electrostatics.

Electrokinetic Phenomena

So far in our discussion of diffuse double-layers, there has been no fluid motion. But since the fluid inside the diffuse cloud is charged, we can exert a force on it by applying an electric field tangent to the surface.

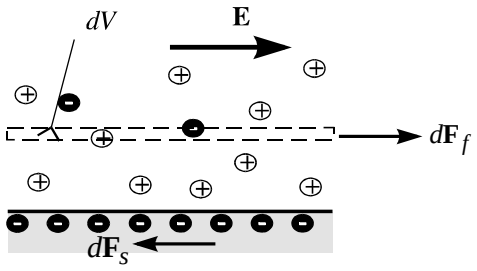

Consider again the distribution of ions near a charged interface. The solution is not electrically neutral. So if an electric field is applied tangent to the surface, the fluid will experience an electrostatic body force:

$$d\mathbf{F}_f = (dq)\mathbf{E} = (\rho_e dV)\mathbf{E}$$

where dq is the net charge on a fluid element having volume dV. The solid is oppositely charged, so it feels a force in the opposite direction. Consequently, at steady state, we can expect the fluid to move relative to the solid, or vice versa.

At least two phenomena are associated with with the relative motion generated by this externally applied electrostatic force:

electrophoresis - migration of charged particles through an otherwise quiescent fluid

electro-osmosis - flow of fluid through a porous solid bearing a surface charge

In both cases, relative motion between the fluid and the solid arises when an electric field is applied externally. Conversely, forcing a fluid to move tangent to a charged interface generates an electric field:

sedimentation potential - the electrical potential (gradient) which arises during sedimentation of charged particles in a gravitational field

streaming potential - the electrical potential (gradient) which arises during flow of fluid through a porous solid which bears a surface charge

These four phenomena depend on the magnitude of the surface charge. Measurements of these induced velocities or induced potentials are the most commonly used techniques for determination of surface charge.

Lecture #24 begins here

Hydrostatic Equilibrium

Since the fluid inside the diffuse cloud is charged, any electric field in the fluid will exert a force on the fluid elements. This body force needs to be included in the Navier-Stokes equations:

$$\text{electrostatic body force/volume} = \rho_e\mathbf{E}$$

which is analogous to the body force exerted by gravity:

$$\text{gravitational body force/volume} = \rho\mathbf{g}$$

Including electrostatics, but neglecting gravity, the Navier-Stokes equation becomes:

$$\rho D\mathbf{v}/Dt = \mu\nabla^2\mathbf{v} - \nabla p + \rho_e\mathbf{E} \qquad (188)$$

In the Gouy-Chapman model described in a previous section, the fluid is stagnant. At hydrostatic equilibrium, any electric field applied to a charged fluid element will lead to a pressure gradient:

$$\mathbf{v} = \mathbf{0}: \qquad \nabla p = \rho_e\mathbf{E} \qquad (189)$$

This is just a more general vector representation of (143). It is also a special case of (188) the Navier-Stokes equation with electrostatic body forces.

Smoluchowski's Analysis (ca. 1918)

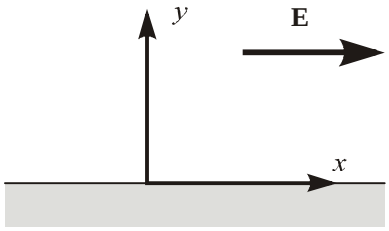

Consider an infinite plate (the y=0 plane in the figure above) in contact with an electrolyte solution. Suppose the plate bears a uniform surface charge density and we somehow externally apply a uniform electric field δE_x tangent to the surface in the $+x$ direction. Let's try to find the velocity profile $\mathbf{v}$ induced by this electric field.

continuity: $\nabla\cdot\mathbf{v} = 0$

NSE: $\rho D\mathbf{v}/Dt = \mu\nabla^2\mathbf{v} - \nabla p + \rho_e\mathbf{E}$ (190)

First, let's distill our description of hydrostatic equilibrium.

Case #1: hydrostatic equilibrium (i.e. $\delta E_x = 0$ and $\mathbf{v} = \mathbf{0}$)

continuity: $0 = 0$

NSE_x: $0 = -\dfrac{\partial p^{eq}}{\partial x}$ so $p^{eq} = p^{eq}(y)$ (191)

NSE_y: $0 = -\dfrac{dp^{eq}}{dy} + \rho_e^{eq} E_y^{eq}$ (192)

Finally Gauss's law gives:

$$\frac{dE_y^{eq}}{dy} = \frac{\rho_e^{eq}}{\varepsilon} \tag{193}$$

which (when written in terms of the electrostatic potential) becomes Poisson's equation

$$\frac{d^2\psi^{eq}}{dy^2} = -\frac{\rho_e^{eq}}{\varepsilon} \tag{194}$$

we have added a superscript "eq" to all variables above to remind us that these apply for hydrostatic equilibrium.

Boundary conditions can be imposed at the wall♣

at y=0: $\psi^{eq} = \psi_0$

and far away (outside the counterion cloud)

as $y \to \infty$: $\psi^{eq} \to 0$ and $p^{eq} = p_\infty$

Case #2: $\delta E_x \neq 0$

We expect the fluid to move in the direction of the applied electrostatic force so v_x must be nonzero. No slip at the wall yields the boundary condition:

at y=0: $v_x = v_y = v_z = 0$

The simplest solution to this problem which has this property is:

$$v_x = v_x(y), \; v_y = v_z = 0$$

Of course, we must allow v_x to vary with y so we can meet the no-slip condition at the surface. Since v_x is independent of x, this solution automatically satisfies continuity.

continuity: $\nabla \cdot \mathbf{v} = \dfrac{\partial v_x}{\partial x} = 0$

Denote by a prefix δ any perturbation in the electric field, electrostatic potential, space charge density or pressure which is caused by externally applying the electric field δE_x:

$$p = p^{eq} + \delta p$$

$$\rho_e = \rho_e^{eq} + \delta\rho_e$$

$$\mathbf{E} = \mathbf{E}^{eq} + \delta\mathbf{E} = E_y^{eq}\mathbf{e}_y + \delta E_x \mathbf{e}_x$$

Recalling that each of the components of the electric field as well as the total electric field are related to the corresponding electrostatic potential by $\mathbf{E} = -\nabla\psi$, we can now deduce the functional form for the electrostatic potential:

$$\psi(x, y) = \psi^{eq}(y) + \delta\psi(x)$$

An important implication of this is that δE_x is independent of y: any y-dependence in $\delta\psi$ would lead to a y-component of $\delta\mathbf{E}$. So if $\delta\mathbf{E}$ is purely in the x-direction, then δE_x must also be independent of y.

Any flow tangent to the plate is not expected to perturb the ion concentration profiles because tangential flow just replaces fluid having a particular concentration with fresh fluid having the same composition (also $\mathbf{v} \cdot \nabla c_i = 0$ since $\mathbf{v}$ and ∇c_i are orthogonal). This suggests that the charge density profile is not perturbed by flow caused either by an externally applied electric field (tangent to plate) or by an externally applied pressure gradient:

$$\rho_e = \rho_e^{eq} \quad \text{or} \quad \delta\rho_e = 0 \tag{195}$$

Gauss's law requires

$$\nabla \cdot \mathbf{E} = \frac{4\pi}{\varepsilon}\rho_e$$

$$\cancel{\frac{dE_y^{eq}}{dy}} + \frac{d\delta E_x}{dx} = \cancel{\frac{4\pi}{\varepsilon}\rho_e^{eq}} + 0$$

The cancellation of two terms above results from substituting (193). Then we get

Gauss: $\dfrac{d\delta E_x}{dx} = 0$ or $\delta E_x = \text{const w.r.t. } x,y$ (196)

The Navier-Stokes equations yield

$$0 = \underbrace{-\frac{\partial p^{eq}}{\partial x}}_{0} - \frac{\partial \delta p}{\partial x} + \mu\frac{d^2 v_x}{dy^2} + \rho^{eq}\delta E_x + \underbrace{\delta\rho}_{0}\delta E_x$$

♣ The surface potential ψ_0 is related to the surface charge density σ. For example see (138).

but two of these terms vanish according to (191) and (195). Dropping these terms leaves

NSE_x: $$\mu\frac{d^2v_x}{dy^2}+\rho_e^{eq}\delta E_x=\frac{\partial\delta p}{\partial x}$$

The y-component of NSE requires

$$0=-\cancel{\frac{dp^{eq}}{dy}}-\frac{\partial\delta p}{\partial y}+\cancel{\rho_e^{eq}E_y^{eq}}$$

Two of these terms cancel according to (192), leaving

NSE_y: $$\frac{\partial\delta p}{\partial y}=0 \quad \text{or} \quad \delta p=\delta p(x)$$

Knowing that δp is independent of y allows us to integrate NSE_x:

$$\underbrace{\mu\frac{d^2v_x}{dy^2}+\rho^{eq}\delta E_x}_{g(y)}=\underbrace{\frac{d\delta p}{dx}}_{f(x)}=\text{const} \qquad (197)$$
$$=\frac{p_L-p_0}{L-0}$$

By applying a pressure gradient along the surface, we could "pump" the fluid past the solid, but this is not the problem we want to address. Thus we set the pressure gradient to zero ($p_0 = p_L$) so there is no pressure-driven flow.

Substituting (194) and $p_0 = p_L$ into (197):

$$\mu\frac{d^2v_x}{dy^2}=\varepsilon\frac{d^2\psi^{eq}}{dy^2}\delta E_x$$

Boundary conditions include

at x=0: $v_x = 0$ and $\psi^{eq} = \psi_0$

as $x\to\infty$: $dv_x/dy \to 0$ or $v_x \to v_{x,\infty}$
$d\psi^{eq}/dy \to 0$ or $\psi^{eq} \to 0$

The b.c.'s on the ψ^{eq} are the same as have been used before [see before (132)]. The first hydrodynamic b.c. ($v_x = 0$) is just "no-slip". The second condition says there is no shear force being applied to the fluid outside the double layer. Shear stress ($\mu\, dv_x/dy$) might result from pressure driving flow or from sliding motion between two parallel plates. Here the only driving force for flow is the electrostatic body force $\rho_e\mathbf{E}$ which vanishes as $x\to\infty$. Since δE_x=const, this can easily be integrated to

$$v_x(y)=\frac{\varepsilon}{\mu}\left[\psi^{eq}(y)-\psi^{eq}(0)\right]\delta E_x$$

Of particular interest is the change in velocity over the diffuse cloud:

$$v_x(\infty)=\frac{\varepsilon}{\mu}\left[\psi^{eq}(\infty)-\psi^{eq}(0)\right]\delta E_x=-\frac{\varepsilon\zeta}{\mu}\delta E_x$$

where $$\zeta\equiv\psi^{eq}(0)-\psi^{eq}(\infty) \qquad (198)$$

is called the "zeta potential".

zeta potential - the electrostatic potential drop across the diffuse part of the double layer.

ζ is an important property of charged surfaces which can be inferred from electrokinetic experiments. It is related to the charge density on the interface: one such relationship is (138).

Substituting $\psi^{eq}(y)$ from (132),

$$v_x(y)=-\frac{\varepsilon\zeta}{\mu}\left(1-e^{-\kappa y}\right)\delta E_x$$

we obtain a velocity profile like that shown below.

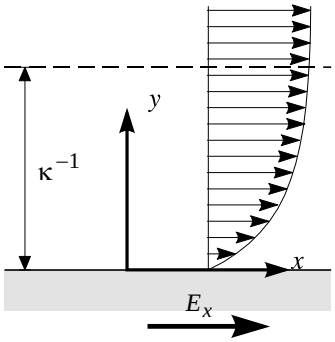

In the analysis above, we took the solid wall to be stationary [i.e. we took $v_x(0) = 0$]. We can easily generalize our result to a moving wall [i.e. let $v_x(0) = v_{x,f}$]. Then the above equation can be rewritten as

$$v_{x,s}-v_{x,f}=\frac{\varepsilon\zeta}{\mu}\delta E_x \qquad (199)$$

which is called ***Smoluchowski's equation***.

Electro-Osmosis in Cylindrical Pores

Consider a long circular capillary tube of radius a. If it is filled with an electrolyte solution and becomes charged, then applying a voltage across the length of the tube will give rise to electro-osmosis through the tube.

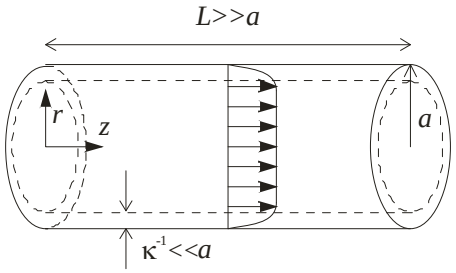

If the capillary radius a is much larger than the Debye length κ^{-1}, then the velocity profile is essentially plug flow except inside the double layer where the velocity suddenly drops to zero at the stationary solid surface

$$v_s = 0$$

$$v_x(r) = v_{x,f} = -\frac{\varepsilon\zeta}{\mu}E_x$$

for all r outside the double layer. Here we have applied (199), but dropped the prefix "δ" since we have no further need to distinguish between the equilibrium and the applied fields.

The volumetric flowrate through the tube is just this velocity times the cross-sectional area:

$\kappa a>>1$: $\quad Q = -\pi a^2(\varepsilon\zeta/\mu)E_x$

So a measurement of the flowrate for a known applied electric field allows us to determine the zeta potential.

Example: A typical value of the ζ potential for aqueous solutions is about 50mV. Plugging in the values of the other parameters

$$\varepsilon\zeta/\mu = 3.5\ \mu\text{m/s per V/cm}$$

Electrophoresis of Large Spheres

Consider a rigid sphere, constructed of some insulating material, immersed in a quiescent electrolyte solution in which we have applied a uniform electric field $\mathbf{E}_\infty$. As a result of any charge on the surface of the sphere, the sphere will be propelled at some terminal velocity $\mathbf{U}_\infty$ which will turn out to be parallel to $\mathbf{E}_\infty$. We now seek that velocity for the case in which the counterion cloud is very thin compared to sphere's radius a; i.e. $\kappa a >> 1$.

While the externally applied electric field $\mathbf{E}_\infty$ is uniform, the presence of the dielectric sphere perturbs that uniformity. We will first try to solve for the disturbance to the electric field. Changes in the electric field are determined by Gauss's equation or Poisson's equation (126).

If the charge layer is very thin, the fluid is electrically neutral nearly everywhere: thus the charge density ρ_e vanishes and Poisson's equation (126) reduces to Laplace's equation:

$$\nabla^2\psi = 0 \qquad (200)$$

at $r=a$: $\quad \partial\psi/\partial r = 0$

as $r\to\infty$: $\quad \psi \to -\underline{\boldsymbol{E}}_\infty r\cos\theta$

The b.c. at $r=a$ assumes that the sphere is an insulator and that no electrical current can be conducted into it. The b.c. as $r\to\infty$ requires that the electric field $\mathbf{E}$ tend to the uniform value $\underline{\mathrm{E}}_\infty$ externally applied. This problem is closely related to potential flow around a sphere. The solution to (200) and its boundary conditions is:

$$\psi(r,\theta) = -E_\infty\left(r + \frac{1}{2}\frac{R^3}{r^2}\right)\cos\theta$$

In particular, we will need the tangential component of the electric field at the surface of the sphere:

at $r = a$: $\quad E_\theta = -(1/r)\partial\psi/\partial\theta = -(3/2)\,\underline{\boldsymbol{E}}_\infty \sin\theta \qquad (201)$

Smoluchowski's equation (199) applies inside the counterion cloud next to a charged sphere. We will solve the hydrodynamic problem in a moving reference frame (so the sphere appears stationary) Taking $v_{x,s} = 0$ and replacing $v_{x,f}$ by v_θ and δE_x by E_θ, (199) yields:

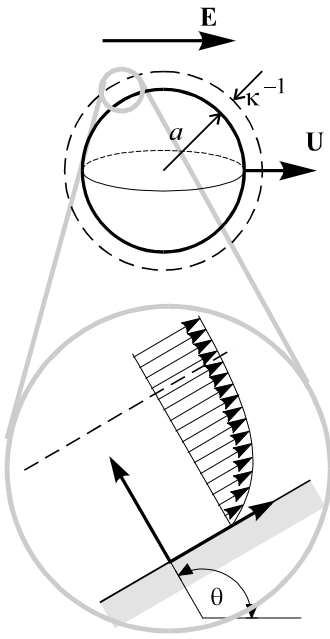

at $r=a+\kappa^{-1}$: $\quad v_\theta = -\frac{\varepsilon\zeta}{\mu}E_\theta \qquad (202)$

in a reference frame in which the sphere is stationary. This is the basis for solving the more complex problem of ***electrophoresis*** of a large sphere. "$r=a$" has been replaced by "$r=a+\kappa^{-1}$" to remind us that this is v_θ evaluated just outside the very thin counterion cloud (since v_θ evaluated at $r=a$ vanishes owing to no slip).

Now let's turn to the fluid flow problem. Outside of the counterion cloud, the fluid is electrically neutral and there are no electrostatic body forces acting on the fluid, even though there might be an electric field:

for $r>a+\kappa^{-1}$: $$\mu\nabla^2\underline{v} = \nabla p \qquad (203)$$

$$\nabla\cdot\underline{v} = 0 \qquad (204)$$

Let's choose a reference frame which moves with the center of the particle. If we define $\underline{U}_\infty$ as the electrophoretic velocity of the sphere in the laboratory reference frame, then the appropriate boundary conditions (in the moving reference frame of the sphere) are:

as $r\to\infty$: $$\underline{v} = -\underline{U}_\infty \qquad (205)$$

at $r = a$: $$\underline{v} = \underline{0}$$

which requires ***no slip*** of the fluid immediately in contact with the sphere. But just outside of the thin counterion cloud, we will have a tangential component of the fluid velocity as specified by (202); however there is still no normal component of fluid velocity:

at $r=a+\kappa^{-1}$: $$v_r = 0 \qquad (206)$$

$$v_\theta = -(\varepsilon\zeta/\mu)E_\theta \qquad (207)$$

(202) is based on (199), which is sometimes called the "slip" boundary condition (as opposed to no-slip). (199) is called that because κ^{-1} is so thin compared to a that the fluid appears to slip over the surface of the sphere.

If there is no pressure gradient imposed on the distant fluid, i.e. if $\nabla p_\infty = \underline{0}$, then the solution to equation (203), subject to (205) and (206) is potential flow:

for $r\ge a+\kappa^{-1}$: $$\underline{v} = \nabla\phi$$

and $$p = p_\infty$$

Recall from Theorem III, that the existence of a potential implies $\nabla\times\mathbf{v} = \underline{0}$. Then the right-hand side of (203) vanishes identically: using Identity F.1

$$\nabla^2\mathbf{v} = \nabla\underbrace{\left(\nabla\cdot\mathbf{v}\right)}_{0} - \nabla\times\underbrace{\left(\nabla\times\mathbf{v}\right)}_{\mathbf{0}} = \mathbf{0}$$

If the pressure is constant everywhere, then potential flow automatically satisfies (203) and (204) becomes:

$$\nabla^2\phi = 0 \qquad (208)$$

(205) becomes: $\phi = -\underline{\boldsymbol{U}}_\infty z$ as $r\to\infty$

(206) becomes: $\partial\phi/\partial r = 0$ at $r=a$

The particular solution to (208) also turns out also to be axisymmetric:

$$\phi(r,\theta) = -U_\infty\left(r + \tfrac{1}{2}\frac{R^3}{r^2}\right)\cos\theta$$

In particular, we will need:

at $r=a$: $$v_\theta = -(1/r)\partial\phi/\partial\theta = -(3/2)\,\underline{\boldsymbol{U}}_\infty\sin\theta \qquad (209)$$

Finally, we need to satisfy (207). Using (201) and (209) in (207), we conclude that

$$\underline{\boldsymbol{U}}_\infty = (\varepsilon\zeta/\mu)\underline{\boldsymbol{E}}_\infty$$

In vector form, we can write:

$\kappa a>>1$: $$\mathbf{U}_\infty = \frac{\varepsilon\zeta}{\mu}\mathbf{E}_\infty \qquad (210)$$

Thus, except for sign, this electrophoretic velocity of a charged sphere through a stagnant fluid is identical to the osmotic velocity of fluid through a stationary solid membrane. Although we have derived this result for a sphere, this result applies for any shape of particle provided the counterion cloud is thin compared to any radius of curvature of the particle (Morrison, 1970).

Electrophoresis of Small Particles

Now let's consider the opposite extreme of a very small particle compared to the thickness of the counterion cloud. In other words, let $\kappa a\to 0$. In this limit, we can treat the particle as a ***point charge***. The force acting on the particle by the applied electric field is given by the definition of electric field:

$$\underline{F}_{el} = Q\underline{E}$$

The particle will begin to move creating a drag force which can be calculated from Stokes' law:

$$\underline{F}_{drag} = -6\pi\mu a\underline{U}$$

The particle continues to accelerate until the drag force exactly balances the electrostatic force and the net force is zero:

$$\underline{F}_{el} + \underline{F}_{drag} = \underline{0}$$

This terminal velocity represents the electrophoretic velocity in the induced electric field:

$$\mathbf{U} = \frac{Q}{6\pi\mu a}\mathbf{E} \qquad (211)$$

Comparing (210) and (211), we see that both electrophoretic velocities are proportional to electric field. The proportionality constant is ***electrophoretic mobility***:

$$\text{electrophor. mobility} \equiv U/E$$

which is positive if the particle moves in the same direction as the electric field and negative if it moves in the opposite direction.

Is the mobility of (211) different from (210)? To compare them, we must first relate Q to ζ. One relationship between charge and zeta potential is given by the Gouy-Chapman equation (138). This was derived for a uniformly-charged, flat plate. It also can be applied near the surface of a sphere which is very large compared to the Debye length (i.e. $\kappa a >> 1$). However in the current problem, the sphere is very small compared to the Debye length (i.e. $\kappa a << 1$). The potential distribution is quite different in this case.

If the particle is a point charge, it seems reasonable to seek a solution in spherical coordinates having the form $\psi = \psi(r)$. In spherical coordinates, the linearized form of the Poisson-Boltzmann equation (130) is

$$\frac{1}{r^2}\frac{d}{dr}\left(r^2\frac{d\psi}{dr}\right) = \kappa^2\psi$$

Appropriate boundary conditions are

as $r\to\infty$: $\psi \to 0$

at $r=a$: $\psi = \zeta$

where once again ζ is the potential drop across the diffuse cloud of counterions surround the point charge. The particular solution to this problem is

$$\psi(r) = \zeta a e^{\kappa a}\frac{e^{-\kappa r}}{r} \qquad (212)$$

Let's denote the charge on our "point charge" as Q. Then global electroneutrality requires that the sum of the this charge and the charge born by the counterion cloud must vanish:

$$Q + \int_a^\infty \rho_e(r)\,4\pi r^2 dr = 0$$

Substituting (129) and (212)

$$Q = \frac{8\pi I e^2}{kT}\int_a^\infty \psi(r) r^2 dr$$

$$= \underbrace{\frac{8\pi I e^2}{kT}}_{4\pi\varepsilon\kappa^2}\zeta a e^{\kappa a}\underbrace{\int_a^\infty r e^{-\kappa r}\,dr}_{\frac{1+\kappa a}{\kappa^2}e^{-\kappa a}}$$

$$Q = 4\pi\varepsilon\zeta a(1+\kappa a)$$

When $\kappa a << 1$, we can neglect it, leaving

$$Q = 4\pi\varepsilon\zeta a$$

(211) becomes $\mathbf{U} = \frac{2\varepsilon\zeta}{3\mu}\mathbf{E}$

which is called ***Huckel's equation***.

Electrophoresis of a Sphere of Arbitrary Size

In the derivation of both Smoluchowski's and Huckel's equation, the distribution of ions within the counterion cloud was computed using either the Gouy-Chapman theory or the Debye-Huckel theory. Both of these theories describe an

equilibrium double layer — ion concentrations given by Boltzmann's equation (electrochemical potential of ions is constant along a normal to particle's surface).

In general, either ion migration in the applied electric field or convection of charge can distort the cloud away from equilibrium. For a more general description of electrophoresis, we must abandon Boltzmann's equation for describing the distribution of ions. That is we must allow for a non-equilibrium double layer:

Transport of ions occurs by convection, diffusion and migration of charges in an electric field. In terms of "driving forces," the flux is given by:

$$\mathbf{J}_i = \underbrace{\mathbf{v}c_i}_{\text{convection}} - D_i\left[\underbrace{\nabla c_i}_{\text{diffusion}} - \underbrace{\frac{z_i\mathcal{F}}{RT}c_i\mathbf{E}}_{\text{migration}}\right] \qquad (213)$$

where $\mathcal{F}/RT = e/kT$

which is called the ***Nerst-Planck equation***. Think of it as Fick's law for electrolytes. The last term in this equation represents migration of ions in the electric field. It's form is obtained by multiplying the terminal velocity by the ion concentration:

migr. flux:

$$\underline{U}_{el}c_i = m_i\underline{F}c_i = (D_i/kT)(z_i e\underline{E})c_i$$

but instead of using Stokes equation for the mobility (as we did to derive Huckel's equation), we used the Nernst-Einstein equation.

Now to find the ion distributions, we solve the steady-state ion continuity equations:

for i=1,2,...,n: $\quad \nabla\cdot\underline{J}_i = 0$

where $\mathbf{J}_i$ is given by the Nernst-Planck equation (213). At equilibrium, $\underline{J}_i = 0$ and continuity is automatically satisfied while the Nernst-Planck equation reduces to Boltzmann's equation. If we are not at equilibrium, we must determine the ion distribution by solving coupled P.D.E.'s:

$$\nabla\cdot\{\underline{v}c_i - D_i[\nabla c_i + (z_i e c_i/kT)\nabla\psi]\} = 0 \quad \text{for } i=1,...,n$$

$$\nabla^2\psi = -(\Sigma z_i e c_i)/\varepsilon$$

$$\mu\nabla^2\underline{v} = \nabla p + (\Sigma z_i e c_i)\nabla\psi$$

$$\nabla\cdot\underline{v} = 0$$

As you can see, all of the variables are now badly coupled. We have 5+n equations in 5+n unknowns ($\underline{v}$,ψ,p,c_i), where n is the number of ion species ($n\geq 2$). Products of unknown appear so the equations are also nonlinear. Boundary conditions are of the form:

at r=a: $\quad \underline{n}\cdot\underline{J}_i = 0$

$$\psi = \zeta$$

$$\underline{v} \to \underline{U}_{el} \qquad \text{(no slip)}$$

as $r\to\infty$: $\quad c_i \to c_{i\infty}$

$$\psi \to -\underline{r}\cdot\underline{E}_\infty$$

$$\underline{v} = \underline{0}$$

The terminal velocity $\underline{U}_{el}$ is determined such that the net force acting on any portion of the system vanishes:

$$\underline{F} = \int_S \underline{n}\cdot\Pi da = \underline{0}$$

where Π is the total stress tensor (viscous+Maxwell). Numerical solutions of this problem for a sphere of arbitrary radius have been published:

Reference – O'Brien & White, *J. Chem. Soc. Faraday Trans. II* **74**, 1607 (1978).

It turns out that the electrophoretic velocity is proportional to the electric field (if it's not too big). The proportionality constant is the electrophoretic mobility

$$\underline{U}_{el} = m_e\underline{E}_\infty$$

where $\quad m_e = m_e(D_+,D_-,\kappa a,\zeta)$

They report their results using the following dimensionless quantities:

$$M \equiv \frac{3\mu}{2\varepsilon\zeta} m_e$$

$$y \equiv e\zeta/kT$$

In terms of these variables, Huckel's equation becomes:

$\kappa a\to 0$: $\qquad M = y$

while Smoluchowski's equation becomes:

$\kappa a\to\infty$: $\qquad M = (3/2)y$

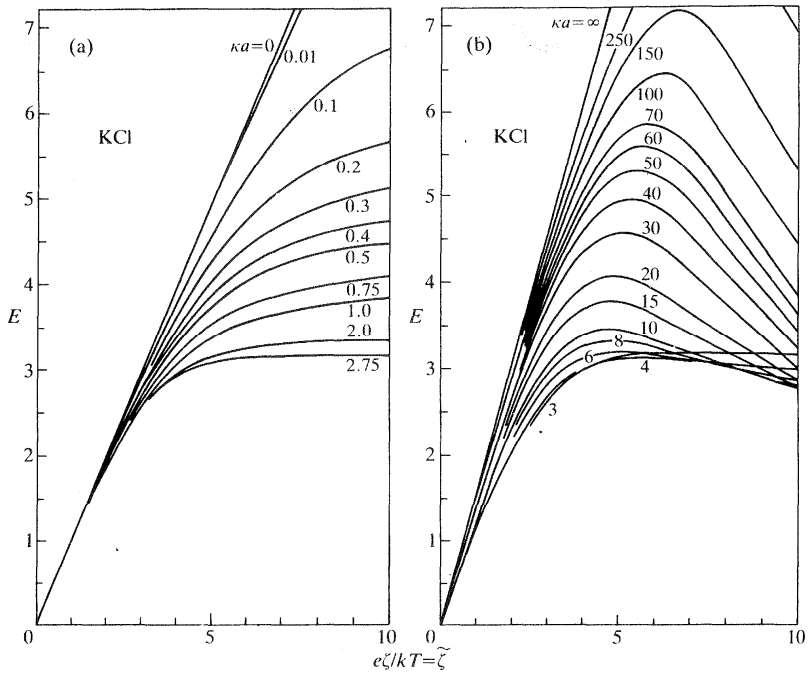

Fig. 1: Electrophoretic mobilities calculated by O'Brien & White (1978).

Although these two limiting cases bound the result for small y, they do not bound the mobility for large y.

Streaming Potential

So far in our discussion of electrokinetic phenomena, we have considered the motion of either fluid or solid that results from the application of an electric field:

Electrophoresis, Electro-osmosis: **E≠0 → U≠0**

Now we would like to consider the inverse situation in which relative motion across a charged interface generates an electric field:

Streaming Potential,
Sedimentation Potential: **U≠0 → E≠0**

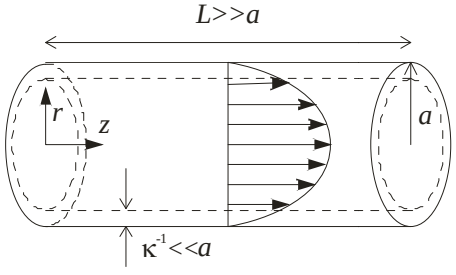

Consider the pressure-driven flow through a large circular capillary.

$$\kappa^{-1} << a << L$$

Owing to the applied pressure drop, we generate a fully developed parabolic velocity profile so familiar for laminar flow:

$$v_z(r) = \frac{1}{4\mu}\frac{dP}{dz}\left(r^2 - a^2\right)$$

The main idea is that this flow causes convection of charge in the counterion cloud which tends to generate a current. However in the absence of electrodes in the two reservoirs, there is no way to form a complete electric circuit. So charge tends to pile up in the reservoir — positive charges on one side of the membrane and negative charges on the other. Coulomb's law exerts a force on these charges which tends to restore electroneutrality to the system and to prevent any steady-state *rate of accumulation* of charge.

Clearly any steady-state electrical current would eventually lead to infinite charge separation and infinite attractive forces. The only way to avoid this is to have ***zero current*** at steady state. This is achieved by an electric field which spontaneously arises inside the bulk of the fluid which creates an electrical current equal but opposite to the convective current:

$$I_{total} = I_{conv} + I_{elec} = 0 \qquad (214)$$

The electrostatic potential drop associated with this induced electric field is called the ***streaming potential***. To calculate it, let's first calculate the current generated by convection of charges inside the cloud.

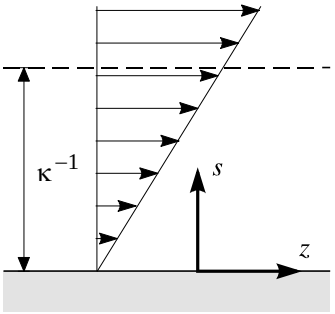

If the charge cloud is very thin compared to the capillary radius, then we need to concentrate on the velocity profile right next to the wall. Here the velocity profile becomes linear:

for $s<<a$: $$v_z(s) = \Gamma s \qquad (215)a$$

where $$s \equiv a - r \qquad (215)b$$

and $$\Gamma = -\left.\frac{dv_z}{dr}\right|_{r=a} = \frac{a}{2\mu}\left(-\frac{dP}{dz}\right) \qquad (215)c$$

Just like we can evaluate the volumetric flowrate by integrating $\mathbf{n}\cdot\mathbf{v}$, the net current I_{total} (not to be confused with the ionic strength) through any surface S is just the integral of the normal component of the current density over the surface:

$$I_{total} = \int_S \mathbf{n}\cdot\mathbf{i}\, da \quad [=] \text{ amps}$$

In our case, we choose a disk of radius a whose normal is parallel to the tube axis.

$$I_{conv} = \int_0^a \rho_e v_z\, 2\pi r dr$$

Since ρ=0 for most of the fluid (except for $r\approx a$), we can approximate this integral as shown by substituting (215):

$$I_{conv} \approx 2\pi a\Gamma \int_0^\infty \rho_e s ds \qquad (216)$$

Since the charge density ρ_e vanishes outside the cloud (which is a small fraction of a), the integrand is zero over most of the domain; thus we can extend the upper limit to ∞ without introducing any additional error. Next, we substitute Poisson's equation (194) for the space charge density:

$$\rho_e = -\varepsilon\, d^2\psi^{eq}/ds^2 \qquad (217)$$

(217) into (216) and integrating by parts:

$$I_{conv} = -2\pi\varepsilon a\Gamma \int_0^\infty \frac{d^2\psi^{eq}}{ds^2} s ds$$
$$= -2\pi\varepsilon a\Gamma\left[\psi^{eq}(z,0) - \psi^{eq}(z,\infty)\right]$$

Substituting (198)

$$I_{conv} = -2\pi\varepsilon a\Gamma\zeta \qquad (218)$$

According to (214), this convective contribution to the current must be balanced an electrical contribution from an induced electric field. The relationship between current and electric field is given by ***Ohm's law*** for electrolyte solutions, which takes the form of

$$\mathbf{i}_{elec} = K\mathbf{E}$$

where K is called the ***specific conductance*** of the solution. Integrating over the cross-section of the tube:

$$I_{elec} = \int_0^a KE_z\, 2\pi r dr \approx \pi a^2 K E_z \qquad (219)$$

where $E_z = -\partial\psi/\partial z = \text{const} = -\Delta\psi/L$

is required by (196), where L is the length of the cylindrical pore. (215)c, (218) and (219) into (214):

$$\pi a^2 K\left(-\frac{d\psi}{dz}\right) = -2\pi\varepsilon a\zeta\frac{a}{2\mu}\left(-\frac{dP}{dz}\right)$$

Integrating over the length L of the capillary:

$$\Delta\psi = -\frac{\varepsilon\zeta}{\mu K}\Delta p$$

which is ***Smoluchowski's equation*** for streaming potential $\Delta\psi = \psi(L) - \psi(0)$. While we have derived this using the geometry of a circular cylinder, the same result applies for any shape (even a porous plug of spherical particles), provided the local radius of curvature a is everywhere large compared to the Debye length.♣ In particular:

$$\kappa a >> \exp\left(\frac{ze\zeta}{2kT}\right)$$

♣ Overbeek, 1952.

Physical Chemistry of Colloids & Surfaces

by

Dennis C. Prieve
Department of Chemical Engineering
Carnegie Mellon University
Pittsburgh, PA 15213

An electronic version of this book in Adobe PDF® format was made available to students of 06-607, Department of Chemical Engineering, Carnegie Mellon University, Spring, 2010.

Table of Contents

